THE INTEGRATED STRESS RESPONSE

DIRECTS CELL FATE DECISIONS IN REPSPONSE TO PERTURBATIONS IN

PROTEIN HOMEOSTASIS

Brian Frederick Teske

Submitted to the faculty of the University Graduate School
in partial fulfillment of the requirements
for the degree
Doctor of Philosophy
in the Department of Biochemistry and Molecular Biology,
Indiana University

May 2013

Accepted by the Faculty of Indiana University, in partial
fulfillment of the requirements for the degree of Doctor of Philosophy.

_____

Ronald C. Wek, PhD., Chair

Doctoral Committee

_____

Martin Bard, PhD.

January 8, 2013

_____

Lawrence L. Quilliam, PhD.

_____

Clark D. Wells, PhD.

DEDICATION

I would like to dedicate this accomplishment to my grandfather Frederick L. Crane.

ACKNOWLEDGEMENTS

I collectively acknowledge my family, friends, colleagues, and mentors for their continued emotional, financial, and intellectual support during my academic training and beyond. Individually, I would like to acknowledge my committee members for their devotion and dedication to the academic process. I thank Dr. Martin Bard for his friendship, extended guidance, and support throughout my research career. I acknowledge Dr. Lawrence Quilliam for his commitment, time, and helpful comments in both formal and informal settings. I thank Dr. Clark Wells for his advice, attention to detail, and scholarly discussions. Finally, I would like to extend a special acknowledgment to Dr. Ronald Wek. The research environment he created for me emphasized quality training, curiosity, camaraderie, scientific discussion, accountability, and academic success. Dr. Wek's personalized training strategy and guidance has given me the tools to open doors for success.

ABSTRACT

Brian Frederick Teske

THE INTEGRATED STRESS RESPONSE

DIRECTS CELL FATE DECISIONS IN REPSPONSE TO PERTURBATIONS IN

PROTEIN HOMEOSTASIS

Disruptions of the endoplasmic reticulum (ER) cause perturbations in protein folding and result in a cellular condition known as ER stress. ER stress and the accumulation of unfolded protein activate the unfolded protein response (UPR) which is a cellular attempt to remedy the toxic accumulation of unfolded proteins. The UPR is implemented through three ER stress sensors PERK, ATF6, and IRE1. Phosphorylation of the α-subunit of eIF2 by PERK during ER stress represses protein synthesis and also induces preferential translation of ATF4, a transcriptional activator of stress response genes. Early UPR signaling involves translational and transcriptional changes in gene expression that is geared toward stress remedy. However, prolonged ER stress that is not alleviated can trigger apoptosis. This dual signaling nature of the UPR is proposed to mimic a 'binary switch' and the regulation of this switch is a key topic of this thesis. Adaptive gene expression aimed at balancing protein homeostasis encompasses the first phase of the UPR. In this study we show that the PERK/eIF2~P/ATF4 pathway facilitates both the synthesis of ATF6 and trafficking of ATF6 from the ER to the Golgi where ATF6 is activated. Liver-specific depletion of *PERK* significantly lowers expression of survival genes, leading to reduced expression of protein chaperones. As a consequence, loss of PERK in the liver sensitizes cells to stress which ultimately leads to apoptosis. Despite important roles in survival, PERK signaling is often extended to the

activation of other downstream transcription factors such as CHOP, a direct target of ATF4-mediated transcription. Accumulation of CHOP is a hallmark of the second phase in the binary switch model where CHOP is shown to be required for full activation of apoptosis. Here the transcription factor ATF5 is found to be induced by CHOP and that loss of ATF5 improves the survival of cells following changes in protein homeostasis. Taken together this study highlights the importance of UPR signaling in determining the balance between cell survival and cell death. A topic that is important for understanding the more complex pathological conditions of diseases such as diabetes, cancer, and neurodegeneration.

Ronald C. Wek, PhD., Chair

TABLE OF CONTENTS

CHAPTER 5. DISCUSSION

LIST OF TABLES

LIST OF FIGURES

ABBREVIATIONS

ATF3	Activating transcription factor-3
ATF4	Activating transcription factor-4
ATF5	Activating transcription factor-5
ATF6	Activating transcription factor-6
bZIP	Basic leucine zipper
BCL	B-cell lymphoma
BIM	Bcl-2 interacting mediator of cell death
CARE	CCAAT-enhancer binding protein activating transcription factor (C/EBP-ATF) response element
CHOP	C/EBP homologous protein
DMEM	Dulbecco's modified eagle's media
DTT	Dithiothreitol
eIF2	Eukaryotic initiation factor-2
eIF2α	Eukaryotic initiation factor-2α
eIF2~P	Eukaryotic initiation factor-2 phosphorylation
ER	Endoplasmic reticulum
ERO1	ER oxidoreductase-1
GAP	GTPase-activating protein
GDP	Guanosine diphosphate
GTP	Guanosine-5' triphosphate
GCN2	General control nonderepressible-2
GDI	GDP-dissociation inhibitor

GADD34	Growth arrest and DNA damage-inducible protein-34
GRP78	Glucose-related protein 78
HRI	Heme regulated inhibitor
ISR	Integrated stress response
IRE1	Inositol requiring enzyme -1
Met-tRNA$_i$	Methionyl-initiator tRNA
MEF	Mouse embryonic fibroblast
PCR	Polymerase chain reaction
PKR	double-stranded RNA-activated protein kinase
PEK	Pancreatic eIF2 kinase
PERK	PKR-like ER kinase
qPCR	Quantitative PCR
TC	Ternary complex
UPR	Unfolded protein response
UTR	Untranslated region
uORF	Upstream open reading frame
WT	Wild-type
WRS	Wolcott-Rallison syndrome

CHAPTER 1. INTRODUCTION

1.1 ER stress and the unfolded protein response

The endoplasmic reticulum (ER) is a cell organelle that serves as a primary site for the folding and assembly of proteins, and also plays an important role in calcium storage, and lipid biosynthesis. The homeostasis of proteins slated for the secretory pathway is controlled by translation associated with the ER, folding and modifications of proteins in the ER, and protein degradation of selected ER proteins. This process is tightly controlled to ensure the proper synthesis and assembly of proteins destined for the secretory pathway. Dysregulation in ER protein homeostasis leading to the accumulation of unfolded proteins can occur in response to elevated expression of secretory proteins or gene alterations altering protein folding, as well as perturbations in calcium levels, redox status, or post-translational modifications in the ER. ER stress and accumulation of improperly folded proteins, a process referred to as proteotoxicity, can be an important contributor to the etiology of diseases including diabetes, cancer and neurodegenerative disorders [1-5].

Proteotoxicity activates the ER resident transmembrane proteins ATF6, IRE1 (ERN1), and PERK (EIF2AK3/PEK), which in turn induce the Unfolded Protein Response (UPR). The UPR regulates expression of specific genes through transcriptional and translational mechanisms to expand the processing capacity of the ER that return it to homeostasis [3-5]. Specifically, changes in the translation of several transcripts upon phosphorylation of eIF2 by PERK facilitate a reduction in nascent polypeptide synthesis, thus limiting the influx of proteins into the overloaded ER [5]. Expression of ER client proteins is also lowered through the cleavage of their mRNAs by IRE1 [6, 7]. ATF6 is also reported to directly activate the synthesis of miRNA which acts to further dampen

the influx of ER proteins [8]. Therefore, each arm of the UPR facilitates a reduction in ER protein load by reducing gene expression. This global reduction of gene expression is thought act as a 'shut-off-valve' that would prevent further organelle stress and cellular damage [5, 9].

In addition to the lowered expression of genes mediated by PERK, IRE1, and ATF6, each of these arms of the UPR are also required for activation of the transcriptional master regulators ATF4, XBP1 and ATF6(N). The details of the activation of the UPR will be introduced in the following sections. Briefly, phosphorylation of eIF2 by PERK facilitates preferential translation of select mRNAs, such as *ATF4*, by a mechanism involving delayed translation re-initiation of inhibitory open reading frames (ORFs) located in the 5'-end of the encoded transcripts [10, 11]. The endoribonuclease activity of IRE1 facilitates the cytoplasmic cleavage of *XBP1* mRNA, leading to the synthesis of the spliced and activated XBP1 (XBP1s) transcription factor. ATF6 is an ER membrane bound transcription factor that upon ER stress transits to the Golgi where the active N-terminus, ATF6(N) is released into the cytoplasm by regulated intramembrane proteolysis (RIP) for subsequent transport to the nucleus allowing transcription of target genes.

Initial targets of ATF4, XBP1, and ATF6 are partially overlapping and include genes involved in adaptive processes such as redox control, protein folding, disulfide bond formation, ER-Golgi trafficking, and calcium homeostasis [3, 5]. Depending on the extent and duration of ER stress, productive folding of proteins may not be restored, resulting in an inability to adapt. This results in a second phase of the UPR, where a terminal unfolded protein response trigger maladaptive processes, such as premature

resumption in protein synthesis, inflammation, and apoptosis. One focus of this thesis is defining gene regulatory networks in the UPR that decide between these adaptive and maladaptive cell fates. Understanding this signaling process, which has been referred to as a binary switch [12, 13], is important for identifying novel biomarkers and potential targets for therapeutic intervention of ER stress associated pathologies.

This thesis investigates both the adaptive and maladaptive phases of the UPR. Results show that PERK mediated phosphorylation of eIF2, and the resulting enhanced expression of ATF4, is required for synthesis and processing of ATF6 that is needed for cell adaptation and survival. The second phase or terminal UPR response that leads to cell death is also a key topic this thesis. A downstream target of ATF4, CHOP can control cell survival in response to alterations in protein homeostasis. We find that the CHOP transcription factor can induce expression of genes favoring remediation of stress damage, as well as those signaling apoptosis. Interestingly, central to the changes in the transcriptome directed by CHOP is the finding that CHOP enhances the expression of many additional transcription factors that comprise additional 'nodes' of a transcription network that reinforce and amplify stress responses. Included among these CHOP-targeted transcription factors is ATF5, which we show is a direct downstream target of CHOP and ATF4. ATF5 serves to potentiate CHOP-dependent apoptosis in response to inhibition of proteasome inhibition, and other disruptions of protein homeostasis. This study of the second phase of the binary switch model places CHOP upstream of a network of transcriptional regulators and identifies new target genes of ATF5 that mediate the apoptotic response to stress.

1.2 Activation of the IRE1-XBP1 axis

IRE1 is a type I transmembrane serine/threonine protein kinase that also serves as an endoribonuclease. There are two isoforms of IRE1, α and β, encoded by distinct genes, with the IRE1α isoform being ubiquitously expressed among tissues, and expression of IRE1β targeted to the digestive system [14]. Upon activation, IRE1 is thought to dimerize and through trans-autophosphorylation induces its endoribonuclease activity that facilitates cytoplasmic splicing of *XBP1* transcript. Following, the cleavage of the XBP1 transcript by IRE1, the joining of the exons is performed by the tRNA ligase, RGL1/TRL1 in yeast *Saccharomyces cerevisiae* [15]. Currently, it is not known which ligase facilitates the splicing of *XBPI* mRNA in mammalian cells. This splicing removes a 26-nucleotide segment leading to expression of the active XBP1s basic leucine zipper transcription factors (bZIP) transcription factor, allowing for the newly synthesized XBP1 to enhance the transcription of UPR target genes involved in protein quality control, disulfide linkage, ERAD, and lipid synthesis [3, 14, 20].

Deletion of *IRE1α* in mice leads to embryonic lethality (e12.5) due to defects in placenta labyrinth vascularization involving VEGF-A [16]. When *IRE1α* mutants are supplied with a wild-type (WT) placenta, the IREα-deficient pups are born alive, which refutes a previous suggestion that lethality in *IRE1*-null animals in due to fetal liver hematopoetic defects [16]. Liver-specific deletion of *IRE1α* also results in hepatic steatosis, in response to tunicamycin induced ER stress, a theme that extends to *ATF6* and *PERK* knockout mice [17, 18]. Deletion of the related gene *IRE1*β that is predominantly expressed in epithelial cells of the gastrointestinal tract, sensitizes mice to chemically induced colitis [19].

XBP1 knockout mice die *in utero* due to fetal anemia which is a manifestation of liver hypoplasia and apoptosis [21]. *XBP1*-specific deletions in lymphatic tissues also revealed that XBP1 was an essential player in B-cell maturation and was the first transcription factor identified in terminal B-cell to plasma cell differentiation required for IgG secretion [14]. The finding that *XBP1*-deficient mice do not mirror or exacerbate those described for the IRE1 isoforms is consistent with the idea that IRE1 endoribonucleases can also alter gene expression through mRNA decay, as noted above. Furthermore, IRE1 was reported to degrade specific miRNAs, which as a consequence would lead to increased expression of genes subject to repression by these small RNAs [22]. This thesis will describe studies showing that *XBP1* expression is dependent on both PERK and ATF4 during ER stress, supporting the idea that there is coordinated expression of multiple branches of the UPR.

1.3 Activation of ATF6

ATF6 is a type II membrane-bound transcription factor that is localized to the ER and serves as both a sensor of ER stress and transcriptional activator of UPR target genes. There are two ER stress-responsive isoforms of ATF6 designate α and β [23-25], with the predominant activator of UPR target genes, ATF6α (ATF6), being the primary focus of this study. Deletion of *ATF6α* and *β* together in mice results in embryonic lethality (e 8.5), but individual deletion of either *ATF6α* or *ATF6β* does not lead to an overt developmental phenotype [26, 27]. *ATF6α* -null mice subjected to pharmacological induction of ER stress showed reduced expression of chaperone proteins and altered metabolic gene expression associated with lipid homeostasis, ultimately leading to

hepatic steatosis not found in the similarly treated WT animals [17, 26-28]. Central to the UPR dysregulation in the *ATF6α*$^{-/-}$ mice is a persistent activation of IRE1, leading to cytoplasmic splicing of *XBP1* mRNA [4, 29, 30].

The ATF6 exists as a transmembrane protein localized to the ER and is constitutively expressed during non-stress conditions. The pool of ATF6 protein in the ER is continually turned over and renewed. The C-terminus of ATF6 extends into the lumen of the ER and is heavily glycosylated on at least three sites containing the consensus motif NxS/T (Figure 1-2). Treatment with the dolichol N-acetyl glucosamine transferase inhibitor, tunicamycin, prevents glycosylation of newly synthesized ATF6 allowing for the differeniation of newly synthesized protein from previously synthesized ATF6 protein in the ER. In the ER membrane, ATF6 is thought to exist as an oligomeric complex organized by two lumenal cysteine residues that participate in inter- and intra-molecular disulfide bridging. In an unstressed state, disulfide linkages between ATF6 polypeptides are promoted due to the oxidative nature of the ER lumen. Enzymatic or chemical reduction of these disulfide linkages is required for ATF6 release from the ER for eventual transport to Golgi for ATF6 cleavage and activation. ATF6 is also bound and sequestered by the ER chaperone BIP that is thought to cover a Golgi-localization signal sequence (GLS) in the ER lumen, preventing trafficking of ATF6 from the ER to Golgi during non-stressed conditions. Therefore ATF6 release from the ER in response to ER stress is thought to involve lumenal disulfide bond reduction and ATF6 release from BIP.

The final step in the release of ATF6 from the ER involves packaging of ATF6 into COPII vesicles. This process minimally involves five proteins, the GTPase SAR1,

SEC23, SEC24, SEC13, and SEC31 [31]. After recruitment to the ER membrane, Sar1 initiates coat formation by GDP to GTP exchange. The SEC23/SEC24 heterodimeric complex, binds to SAR1 GTP and the second complex, SEC13/SEC31, then initiates membrane curvature necessary to pinch of the vesicle. Cargo selection is thought to involve protein-protein interactions between SEC24 and cytosolic motifs of vesicle cargo, in this case ATF6. Overexpression of dominant-negative SAR1 has been shown to inhibit COPII vesicle formation and block transport of ATF6 [32].

In the Golgi, ATF6 is processed by regulated intramembrane proteolysis (RIP) involving consecutive cleavage by site-1-protease (S1P) and site-2-protease (S2P) liberating the N-terminal portion of ATF6 [3, 33, 34]. The S1P cleavage and S2P cleavage sites are conserved between mouse and human (Figure 1-2). Cleavage by S1P removes a bulky C-terminal region in the lumen of the Golgi allowing for subsequent S2P access and cleavage to occur in the plane of the membrane [34]. Following cleavage by S2P the N-terminus of ATF6 diffuses away from the Golgi membrane and transits to the nucleus to activate expression of target genes. Reduced (-SH) ATF6 monomers are thought to be the preferred substrate for this cleavage process and oxidized (S-S) monomers are proposed to be recycled back to the ER from the Golgi [35]. ATF6 is released as a N-terminal transcription factor, ATF6(N) which enters the nucleus and binds to ER stress response elements and unfolded protein response elements (ERSEs and UPREs) located in the promoters of UPR targeted genes [3, 26, 27, 36, 37]. This results in increased transcription of a network of genes, including genes encoding ER chaperones, such as *BIP/GRP78*, and components of the ER-associated degradation (ERAD) pathway [3, 26, 27, 37]. It should be emphasized that genes transcriptionally

targeted by ATF6 are necessary for an increase in ER lumen folding capacity and are critical for cell survival.

As mentioned above ATF6β is not a predominant activator of UPR gene expression. Although activation of ATF6β is stress-dependent, its release from the ER and subsequent cleavage in the Golgi in response to ER stress is delayed with respect to ATF6α [23]. The structure of the N-terminal trans-activation domain (TAD) also differs between the α and β isoforms, with the ATF6β isoform possessing an 8 amino acid insert in the TAD that is thought to disrupt the potency of gene activation. Additionally, ATF6β has been shown to serve as a direct repressor of ATF6α mediated gene activation through hetero-dimerization between their bZIP domains [23].

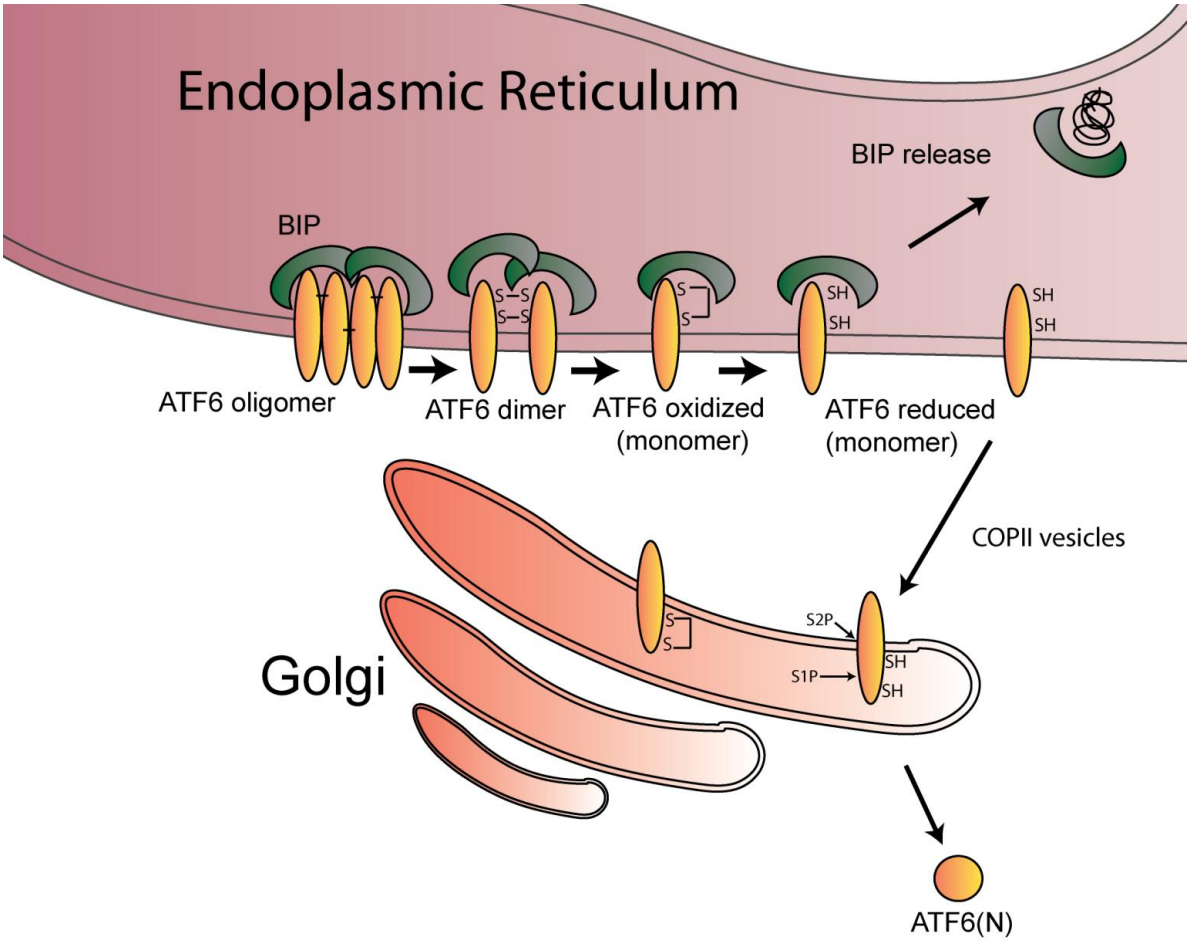

Figure 1-1 Activation of ATF6 in response to ER stress. The chaperone BIP/GRP78 inhibits ATF6 activation by binding to the the C-terminus of ATF6 in the lumen of the ER. Two cysteine residues in the lumenal domain are involved in inter- and intra-molecular disulfide bonding allowing for oligomerization. Upon activation during ER stress, ATF6 undergoes deoligomerization and BIP release which leads to formation of ATF6 monomers that traffic to the Golgi. At the Golgi, ATF6 is first processed by S1P cleavage, followed by regulated intermembrane proteolysis by S2P. Intermembrane cleavage liberates the activated form of ATF6, designated ATF6(N), which then is transported to the nucleus. ATF6(N) then binds to the promoters of UPR target genes facilitating activation of transcription.

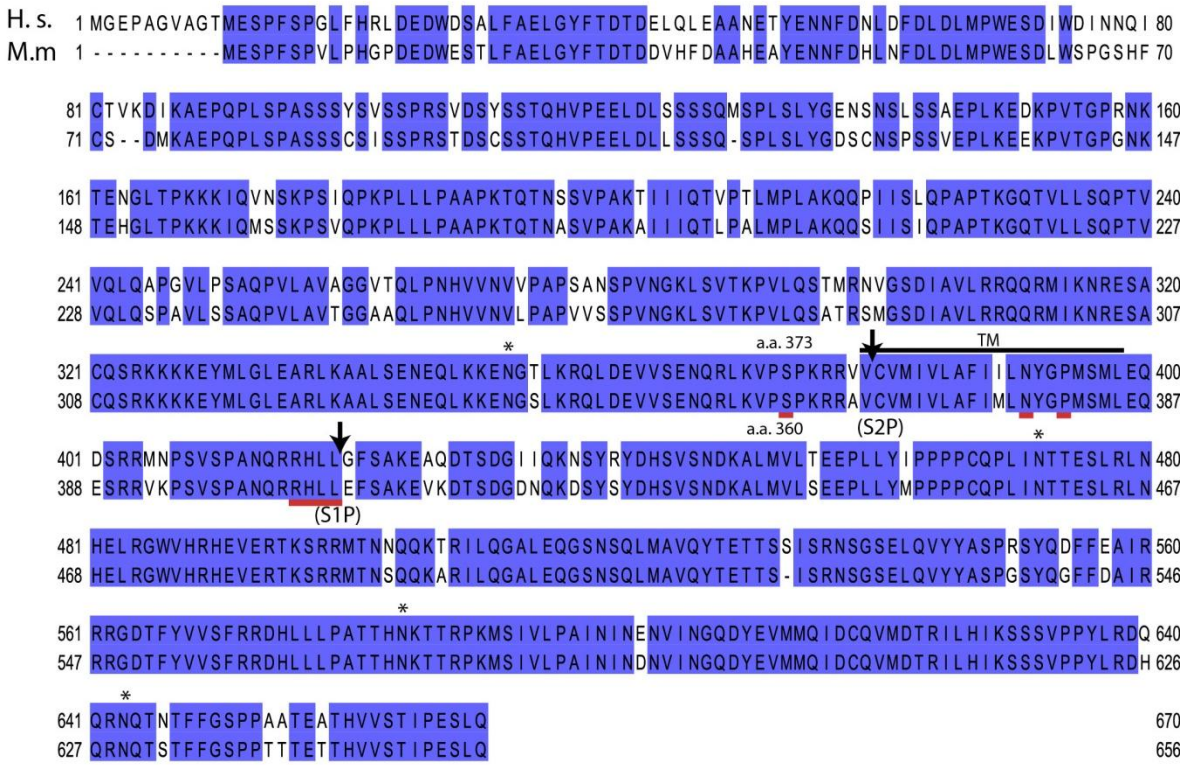

Figure 1-2 Sequence homology between mouse (M.m.) and human (H.s.) ATF6α.

Sequence alignment between the mouse and human orthologs of ATF6α. Sequences identities are shown in blue highlights, with putative N-glygosylation sites (N-X-S/T) labeled with a "*". Arrows indicate the S1P and S2P cleavage sites, and the transmembrane domain is shown with a black line. The residue underlined in red at position 373 (H.s.) or 360 (M.m.) represents the C-terminal residue in the active ATF6(N) fragment that is used in overexpression studies. Other underlined residues indicate amino acids required for cleavage by S1P or S2P.

1.4 PERK dependent translation control and the integrated stress response

The translational control arm of the UPR is directed by PERK phosphorylation of eIF2, a translation initiator factor that combines with GTP and delivers the initiator Met-$tRNA_i^{Met}$ to the translational machinery (Figure 1-3). Phosphorylation of the α subunit of eIF2 at serine-51 blocks the activity of eIF2B required for the exchange of eIF2-GDP to the active version, eIF2-GTP [5, 38]. The subsequent reduction in protein synthesis conserves cellular energy and prevents further influx of nascent polypeptides into the ER. Reduced protein synthesis also provides the cell ample time to implement the UPR reprogramming of the transcriptome. Accompanying the repression of global protein synthesis, eIF2 phosphorylation (eIF2~P) also enhances the translation of select mRNAs, such as that encoding ATF4, a transcriptional activator of genes involved in metabolism, cellular redox status, and regulation of apoptosis [3, 5, 10, 39-41].

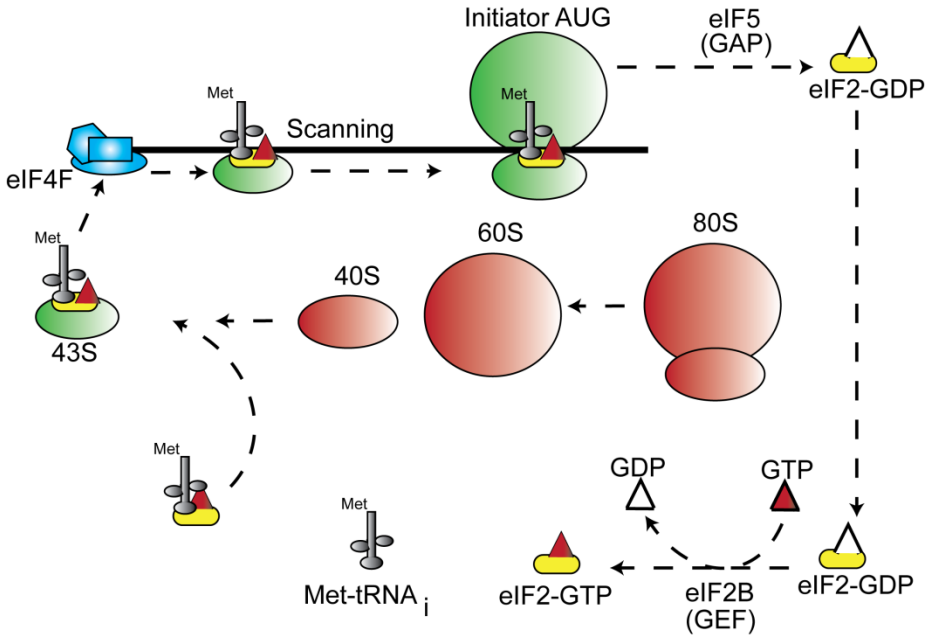

Figure 1-3 eIF2-GTP facilitates delivery of charged initiator tRNA to the ribosome during translation initiation. eIF2 bound to GTP is required for recruitment of the initiator Met-tRNA$_i^{met}$ to the 40S ribosome, leading to formation of the 43S preinitiation complex (PIC) that associates with the 5'-cap structure of mRNAs [38]. The small ribosomal complexes then scans in a 5' to 3' direction along the 5'-leader of the transcript until the appropriate initiation codon is recognized and placed in the P site. eIF2-GTP is hydrolyzed with the aid of eIF5 to generate eIF2-GDP, which is released prior to the 40S ribosomal subunit joining with the 60S ribosomal subunit. The eIF2-GDP is recycled to the active eIF2-GTP by the guanine nucleotide exchange factor, eIF2B. The newly recycled eIF2 bound to GTP can then be used for subsequent rounds of translation initiation.

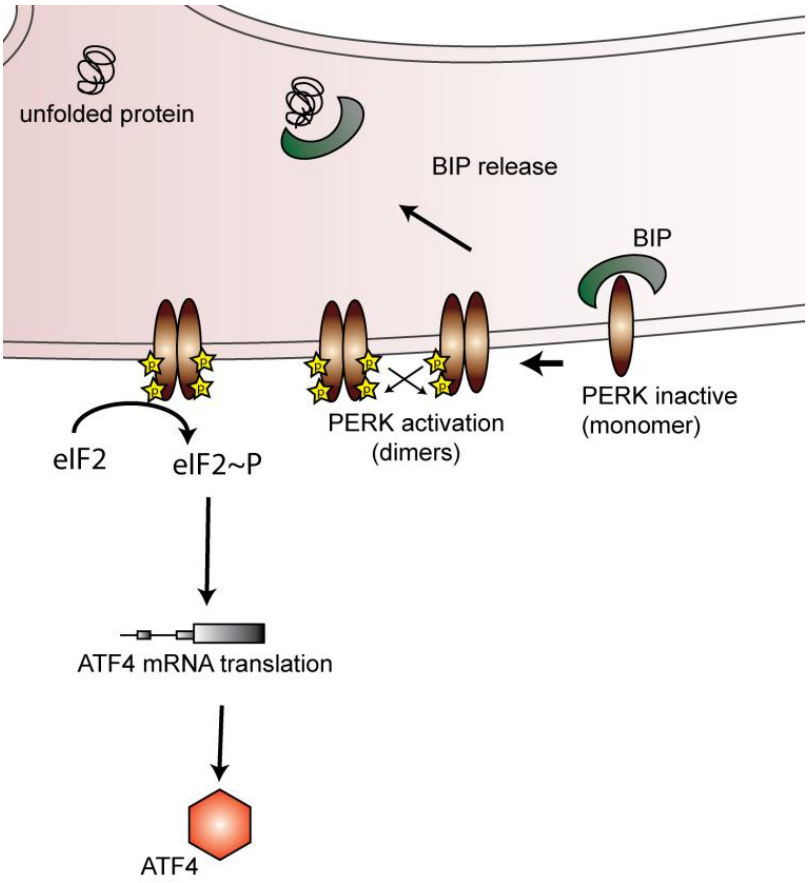

Figure 1-4 Activation of PERK during ER stress. The luminal domain of PERK is bound by the ER chaperone BIP/GRP78 to maintain PERK monomers in an inactive state. Upon ER stress, BIP is released from the N-terminus of PERK resulting in formation of PERK homodimers. Homodimers of PERK are capable of trans-autophosphorylation of neighboring dimers, leading to activation of the protein kinase. Activated PERK then phosphorylates eIF2, facilitating preferential translation of *ATF4* mRNA.

1.5 eIF2~P activation of ATF4 is not unique to ER stress

In addition to ER stress, preferential translation of *ATF4* occurs in response to diverse stress conditions that regulate three other eIF2 kinases [5, 38, 42]. For example, in response to starvation for amino acids, the eIF2 kinase GCN2 serves to conserve nutrients [42-44], while HRI insures that globin synthesis is coupled to heme availability in erythroid tissues [45]. The eIF2 kinase PKR participates in the anti-viral defense mechanism directed by interferon. In each case, eIF2~P abruptly blocks translation initiation by reducing the recycling of eIF2-GDP to eIF2-GTP, while preferentially translating *ATF4*, a master transcriptional regulator of stress-related genes [2, 4, 40]. The idea that ATF4 is an induced downstream factor that integrates signaling from PERK and other eIF2 kinases has led to the designation of the eIF2~P/ATF4 pathway as the Integrated Stress Response (ISR) [40].

Early signaling in the ISR network is critical for ameliorating stress conditions, such as those afflicting the ER organelle, as genetic perturbations of the eIF2 kinases have significant medical consequences. For example, PERK disruption leads to Wolcott-Rallison syndrome, which is characterized by neonatal diabetes, atrophy of the exocrine pancreas, skeletal dysplasia, growth retardation, and hepatic complications resulting in morbidity [46-48]. These pathologies were recapitulated in *PERK*-deficient mice [49, 50], where the molecular and cellular mechanisms have been investigated [51-54].

1.6 Dephosphorylation of eIF2

Translation control through eIF2~P can also be regulated by protein phosphatases. eIF2~P is dephosphorylated by protein phosphatase type 1 (PP1c), which requires a targeting subunit for holoenzyme function [55]. Under non-stressed conditions, the CReP-PP1c complex is responsible for maintaining eIF2/eIF2~P homeostasis. CReP is rapidly turned over and therefore continual synthesis of CReP is required to maintain the eIF2/eIF2~P balance within the cell. As part of a feedback mechanism, there is increased synthesis of the PP1c targeting subunit, GADD34. *GADD34* mRNA is induced by the ISR pathway via ATF4/CHOP transcriptional activation and *GADD34* is also preferentially translated by a mechanism involving eIF2~P; thus there are multiple layers of regulation that facilitate this negative feedback loop. GADD34 feedback appears to be necessary for resumption of global protein synthesis once the transcriptome has been reprogrammed to alleviate stress. However, premature resumption of protein synthesis by GADD34 can also lead to further ER overload and initiate a terminal ER stress response. Therefore, GADD34 can have significant proapoptotic functions during chronic stresses [56].

CReP/GADD34 mediated eIF2~P dephosphorylation can be targeted pharmacologically with salubrinal, Sal003, and a GADD34-specific inhibitor guanabenz [57, 58]. These drug inhibitors elicit robust eIF2~P and activation of ATF4. In cell culture experiments, removal of these inhibitors from treatment media rapidly reverses eIF2~P and reduces levels of ATF4 and its target genes.

The importance of regulation of eIF2~P can also be seen in several mouse models. First, mice containing an alanine substituted for the phosphorylation site serine-

51 in eIF2α (S51A, designated A/A mice) can be born alive, suggesting that regulation of translation initiation through eIF2~P is not required for embryogenesis. However, in A/A mice liver gluconeogenesis was severely diminished, which is suggested to contribute to perinatal lethality in these animals [59]. Alternatively, hyperphosphorylation of eIF2 by genetic disruption of PP1c regulatory subunits CREP and GADD34 in mice leads to altered levels of eIF2~P, translation control, and has health consequences [56]. GADD34 knockout mice do not appear to be developmentally different from WT mice and display slight resistance to ER stresses. By comparison, CREP knockout animals are born alive but are of low birth weight, fail to nurse, and die in the post natal period within the first day of life. Double disruption of both PP1c regulatory subunits results in embryonic lethality [60].

1.7 Distal ISR signaling initiates maladaptive stress responses

It is also important to note that while the ISR serves essential adaptive functions in response to ER stress and other stress arrangements, perturbations in or unabated induction of these stress responses can contribute to morbidity. The immediate downstream target of eIF2~P is the ISR master transcriptional regulator ATF4. Genetic disruption of *ATF4* in mice is not lethal although knockout mice display low fertility, fetal anemia, and developmental defects in lens formation [61]. ATF4 activates genes by a specific CCAAT-enhancer activating transcription factor response element (CARE) [62, 63]. Binding of ATF4 at these CARE elements is thought to be dynamic where the ATF4 transcriptional signal can be differentially modified by the association with partner proteins as heterodimers [62].

The processes by which the ISR can adversely affect cells is not well understood, but central to this process is the ATF4-target gene, *CHOP* (*GADD153*/*DDIT3*), a transcriptional regulator whose extended expression during stress can trigger apoptosis [3, 56, 64-66]. Thus the ISR pathway is often extended to include genes downstream of eIF2~P and ATF4, such as *ATF3* and *CHOP*, which collectively participate in regulation of ISR-target genes [5, 63, 67]. CHOP is implicated in many different stress conditions and is central for apoptosis during selected stress conditions [2, 4, 56]. Several CHOP targets genes involved in the regulation of apoptosis include *BCL2*, *ERO1*, *DR5*, *BIM* and *GADD34*; however the transcription factor network regulating these genes has been poorly defined.

1.8 Induction of the ISR network extends to ATF5

This thesis identifies ATF5 as an important transcription factor in the ISR, which is downstream of CHOP and sensitizes cells to apoptosis. ATF5 is another member of the ATF/CREB family of bZIP proteins. Two alternatively spliced *ATF5* transcripts (*ATF5*α/β) have been identified with distinct 5'-leaders that encode different uORF arrangements [68]. *ATF5α* is the more abundant transcript, expressed highly in liver but also detected in brain, heart, lung and kidney [68], and will be a focus of this study. *ATF5* has been shown to be regulated at both the transcriptional and translation level [69, 70] and can also be regulated post-translationally by p300 directed acetylation at lysine-29 [71]. At the translational level, *ATF5* expression is regulated by two uORFs and the synthesis is dependent on eIF2~P and a mechanism involving delayed ribosome

reiniation that was described for ATF4 [70]. *ATF5β* appears to be largely restricted to early development, and is not subject to translational control by eIF2~P.

1.9 Cross-talk in the ISR network reinforces cell fate decisions

The results in Chapter 3 of this thesis center on the early survival pathways that are controlled by the ISR. As described in introductory sections 1.2 to 1.4, activation of ATF6, IRE1, and PERK in response to ER stress is thought to occur in parallel, but the timing and duration of each may differ. Although the complete mechanistic details are not yet resolved, it has been proposed that the ER luminal portions of each of these sensory proteins can be bound and repressed by BiP [3, 72]. Accumulation of unfolded proteins in the ER lumen is suggested to compete with the sensory proteins for BIP binding, enhancing release of this ER chaperone from each ER sensor and thus leading to their activation [3, 72-75]. Alternatively, it has been proposed that unfolded proteins can directly interact with the ER sensor proteins, such as IRE1, which then facilitates oligomerization and activation [3, 76-79]. These models posit that activation of the sensory proteins in response to ER stress occurs largely by independent rather than by interconnected processes. We wished to determine if the translational control arm of the UPR is coupled to the regulation of the transcriptional components of this stress response, insuring coordinate control of the transcription and translation phases of the UPR. Our studies show that the PERK/eIF2~P/ATF4 pathway is required to facilitate activation of ATF6 in response to ER stress both *in vivo* and in cultured cells. As a consequence, liver-specific deletion of *PERK* leads to enhanced apoptosis in response to ER stress, along with hepatic dysfunctions, features that are similar to those described for *ATF6*-null

mice. In this model, loss of PERK mediated translational control of the UPR also significantly blocks the transcriptional arms, resulting in dysregulation of the UPR network that would ultimately contribute to disease.

Results in Chapter 4 of this thesis investigate UPR signaling involved in maladaptive cell fates. Specifically, this study focuses on defining transcription factor networks directed by the ISR pathway in response to perturbations in protein homeostasis. Among ISR genes, CHOP is considered a central inducer of stress induced apoptosis [2, 56]. Several CHOP target genes have been suggested to be involved in the switch to apoptosis. For example, *ERO1α* is involved in the formation of disulfide bonds in the ER lumen, a process that eventually leads to oxidative damage if accumulation of unfolded protein is not resolved. As noted earlier, expression of *GADD34* restores translation initiation, which can further exacerbate an overloaded ER and can therefore be viewed as maladaptive during chronic stress. This dual nature of ISR signaling that involves signaling decisions between adaptive and maladaptive cell fates has been referred to as a "binary switch" [12, 13], A focus of this study is to define gene regulatory networks controlling of the switch between cell fates. The signaling events are not well defined, but induction of CHOP is suggested to be a central event. Therefore a major goal of Chapter 4 is to define and characterize novel transcription factors downstream of CHOP that may play a role in ISR signaling toward cell death. We found that *ATF5* is a direct downstream target of CHOP and that ATF5 serves to potentiate CHOP-dependent apoptosis in response to diverse stress conditions.

CHAPTER 2. EXPERIMENTAL METHODS

This section will describe the methods used in experiments described in this thesis. These experimental methods will also highlight critical considerations and useful tips in designing and conducting experiments analyzing the ISR and UPR.

2.1 Cell Culture

PERK$^{-/-}$, *ATF4*$^{-/-}$, *CHOP*$^{-/-}$ and *A/A* MEF cells, and their WT counterparts, have been described previously [39, 80]. MEF cells were grown in Dulbecco's Modification of Eagle's Medium (DMEM) (4.5 g/L glucose), supplemented with 1X MEM non-essential amino acids (HyClone SH30238.01) and 50 μM β-mercaptoethanol, as described previously [40]. HEK293 and the mouse hepatoma cell line, HEPA1-6, were also cultured in DMEM (4.5 g/L glucose). Cultured cells were treated with 2 μM tunicamycin, 1 μM thapsigargin, 1 μM MG132, 10 μM actinomycin D, 50 μg/ml cycloheximide, and 5 μg/ml brefeldin A, and 10 μM Sal003, as indicated. Sal003 was added at a final concentration of 10 μM, by first diluting a 10 mM stock to 100 μM in warm media prior to adding to the cultured cells. Specific experimental details regarding pretreatments or co-treatments are provided in the figure legends. When designing stress response experiments, it was important to consider the dosage and duration of stress exposure. The selected concentrations were determined to be optimal for the induction of the UPR and ISR, or in the case of actinomycin D and cycloheximide, for repression of transcription or protein synthesis, respectively. The timing of the chemical induction of stress response is also critical. Transcriptional regulators of the ISR often appeared early in a stress time course. For example, eIF2~P and ATF4 can be detected in cultured cells

within about 1-2 hours of treatment with agents that can induce ER stress, while CHOP is induced between 3 and 6 hours. By contrast, measurements of apoptotic markers were detectable between 12 and 24 hours of stress induction.

2.2 Measurement of eIF2~P and the ISR by immunoblot analyses

Cellular lysates were prepared from cultured cells using RIPA-buffered solution containing 50 mM Tris-HCl (pH 7.9), 150 mM sodium chloride, 1% nonident P-40, 0.1% sodium dodecyl sulfate (SDS), 100 mM sodium fluoride, 17.5 mM β-glycerophosphate, 0.5% sodium deoxycholate, and 10% glycerol that was supplemented with EDTA-free protease inhibitor cocktail tablet (Roche). Protein content was determined for each preparation by a modified Bradford or Lowry assay, such as that offered by the Bio-Rad protein quantification kit for detergent lysis (cat no. 500-0114) following the manufacturer's instructions. Equal amounts of protein preparations, typically 10 to 30 μg, was prepared in 2X SDS sample buffer, heated at 95˚C, and then separated by electrophoresis using an SDS polyacrylamide gel. The percentage of acrylamide for these gels was 7.5%, 10%, or 12% to insure linearity for the size of the measured proteins. Polypeptide markers of known molecular weight were included to determine the size of proteins identified in the immunoblot analysis. Proteins separated by gel electrophoresis were then transferred to nitrocellulose filters, and the membranes were then incubated in 5% (w/v) nonfat milk powder in PBS followed by incubation with antibody that specifically recognizes the proteins of interest. After washing the filters to remove unbound antibody, secondary antibody was added (dilution 1:3000 to 1:10,000). The secondary antibodies contained a dye label for visualization of the target protein with

the Odyssey infrared imaging system (LI-COR). Alternatively, secondary antibodies conjugated to horse radish peroxidase (HRP) were used for detection with an enhanced chemiluminescent (ECL) immunoblot protocol. This ECL protocol used "homebrewed" solutions that were made fresh or in bulk and kept at 4˚C for several weeks. For detection, equal volumes of solution 1 and solution 2 were mixed and applied evenly to the membrane filter for 1-2 minutes followed by film detection. Solution 1 contained 100 mM Tris-HCl (pH 8.5), 2.5 mM 3-aminophthalydrazide (Luminol; Sigma-Aldrich #A-8511) and 0.4 mM P-coumaric acid (Sigma-Aldrich #C-9008) and Solution 2 contained 100 mM Tris-HCl (pH 8.5) and H_2O_2 (stock 30%) at a final concentration of 0.02%. Freshly prepared solutions usually gave the more intense signal, but SuperSignal West Femto from Thermo Scientific (Prod #34094) was used for immunoblot analyses when more sensitivity was needed, such as immunoblots measuring eIF2~P. A common troubleshooting practice involved the use of the more sensitive West Femto substrate after faint unmanageable protein bands appeared with the less sensitive ECL solutions. The coupled use of LI-COR and ECL immunoblot detection allowed for detection of multiple different proteins from a single immunoblot filter. Thus this bypassed the need for multiple rounds of membrane filter stripping and also allowed for detection of proteins of similar size from one blot when cutting the membrane was not an option.

Antibodies for eIF2~P (Ser51), cleaved caspase-3, and Grp78/BiP were purchased from Cell Signaling Technology, total eIF2 and CHOP were purchased from Santa Cruz Biotechnology, and actin from Bethyl Laboratories. Secondary antibodies were purchased from Jackson Laboratories. ATF6 antibody was prepared in rabbits using the mouse ATF6 N-terminal amino acids 6-307 as the antigen. ATF6 antibody was

used at a concentration of 1:500 in 5% milk powder in PBS. ATF4 and ATF5 antibodes prepared against full-length recombinant human ATF4, were affinity purified, and used in immunoblot analyses.

There are many different antibody preparations for measuring eIF2~P and ISR target proteins that are available commercially. However, these commercial antibodies can vary in their affinity and specificity. Even when commercial antibodies are indicated in publications, it is important to appreciate that the efficacy can vary between commercial antibody preparation, even when procuring antibodies with the same product number and lot number. Establishing criteria for antibody specificity, in conjunction with suitable control lysate preparations, is important, especially when characterizing new cultured cell lines or tissue types. The following are guidelines for antibody usage based on our laboratory experience. Antibodies against eIF2~P typically worked well among different vertebrate protein preparations, as the sequences flanking the serine-51 are well conserved. Antibody against eIF2~P was typically used at a concentration of 1:250, but depending on the commercial antibody preparation, dilutions often varied in the range of 1:50 and 1:1000. Measurements of total eIF2 were important to insure that induced eIF2~P was not a function of changes in the levels of the translation factor. CHOP antibodies were also typically reliable and were used at a concentration range of 1:1000 to 1:3000. Immunoblot analyses of CHOP protein sometimes resulted in a doublet band that may represent CHOP phosphorylation [81].

Immunoblot analyses measuring ATF4 protein offered the greatest technical hurdles. The predicted molecular weight of ATF4 is 38 kD, but ATF4 typically migrated with a size between 45 to 52 kD by SDS-PAGE. Furthermore, ATF4 often migrated as a

broad band in immunoblots, which upon closer inspection seemed to represent multiple bands that appeared to be a consequence of protein phosphorylation [5, 82-84].

It is important not to grow cultured cells to more than 70% confluency prior to treatment. Confluent growth of cultured cells is by nature a stress that can induce eIF2~P. High basal eIF2~P levels in the absence of added stress agents is not an uncommon dilemma in experiments, and this can lead to experimental misinterpretations when appropriate controls are not included in the studies. As noted above, when studying new stress conditions or cell types for induction of eIF2~P it is helpful to conduct a dose response at a fixed time point, such as 6 hours of exposure. Once an optimum stress condition is determined, keeping in mind the physiological parameters for a given stress, this can be followed with a time course.

Liver tissue samples were prepared for SDS-PAGE as previously described [85]. Tissues were homogenized in 7 volumes of a solution consisting of 20mM *N*-2-hydroxyethylpiperazine-*N*'-2-ethanesulfonic acid (pH 7.4), 100 mM KCl, 0.2 mM EDTA, 2 mM EGTA, 1 mM dithiothreitol, 50 mM sodium fluoride, 50mM β-glycerophosphate, 0.1 mM phenylmethylsulfonyl fluoride, 1 mM benzamidine, and 0.5 mM sodium orthovanadate. Following electrotransfer to nitrocellulose filter, immunoblots were incubated with primary and secondary antibodies, and then were visualized using enhanced chemiluminescence reagents (ECL) (GE Biosciences).

To measure the half-life of ATF6(N), plasmid p913 encoding an N-terminal HA-tagged version of ATF6 residues 1-373 (HA-ATF6-1-373) was transfected into WT or *ATF4*$^{-/-}$ MEF cells. After 24 hours, cells were pre-treated with 2 μM tunicamycin for 3

hours, or exposed to no ER stress, followed by the addition of 50 μg/ml cycloheximide. Cells were then incubated for up to 8 hours.

2.3 Interpreting whether the observed induction of eIF2~P and the ISR results from ER stress

An observed increase in eIF2~P and the ISR is not necessarily a demonstration of ER stress, as many different stress conditions involving other cellular compartments can activate the eIF2 kinase family. There are four strategies to ensure that an observed increase in eIF2~P is a consequence of ER stress. Each offers certain advantages and deficiencies, which should be recognized during the design of the proposed ER stress experiments. The first strategy is indirect, and involves measuring the activity of the UPR sensors, IRE1 or ATF6, in conjunction with eIF2~P. These UPR sensors are thought to be exclusively activated by ER stress. IRE1 facilitates cytoplasmic splicing of *XBP1* mRNA, which then leads to synthesis of the transcription activator of UPR genes [86]. Splicing of *XBP1* mRNA can be measured by qPCR [87, 88], and enhanced eIF2~P combined with spliced *XBP1* mRNA gives one a degree of confidence that the underlying stress being studied perturbs the ER. It is noted that there are some stresses that have been reported to have discordant activation or amplification of PERK and IRE1 [88-90], which can complicate negative experimental findings.

Additional strategies for establishing whether a studied stress induces eIF2~P due to ER stress includes measuring eIF2~P in *PERK*$^{-/-}$ mouse embryo fibroblast (MEF) cells, or specifically knocking down this eIF2 kinase using shRNA [80, 91-93]. A collection of MEF knockout cells have been described that are deleted for one or more of the eIF2

kinase genes, and significant reductions in levels of stress induced eIF2~P in *PERK* depleted cells supports the idea that there is an underlying ER stress [80]. However, it is noted that longer periods of ER stress exceeding 6 hours can induce eIF2~P in *PERK*$^{-/-}$ cells. It is suggested that secondary eIF2 kinases are activated during these extended periods of stress. Another related strategy is to measure the phosphorylation status of PERK, which is known to occur during the activation of this eIF2 kinase. Commercial antibodies are available for measuring phosphorylation of PERK at the activation loop (threonine-980), and measuring phospho-PERK by immunoblot analysis along with total PERK levels is a strategy for determining whether a stress activates this ER-stress inducible eIF2 kinase [50, 73, 94]. It is noted that immunoblot analysis of phospho-PERK can be problematic, as PERK is a large membrane-bound protein (~125 kD), and the phosphorylated version of this eIF2 kinase can migrate as several tightly packed bands in SDS-PAGE. In fact the increase in migration of PERK was originally used to establish its phosphorylation and activation during ER stress [73, 94]. Frequently measures of phospho-PERK have involved first immunoprecipitating PERK, which can improve the sensitivity and specificity of the phospho-PERK antibody in immunoblot analysis [39, 50, 87]. A final strategy for establishing whether eIF2~P is a consequence of ER stress and activation of PERK is to carry out *in vitro* kinase assays using recombinant eIF2 substrate and immunoprecipitated PERK prepared from stressed cells showing enhanced eIF2~P[95]. Increased PERK eIF2 kinase activity in this *in vitro* assay would provide confidence that the studied stress condition involves ER stress and the UPR.

2.4 Animals

The animal study protocol was approved by the Institutional Care and Use Committee at the Indiana University School of Medicine-Evansville. Mice homozygous for the *LoxP* allele of *PERK* (*PERK*$^{fl/fl}$) were mated with transgenic mice heterozygous for Cre recombinase expressed from the albumin gene promoter (*AlbCre*) to create a liver-specific deletion of PERK, LsPERK-KO (*AlbCre*$^{+}$, *PERK*$^{fl/fl}$). This mating also produced littermates that are Cre negative that express a WT version of PERK (*AlbCre*$^{-}$, *PERK*$^{fl/fl}$) [85, 96]. The LsPERK-KO mice were derived from a cross between C57BL/6 and 129SvE mice. Genotyping that showed efficient *PERK* gene deletion in the LsPERK-KO livers was reported [85], which is consistent with lowered eIF2~P levels in response to tunicamycin treatment. Male and female adult mice (n=5-8 per treatment group), ages 3 to 6 months, were individually housed in wire-bottomed cages, maintained on a 12 hour light/dark cycle, and provided unrestricted access to food (7017 NIH-31 Open Formula Mouse/Rat Sterilizable diet, Harlan Teklad) and water. The key gene expression, triglyceride, and apoptotic findings reported in this study were similar between the male and female mice. Among the assays in which n=8, there were between 4-7 males, and between 1-3 females. Analysis of ATF6 activation includes independent liver samples prepared from at least one male and one female in each treatment group. Mice were administered tunicamycin by intraperitoneal (i.p.) injection at a dose of 1 mg/kg body weight or an equivolume of excipient (0.3% DMSO in phosphate buffered saline) [97]. Mice were euthanized by decapitation at 6, 12, 24, or 36 hours after injection.

Dissected livers were rinsed in ice-cold PBS, weighed, and either snap-frozen in liquid nitrogen or fixed in 4% paraformaldehyde.

2.5 Reverse Transcription and Real-Time PCR

Total RNA was extracted from frozen tissue using TriReagent (Molecular Research Center, Inc.) followed by a DNase treatment (VersaGene DNase kit, Gentra Systems). To inactivate the reaction, the samples were heated to 70°C for 5 min. RNA samples were further purified using the RNeasy mini kit (Qiagen), yielding preparation with an A_{260}/A_{280} ratio between 1.8 and 2.0. The levels of the indicated mRNAs were determined by qPCR. Approximately 1 μg of each of the RNA solutions was used for reverse transcription, which employed the High-Capacity cDNA Reverse Transcription Kit (Applied Biosystems, Foster City, CA, USA) according to the manufacturer's instructions. TaqMan Gene Expression Master Mix (Roche) and TaqMan Gene Expression Assays (Applied Biosystems) were used for the quantitative PCR. Amplification and detection were performed on the LightCycler 480 (Roche). For measurement of the spliced version of the *XBP1* mRNA, the forward primer 5'-GAGTCCGCAGCAGGTG-3' and reverse primer 5'-CTCTGGGAGTTCCTCCAGACT-3' were used in the qPCR. All measurements were in triplicate and normalized to β-actin or 18S mRNA. Results were obtained by the comparative Ct method, and results were expressed as fold change with respect to the non-stressed control. qPCR was also performed on RNA extracted from cultured cells.

Total RNA was extracted from MEF cells using TriZol reagent following the manufactures instructions for adherent cells. The levels of the indicated mRNAs were

determined by qPCR. Approximately 1 μg of each of the RNA solutions was used for reverse transcription, which employed the High-Capacity cDNA Reverse Transcription Kit (Applied Biosystems) according to the manufacturer's instructions. Primers for SYBR green detection of cDNA are listed in Table 1. Amplification and detection were performed on the LightCycler 480 (Roche) or the Realplex^2 Master Cycler (Eppendorf). All measurements were recorded in biological and technical triplicates and normalized to *β-actin* mRNA. Results were obtained by the comparative Ct method, and results were expressed as fold change with respect to the untreated control.

Table 2-1 Sequence of oligonucleotides for SYBR green based qRT-PCR.

Primer name	Sequence
mCHOP	5'-CCTAGCTTGGCTGACAGAGG-3' 5'-CTGCTCCTTCTCCTTCATGC-3'
mATF4	5'-GCCGGTTTAAGTTGTGTGCT-3' 5'-CTGGATTCGAGGAATGTGCT-3'
mβ-Actin	5'-GTATGGAATCCTGTGGCATC-3' 5'-AAGCACTTGCGGTGCACGAT-3'
mGADD34	5'-AGGACCCCGAGATTCCTCTA-3' 5'-CCTGGAATCAGGGGTAAGGT-3'
mATF5	5'-GGCTGGCTCGTAGACTATGG-3' 5'CCAGAGGAAGGAGAGCTGTG-3'
mNOXA	5'-GACAAAGTGAATTTACGGCAGA-3' 5'-GGTTTCACGTTATCACAGCTCA-3'
mAPAF1	5'-GTTCAAAGCCGAGACAGGAG-3' 5'-ATTGACTTGCTCCGAGTGCT-3'
mTXNIP	5'-TATGTACGCCCCTGAGTTCC-'3 5'-GCTCACTGCACGTTGTT-3'

Each of these indicated genes are derived from mouse, as indicated by the "m" designation preceding each.

2.6 Histology

Tissues fixed in 4% paraformaldehyde were frozen and then sectioned (10 μm) using a cryostat. TUNEL assays were performed according to the manufacturer's instructions (Trevigen TACS 2 TdT-Blue Label *in situ* Apoptosis Detection kit, R&D Systems). TUNEL-positive cells were measured from 3 equal sized areas per section. Digital images of selected areas captured at 200X were imported into Scion Image for Windows (Scion Corporation, Inc.), and TUNEL-positive cells were manually marked and counted using the counting tool. The TUNEL-staining showed pyknotic bodies, and the nucleus was stained darker than the cytoplasm portion in the tissue preparations. Frozen sections were also stained with Oil Red O and counter stained with hematoxylin to visualize lipid content and tissue morphology.

2.7 Triglyceride Measurements

Triglycerides were measured using the Triglyceride Quantification Kit from BioVision Research Products (Mountain View, CA) following the manufacturer's instructions. Tissue samples (~40 mg) were weighed and homogenized in 10 volumes of a 5% NP-40 solution. Samples were heated to 85˚C then subjected to centrifugation at 10,000 x g for 2 minutes at room temperature. The resulting supernatants were diluted 1:500 with sterile water, and a volume of 50 μl of diluted supernatant was added to 50 μl of reaction mix and absorbance levels were measured at 570 nm. The absorbance of the standards was plotted and test sample readings were applied to the standard curve to calculate the triglyceride concentrations.

2.8 Microarray analysis

Microarray analysis was carried out using RNA prepared from livers obtained from WT and LsPERK-KO mice injected with 1 mg/kg body weight of tunicamycin or excipient for 6 hours, as highlighted above in the Animals section of the Experimental Methods. Three mice from each control and four mice from each experimental group were analyzed, for a total of 14 preparations analyzed. Total RNA was isolated from liver tissue using TRIzol reagent (Invitrogen) following the manufacturer's instructions, and an RNeasy mini kit (Qiagen, Gaithersburg, MD) was used to further purify samples. The RNA was then labeled using the standard Affymetrix protocol for 3'-IVT arrays (Affymetrix, Santa Clara, CA). Labeled cRNA was hybridized for 17 hours to the Affymetrix mouse 430 2.0 array. The signal values and detection calls were derived using the MAS5 algorithm in Affymetrix GeneChip Operating Software. Probe sets were eliminated from further analysis if an absent call was determined in greater than 50% of the samples in both the WT treated/untreated and LsPERK-KO treated/untreated.

Filtered data was imported into Partek Genomics Suite (Partek, Inc.) where hierarchical clustering and principal components analysis were used to detect any outlier arrays, none were found. P-values were determined for treatment condition (stress/no stress), genotype (WT/LsPERK-KO), and interaction terms by 2-Way ANOVA using the Partek software. False discovery rates (FDR) were calculated according to Benjamini and Hochberg [98]. Probe sets that were not significantly changed during tunicamycin treatment were filtered out ($p>0.05$ or FDR>0.15), such that the resulting data set would further represent ER stress-dependent genes. From this ER stress-dependent data, probe

sets that had an interaction p-value (condition*genotype) of $p>0.05$ were removed to enrich for the subset of *PERK*-dependent genes.

The following gene ontology (GO) terms were used to identify genes in the PERK-dependent dataset that were linked with ER to Golgi transport: Primary GO term, Biological process: 0006810 (transport). Secondary GO terms, Gene Ontology Cellular Compartment: 0005783 (endoplasmic reticulum), 0005789 (endoplasmic reticulum membrane), 0000139 (Golgi membrane), 0005794 (Golgi apparatus). Microarray data have been deposited in GEO (gene expression omnibus) (www.ncbi.nlm.nih.gov/geo/) under the accession number GSE29929.

Microarray technology was also used to distinguish differential transcription profiles between WT, *CHOP*$^{-/-}$ and *ATF5*-kd cells. Total RNA was extracted from WT and *CHOP*$^{-/-}$ MEF cells using TRIzol reagent following the manufacturer's instructions for adherent cells. The crude RNA pellet was purified using an RNeasy kit (Qiagen, Gaithersburg, MD), and array hybridizations were carried as highlighted above and previously described [18]. Filtered data was imported into Partek Genomics Suite (Partek, Inc.) where hierarchical clustering and principal components analysis were used to detect any outlier arrays, none were found. With respect to drug treatment significance was determined by t-test and genes were considered significantly changed if the p-value was less than 0.05 in the WT samples. *CHOP* dependence was further defined from within this set of genes where a p-value of 0.05 between the WT and *CHOP*$^{-/-}$ treated cells and fold change of WT/*CHOP*$^{-/-}$ treated samples was greater than 1.0. Alternatively, cRNA derived from WT and *ATF5*-kd cells were hybridized to an Affymetrix Mouse 1.0 ST array. Venn Diagrams were created with the help of an online

Venn diagram program (Venny). CHOP dependent genes were also analyzed using Ingenuity Pathway analysis software package (Redwood, CA).

2.9 Luciferase assays

Luciferase assays were carried out in 6-well plates using the Dual-Luciferase reporter assay system (Promega, Madison, WI) following the manufacturer's instructions. The *ATF6* expression plasmids were described by Prywes and colleagues [99]. For measurements of ATF6 transcriptional activity, plasmid p912 encoding five ATF6-binding elements fused to the firefly luciferase reporter gene was co-transfected with a *Renilla* normalization plasmid into *PERK*$^{-/-}$, *ATF4*$^{-/-}$, *A/A,* and WT MEF cells. Measurements were determined as the RLU of the firefly luciferase normalized to *Renilla* luciferase. Plasmid p1018 expressing *ATF6* encoding residues1-500Δ431-475 [72] was co-transfected with p912 and the *Renilla* normalization plasmid into WT and *ATF4*$^{-/-}$ MEF cells, and the ATF6 transcriptional activity with the co-transfection of ATF6-1-500Δ431-475 was determined. The activity of the *ATF6* gene promoter was measured by using a luciferase reporter assay. A DNA segment encoding -1500 to -1 bp relative to the transcriptional start site of the *ATF6* gene was amplified using the primers F5'-GGGACGCGTGCAAACGTGCAGCCTGGTCTGTATGTGGGTCCCC-3' and R5'-GGGCTCGAGCACCGCCCCGTGGCCTCCTGCCGCGCCCAGCCTTTCTAGG-3' , with the *Mlu1* and *Xho1* restriction sites underlined. The resulting PCR product was then digested and the DNA fragment was inserted using the *Mlu1* and *Xho1* restriction sites of the pGL3-basic vector (Promega), resulting in p1052. The plasmid p1052 was co-

transfected with the *Renilla* vector into, *ATF4*$^{-/-}$, and WT MEF cells and the ATF6 promoter activity was determined using the dual luciferase assay.

Table 2-2 Plasmids used in this study.

WB ID#	**Description**	**Source**
912	5X ATF6 in pGL3 luciferase. Contains 5 optimized ATF6 binding elements in tandem.	Prywes
984	pMDLg/pRRE Lenti (packaging) from Addgene 3rd generation plasmids, AmpR	Cornetta
985	pRSV-REV Lenti(packaging) from Addgene 3rd generation plasmids, AmpR	Cornetta
986	pVSV-G Lenti (envelope) from Addgene 3rd generation plasmids, AmpR	Cornetta
1015	pGL3 basic ATF5 promoter -3000bp AmpR	This study
1016	p3X Flag ATF6, AmpR	Prywes
1017	p3X Flag ATF6 (S1P-) S1P cleavage site point mutation that generates Nhe1 restriction site, AmpR	Prywes
1018	p3X Flag ATF6 1-500 (Δ431-475) deletion of BIP binding site, Also deletes lumenal cysteines. Also referred to as ATF6 constitutively active mutant (ATF6-CAM), AmpR	Prywes
1019	p3X Flag ATF6 1-500 (Δ431-475) S1P- deletion of BIP binding site and lumenal cysteines. Contains S1P point mutation generating unique Nhe1 site. Golgi localized. AmpR	Prywes
1027	pCMV-hATF5, AmpR	Kirk
1048	pGL3 basic luciferase reporter, AmpR	Promega
1052	pGL3 basic with -1500 to -1 of the ATF6 promoter by Mlu1/Xho1, AmpR	This study
1006	hCHOP, AmpR	Kilberg
1084	pLKO.1 scramble shRNA, AmpR	Quilliam
1142	shRNA hCHOP TRC identifier (last 2-digits) #28, AmpR	Sigma-Aldrich
1143	shRNA hCHOP TRC identifier (last 2-digits) #63, AmpR	Sigma-Aldrich

1144	shRNA hCHOP TRC identifier last (2-digits) #64, AmpR	Sigma-Aldrich
1145	shRNA hCHOP TRC identifier (last 2-digits) #65, AmpR	Sigma-Aldrich
1146	shRNA hCHOP TRC identifier (last 2-digits) #67, AmpR	Sigma-Aldrich
1147	shRNA mNOXA TRC identifier (last 2-digits) #06, AmpR	Sigma-Aldrich
1148	shRNA mNOXA TRC identifier (last 2-digits) #07, AmpR	Sigma-Aldrich
1149	shRNA mNOXA TRC identifier (last 2-digits) #08, AmpR	Sigma-Aldrich
1150	shRNA mNOXA TRC identifier (last 2-digits) #16, AmpR	Sigma-Aldrich
1151	shRNA mNOXA TRC identifier (last 2-digits) #57, AmpR	Sigma-Aldrich
1160	shRNA mATF5 TRC identifier (last 2-digits) #49, AmpR	Sigma-Aldrich
1161	shRNA mATF5 TRC identifier (last 2-digits) #46, AmpR	Sigma-Aldrich
1162	shRNA mATF5 TRC identifier (last 2-digits) #57, AmpR	Sigma-Aldrich
1163	shRNA mATF5 TRC identifier (last 2-digits) #70, AmpR	Sigma-Aldrich
1164	shRNA mATF5 TRC identifier (last 2-digits) #82, AmpR	Sigma-Aldrich

2.10 Statistics

Data were analyzed using two-way analysis of variance to assess the main and interaction effects, with drug, and genotype as the independent variables (StatSoft, Tulsa, OK). When a significant overall effect was detected, differences among treatment groups were assessed with Duncan's Multiple Range post-hoc test. The level of significance was set at $p<0.05$ for all statistical tests.

2.11 Lentivirus shRNA knockdown

The protocol for Lentivirus particle preparation from Addgene 3rd generation series of plasmids was used in conjunction with the validated mission shRNA TRC clones (Sigma) for generating lentivirus particles. Briefly, three viral plasmids WB984, WB985, WB986, encoding packaging and envelope components, and one shRNA plasmid were co-transfected into HEK293T cells using Fugene 6 as a transfection reagent. The following day media was removed and replaced with fresh growth media containing 25 mM HEPES. Lentivirus containing media was collected and subject to centrifugation at 3,000 x g. WT MEF cells or Hepa1-6 cells were transduced by replacing growth media with lentivirus containing media and the following day media was replaced with puromycin (10 μg/ml) containing media. Cells were selected in the presence of puromycin until there were no surviving cells on the non-transduced plate. The shRNA expressing cells were then expanded and used for experiments.

2.12 Chromatin immunoprecipitation

ChIP assay was performed essentially as described in a previous publication (Chen et al., 2004) with the following minor modifications. About 5~10 X 10^6 immortalized mouse embryonic fibroblasts (MEF) were used per treatment. Cells were cultured in Dulbecco's modified Eagle's medium (DMEM), pH 7.4 (Mediatech, Herndon, VA) supplemented with 1 X nonessential amino acids, 2 mM glutamine, 100 mg/ml streptomycin sulfate, 100 U/ml penicillin G, 0.25 mg/ml amphotericin B, 10% (vol/vol) fetal bovine serum (FBS), and 1μM 2-Mercaptoethanol (#21985-023, Invitrogen, Carlsbad, CA) and maintained at 37°C in an atmosphere of 5% CO_2 and 95%

air. The cells were cultured to ~60-70% confluence so that the cells were still in a growth phase during the experiment. At 12 to 16 h before initiation of treatment, cells were given fresh medium and serum to ensure that no nutrient deprivation took place before the start of experimental incubations. To elicit the desired stress, cells were replenished with the medium containing 2 μM tunicamycin, 1 μM thapasgargin, or 1 μM MG132 for 12 hours. To fragment the chromatin, isolated nuclei were resuspended in 1 ml lysis buffer and sonicated for 2 times with the Fisher model 100 sonicator power level at 15 watts. Antibodies used in the ChIP assays include rabbit anti-ATF4 polyclonal (custom made by Cocalico Biotechnology Inc., Reamstown, PA), rabbit anti-GADD153 (CHOP) polyclonal antibody (Santa Cruz, CA, sc-575), and normal rabbit IgG (Santa Cruz, CA, sc-2027) was purchased from Santa Cruz Biotechnology, Inc. DNA enrichment was analyzed with RT-qPCR with a DNA Engine Opticon 3 system (Bio-Rad) and detection with SYBR Green. The reaction mixtures contained 2 μl purified DNA, 10 μl of SYBR Green master mixture and 5 pmol of forward and reverse primers in a total volume of 20 μl. Samples were incubated at 95°C for 15 min, followed by amplification at 95°C for 15 s and 60°C for 60 s for 35 cycles. All experiments were performed in triplicate. The result was described as the ratio to a partial of total input DNA.

2.13 Cell survival assays

The CellTiter 96 Non-Radioactive Cell Proliferation Assay (Promega G4001) is a colormetric assay the ability of living cells to convert a tetrazolium salt [3-(4,5-dimethylthiazol-2-yl)-2,5-diphenyltetrazolium bromide] in the dye solution into a colored formazan product. This assay was used to determine cell viability in response to different

stress arrangements. The assay was performed in a 96 well plate format and measurements of formazan product were carried out using a plate reader at an absorbance of 570 nm. 5,000 cells were plated per well in a 0.1 ml volume of DMEM supplemented with 10% FBS, 1 mM non-essential amino acids, 100 units/ml penicillin, and 100 µg/ml streptomycin. After an overnight incubation, cells were cultured in the presence of 1 µM MG132 for 1, 3, 6, 12, or 18 hours, or no treatment. Alternatively cells were incubated in the presence of 2-fold dilutions of 1 µM MG132 for 24 hours. At the indicated time, the media containing the stress agent was removed by gentle aspiration with 0.5-10 µl pipet tips, and cells were then washed with warm media prior to incubation in DMEM in the absence of stress for a total of 24 hours from the beginning time of the stress treatment. For example, cells treated with MG132 for 1 hour, were washed and then cultured in the absence of this stress agent for 23 hours. After the 24 hour period, 15 µl of the dye solution was added to a final volume of 115 µl, and then incubated with the cells for 4 hours, followed by the addition of 100 µl solubilization solution, as described by the manufacturer's protocol. The formazan crystals were verified to be completely solubilized by inspection under the microscope and the absorbance of the solution was measured at 570 nm using a Spectra Max 340 96-well plate reader (Molecular Devices, Sunnyvale, CA).

CHAPTER 3. RESULTS: THE ISR IS REQUIRED FOR ATF6 ACTIVATION

3.1 Loss of *PERK* disrupts the UPR and renders the liver susceptible to ER stress

To address the role of *PERK* in the UPR in liver, mice were bred with a liver-specific knockout of *PERK* (LsPERK-KO). LsPERK-KO mice were produced by deletion of floxed $PERK^{fl/fl}$ using *cre* expression driven by the liver-specific albumin promoter, as described previously [49, 85]. Consistent with *PERK* depletion from the liver, there was significantly reduced eIF2~P following 6 hours of injection with tunicamycin (1 mg/kg), a potent ER stress agent that blocks N-glycosylation of proteins (Figure 3-1, A and B). Disruption of eIF2~P in the LsPERK-KO livers was also observed following 24 and 36 hour treatments with tunicamycin. In addition to translational expression of *ATF4*, induced eIF2~P enhances the transcription of *ATF4* and its target gene *CHOP*, and the levels of both mRNAs were sharply reduced in the LsPERK-KO mice during ER stress (Figure 3-1C). Expression of *CREB-H*, which has been previously linked to the UPR [100], was unchanged during the treatment with tunicamycin. Accompanying this block in PERK activity and downstream gene expression, livers for the LsPERK-KO mice displayed substantial Oil red O staining, indicating the presence of fat deposits in response to 12 hours tunicamycin treatment (Figure 3-2A). This staining was significantly reduced in the wild type (WT) mice. Triglycerides were also increased in livers of the LsPERK-KO mice treated with tunicamycin as compared to the WT (Figure 3-2B). After 24 hours of the ER stress, increased TUNEL staining of hepatocytes in *PERK*-deficient mice, indicated enhanced apoptosis in the liver (Figure 3-2, C and D). This was accompanied by elevated cleavage of caspase-3 in the LsPERK-KO livers (Figure 3-2E). As expected, induction of CHOP

protein in response to ER stress was substantially diminished in the LsPERK-KO livers, consistent with the idea that activation of the ISR was blocked as illustrated by the lowered levels of eIF2α~P. Interestingly, the mRNA and protein levels of the ER chaperone BiP were also substantially reduced with loss of *PERK* function, with only modest levels of BiP protein in the LsPERK-KO liver samples following 36 hours of tunicamycin treatment (Figures 3-1C and 2E). These results suggest that PERK deficiency blocks induction of eIF2~P and the translational control arm of the UPR, which leads to disruption of liver homeostasis and increased apoptosis during ER stress.

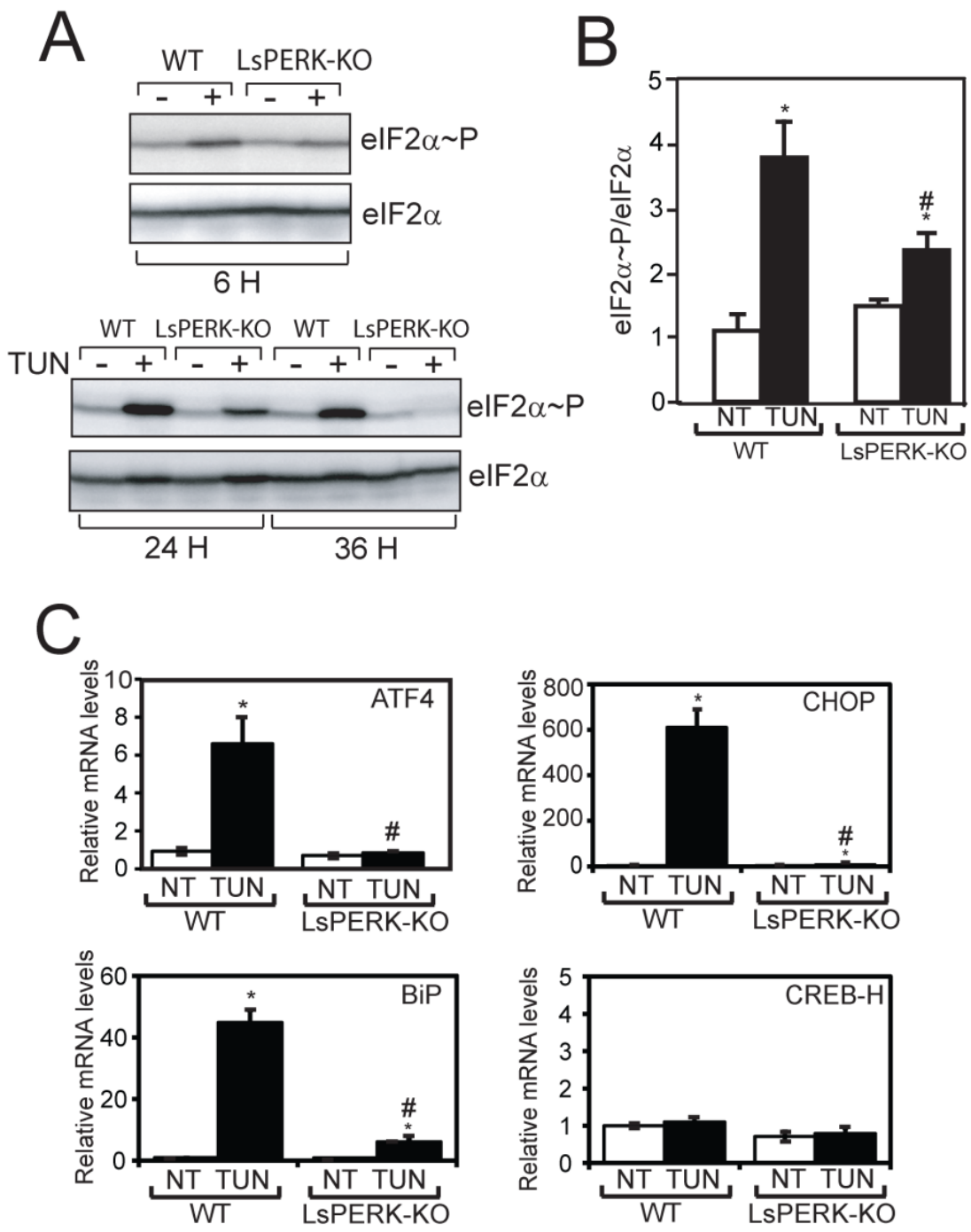

Figure 3-1 Liver-specific knockout of *PERK* reduces eIF2~P and the ISR in response to tunicamycin treatment. (A) WT and LsPERK-KO mice were injected

intraperitoneally with tunicamycin (TUN), and following 6, 24, or 36 hours of exposure to this ER stress agent, the levels of eIF2~P and total eIF2 in livers were measured by immunoblot analyses. The "+" indicates treatment with tunicamycin, and the "-" indicates injection with only excipient. Results shown in each panel are representative of at least three independent experiments. (B) Quantification of the levels of total and phosphorylated eIF2 in the WT and LsPERK-KO livers following 6 hours of treatment with tunicamycin (TUN) or with excipient (NT, no treatment). (C) The levels of *ATF4*, *CHOP*, *BiP* and *CREB-H* mRNAs in the WT and LsPERK-KO livers exposed to tunicamycin for 6 hours, or to no treatment, were measured by quantitative PCR. "*" indicates statistically significant differences ($p<0.05$) between the levels of tunicamycin treated (TUN) and no treatment (NT) samples; "#" indicates statistically significant differences ($p<0.05$) between WT and LsPERK-KO mice. The error bar represents the S.E.M.

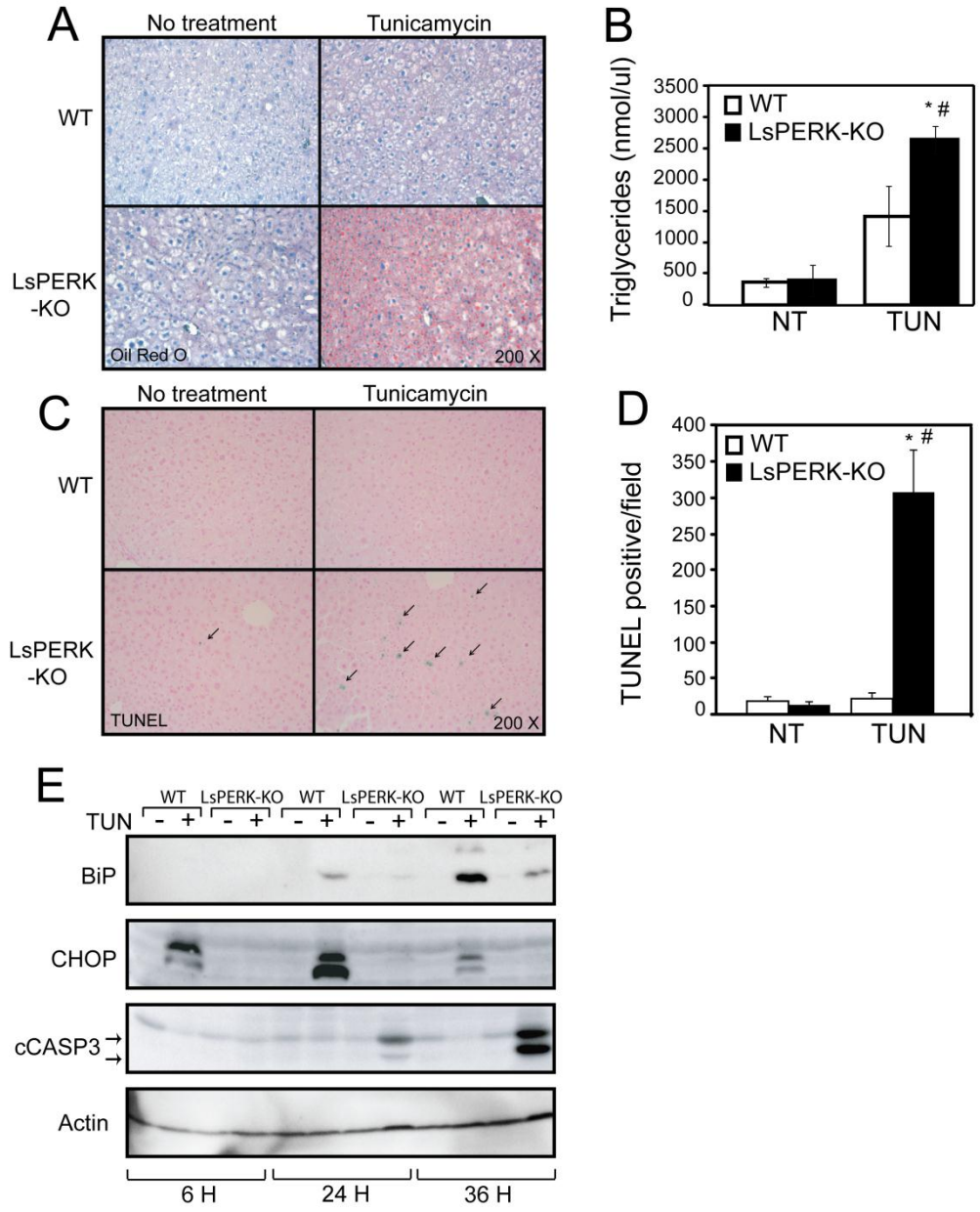

Figure 3-2 Loss of *PERK* enhances liver apoptosis in response to ER stress. (A) WT and LsPERK-KO mice were injected intraperitoneally with tunicamycin or excipient (NT, no treatment). Following 12 hours of exposure to the ER stress agent, a histological analysis of the livers was carried out using Oil Red O stain to visualize triglycerides, and liver sections were counter stained with hematoxillin. (B) Quantification of triglyceride levels in WT and LsPERK-KO liver samples following treatment with tunicamycin

(TUN) or vehicle control (NT). (C) WT and LsPERK-KO mice were treated with tunicamycin for 24 hours and a TUNEL analysis was carried out on liver histological sections, with the arrows indicating TUNEL-positive cells in a representative field. (D) Quantification of the TUNEL-positive levels in WT and LsPERK-KO livers following the treatment with tunicamycin (TUN) or with no treatment (NT). The error bar represents the S.E.M., and the "*" indicates statistically significant differences ($p<0.05$) between the tunicamycin treated and no treatment samples; "#" indicates statistically significant differences ($p<0.05$) between WT and LsPERK-KO mice. (E) WT and LsPERK-KO mice were treated with tunicamycin (+) or vehicle only (-) for 6, 24, or 36 hours and the levels of BiP, CHOP, and cleaved caspase-3 in liver lysates were measured by immunoblot analysis.

3.2 Loss of *PERK* in liver blocks activation of the UPR transcriptome

An analysis of gene expression changes in the LsPERK-KO mice indicated that there was significantly diminished induction of *BiP* expression in response to ER stress. This suggested that in the liver, PERK normally enhances the expression of key ER chaperones, a function previously ascribed to ATF6 and IRE1/XBP1 [3, 4, 36, 101]. To investigate changes in UPR genes which require *PERK*, total RNA was isolated from WT and LsPERK-KO livers and analyzed by Affymetrix microarrays. In WT livers, 9,645 probe sets were significantly changed by tunicamycin treatment, with nearly 50% of these being induced by 2.0-fold or greater (Table 3-1; $p \leq 0.05$, fdr ≤ 0.15). A comparison between the induction ratios (stress/control) for the ER stress-induced genes in the WT versus the *PERK*-deficient livers indicated that 63% (4599/7324) displayed a significantly lower induction ratio in the LsPERK-KO mice. Furthermore, among those genes enhanced ≥2-fold by tunicamycin treatment, 74% (3523/4737) showed a requirement for *PERK* for full induction in response to ER stress (Table 1). These finding are illustrated in Figure 3-3A, which features a comparative analysis between the stress-induced transcriptome changes in WT (x-axis) versus LsPERK-KO (y-axis). The *PERK* requirement for changes in the UPR transcriptome is supported by the large number of probe sets which were increased in the WT livers upon ER stress, but lie below the diagonal where y=x.

Table 3-1 PERK facilitates expression of a large number of UPR target genes.

		Fold Change (Treated/Untreated)[a]			
Dependence	Total	> 1.0	≥ 2.0	< 1.0	≤ 0.5
WT	9645[b]	7324	4737	2321	797
PERK-dep	4948[c]	4599	3523	349	190

[a] Expression profile summary of gene transcripts, as defined by probe set, that were significantly changed after treatment with tunicamycin (1mg/kg). The number of induced genes are shown for both the >1.0 fold and ≥2.0 fold thresholds. The repressed genes are also shown for the < 1.0 and < 0.5 fold thresholds
[b] The total number of transcripts significantly changed ($p \leq 0.05$) by ER stress.
[c] The number of PERK-dependent transcripts that were significantly changed by ER stress.

These results indicate that PERK is a major participant in the transcriptional phase of the UPR, with a majority of activated genes requiring PERK function for full induction. As expected, these PERK-dependent genes included canonical ISR target genes such as *ATF4*, *CHOP*, *GADD34*, *ATF3*, and *TRIB3* (Figure 3-3B). However, many UPR target genes also required PERK for full induction in response to tunicamycin treatment, including those involved in protein folding and ERAD (Figure 3-3C). To address the apparent overlap between PERK and ATF6 transcriptional target genes, we compared a previously reported microarray characterization of livers from *ATF6* knockout mice treated with tunicamycin with our LsPERK-KO dataset [17]. A total of 2,487 genes were significantly induced by ER stress in both datasets, with 39% (969/2,487) of these requiring ATF6 for full induction (Figure 3-3D). Importantly, among these ATF6-target genes, 69% (671/969) were also dependent on PERK for full induction. We conclude that PERK facilitates not only the expression of the ISR genes, but also a majority of the UPR genes, including those targeted by ATF6.

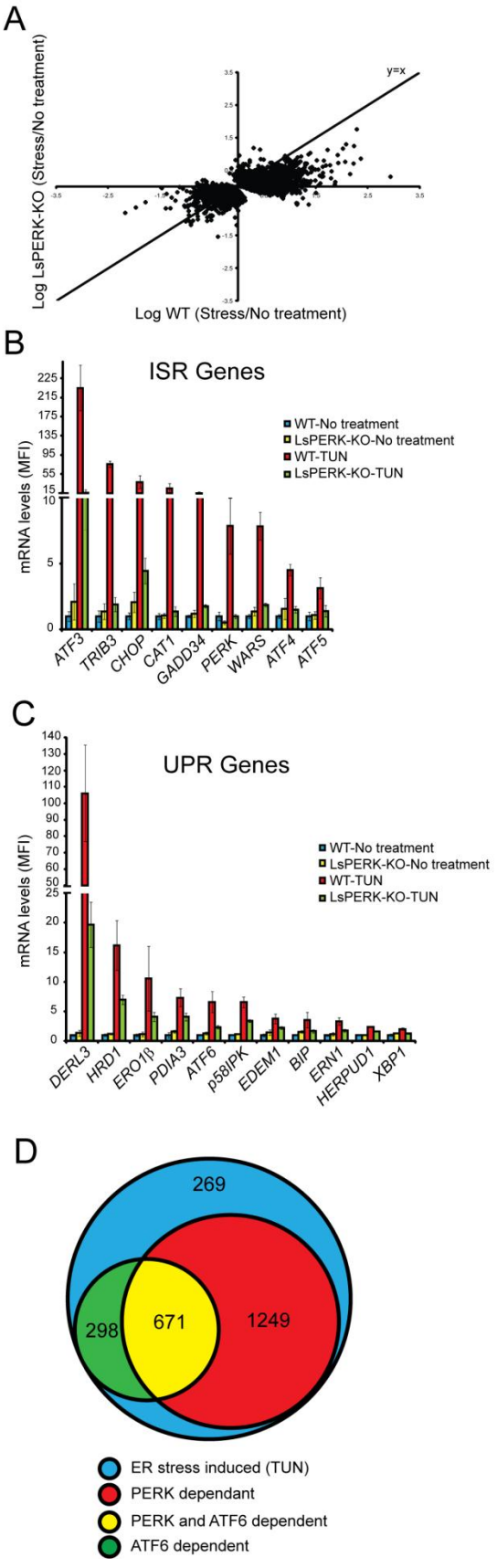
A
y=x
Log LsPERK-KO (Stress/No treatment)
Log WT (Stress/No treatment)
B
ISR Genes
mRNA levels (MFI)
WT-No treatment
LsPERK-KO-No treatment
WT-TUN
LsPERK-KO-TUN
ATF3
TRIB3
CHOP
CAT1
GADD34
PERK
WARS
ATF4
ATF5
C
UPR Genes
mRNA levels (MFI)
WT-No treatment
LsPERK-KO-No treatment
WT-TUN
LsPERK-KO-TUN
DERL3
HRD1
ERO1β
PDIA3
ATF6
p58IPK
EDEM1
BIP
ERN1
HERPUD1
XBP1
D
269
298
671
1249
ER stress induced (TUN)
PERK dependant
PERK and ATF6 dependent
ATF6 dependent

Figure 3-3 PERK is required for full induction of a majority of the UPR-targeted genes. (A) The scatter plot is the log ratio of stressed vs no stress for WT (x-axis) and LsPERK-KO (y-axis). This comparative analysis of gene transcripts induced or repressed by ER stress in the livers of WT mice and LsPERK-KO mice displays all significant probe sets ($p<0.05$) following treatment with 2 μM tunicamycin for 6 hours. Microarray measurements of gene transcripts targeted by the ISR (B) and the UPR (C) shown as mean fluorescent intensity (MFI) for each transcript is shown as a histogram, along with the S.D. Each of these representative genes showed a significant induction in response to ER stress that was dependent on *PERK* ($p\leq0.05$, fdr≤0.15). (D) Comparative analysis of genes induced by tunicamycin in mice livers. The LsPERK-KO microarray analysis described here was compared with microarray measurements derived from *ATF6* liver-specific knockout mice as reported by Rutkowski et al [17]. Genes significantly induced by ≥ 2-fold were plotted by the Venn diagrams. Shown here are genes induced by tunicamycin in liver that were present in both microarray datasets (Blue), with ATF6-dependent genes (Green), PERK-dependent genes (Red), and PERK and ATF6-dependent genes (Yellow).

Turnover of a large number of gene transcripts is enhanced in response to ER stress [6, 7]. There were 2,321 gene transcripts that were significantly reduced in WT livers upon tunicamycin treatment, with 797 being lowered by at least 2-fold (Table 3-1). PERK contributed to 24% of those genes repressed by 2-fold or greater (190/797). This is illustrated in Figure 3-3A, with the repressed transcripts in WT livers (x-axis) lying above the y=x diagonal. Turnover of a large number of mRNAs is known to be enhanced in response to ER stress, and the endoribonuclease activity of IRE1 is thought to facilitate the decay of many of these mRNAs [6, 7]. These results suggest that PERK is also a significant contributor to the repression of the transcriptome in response to ER stress.

3.3 PERK facilitates activation of ATF6 in response to ER stress

Our microarray analysis suggested that both *ATF6* and *XBP1* mRNA expression were substantially diminished in LsPERK-KO mice subjected to tunicamycin treatment compared to WT, results that were confirmed by qPCR measurements (Figures 3-3C and 3-4A). These findings support the idea that PERK can facilitate activation of the UPR transcriptome by contributing to the activation of ATF6 and XBP1 during ER stress. While loss of *PERK* lowered the total levels of *XBP1* mRNA, and as a consequence the amount of spliced *XBP1* mRNA in response to ER stress, the ratio of spliced/total *XBP1* transcript was unchanged between the LsPERK-KO and WT mice (Figure 3-4A). This suggests that within this timeframe of ER stress, IRE1 endoribonuclease activity for *XBP1* mRNA cleavage is not significantly altered by loss of PERK function.

Given the larger than expected role for PERK in UPR-directed gene expression, we next addressed whether loss of this eIF2 kinase could adversely affect the activation

of ATF6 in response to ER stress. Consistent with our previous results, PERK deficiency significantly reduced eIF2~P following 6 hours of tunicamycin treatment (Figure 3-4B). Immunoblot analyses comparing the levels of the full-length (ATF6-FL/G) and processed ATF6(N) protein in WT and LsPERK-KO indicated that activation of ATF6 was dramatically reduced with loss of PERK function (Figure 3-4B). Following treatment of the WT mice with tunicamycin, there was accumulation of unglycosylated full-length ATF6 (ATF6-FL/UG), along with the proteolytically cleaved and activated ATF6(N). Cleavage of ATF6 was dependent on *PERK* following 6 hours of ER stress. We note that the size of the ATF6(N) protein is consistent with that determined using an *ATF6* expression plasmid encoding residues 1-373 (HA-ATF6-1-373) transfected into cultured mouse embryonic fibroblasts (MEF) (Figure 3-5). Furthermore, ATF6 was reported to be glycosylated at multiple sites [102], and as described below, the ATF6-FL/UG was detected in MEF cells treated with tunicamycin, but not detected in response to thapsigargin, another well-characterized ER stress agent that does not directly inhibit protein glycosylation [4, 102]. These results indicate that PERK facilitates activation of ATF6 in response to ER stress, providing an important rationale for why loss of *PERK* has such a broad impact on the UPR transcriptome.

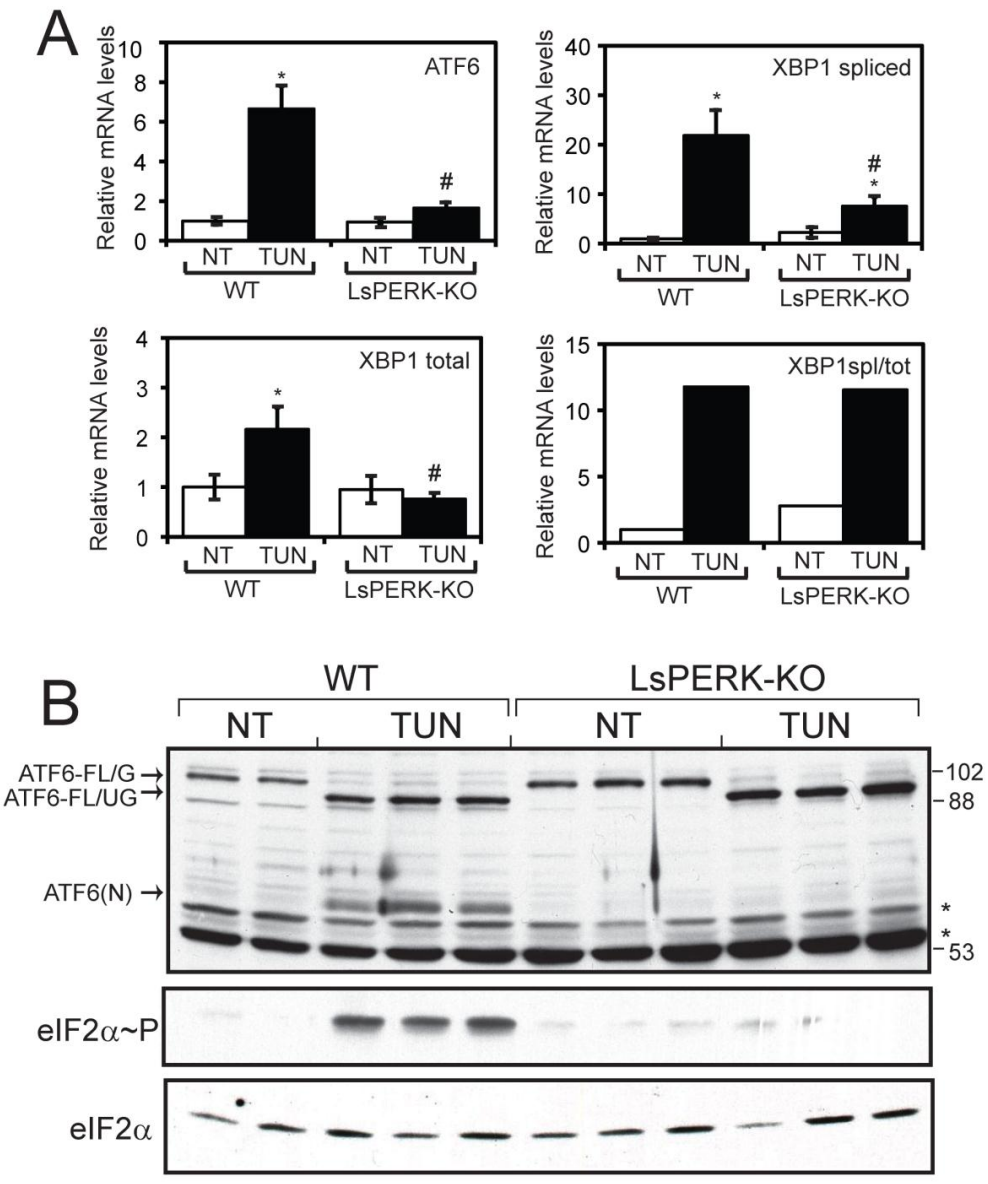

Figure 3-4 PERK facilitates activation of ATF6 in the liver following tunicamycin treatment. (A) WT and LsPERK-KO mice were treated with tunicamycin (TUN) or excipient (NT, no treatment) for 6 hours and the levels of *ATF6*, *XBP1*, and spliced *XBP1* mRNA were measured by quantitative PCR. The ratio of spliced *XBP1* mRNA versus total *XBP1* transcripts was also determined (XBP1spl/XBP1tot). The error bar represents the S.D., and the "*" indicates statistically significant differences (p<0.05) between

tunicamycin treatment and non ER stress. The "#" symbol indicates significant differences ($p<0.05$) between the WT and LsPERK-KO livers. (B) Activation of ATF6 was measured by immunoblot analysis using whole cell lysates prepared from WT and LsPERK-KO livers following tunicamycin treatment for 6 hours or no treatment (NT) control. The arrows indicate full-length glycosylated ATF6 (ATF6-FL/G), full-length unglycosylated (ATF6-FL/UG), and the cleaved ATF6(N) proteins. Two or three different liver samples are shown for each treatment group in the immunoblot panels. The position of the molecular weight standards (KDal) in the SDS-PAGE are shown to the right of the panel, and "*" designations indicate proteins that cross-react with the antibody prepared against recombinant ATF6 protein. Additionally, the levels of eIF2~P and total eIF2 were measured by immunoblot analyses using antibodies specific to each version of this translation initiation factor.

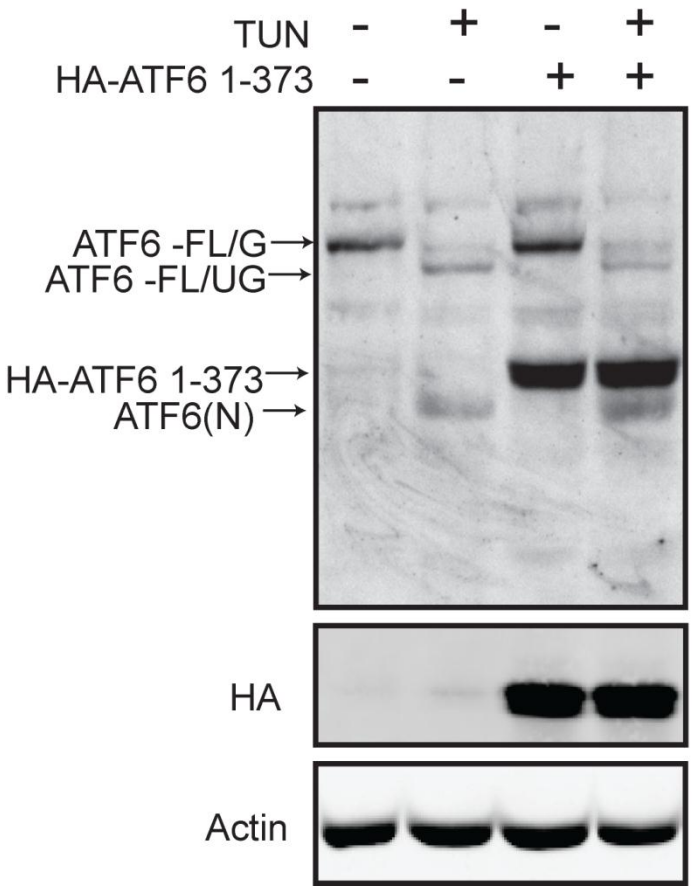

Figure 3-5 ATF6 antibody detects endogenous and over-expressed ATF6 in MEF cells. WT MEF cells were transfected with an HA-tagged ATF6 expression plasmid encoding residues 1-373 (+), or no expression plasmid (-). Cells were then treated (+) for 3 hours with 2 μM tunicamycin, or left untreated (-). Cell lysates were prepared and analyzed by immunoblot using antibody that recognizes ATF6, the HA tag, or actin.

We next addressed whether PERK also facilitates activation of ATF6 in cultured MEF cells exposed to ER stress agents. WT MEF cells were treated with tunicamycin, thapsigargin, or DTT for up to 6 hours and ATF6 levels were measured by immunoblot analyses. Consistent with our liver analysis, we found that tunicamycin triggered accumulation of the cleaved ATF6(N), initiating at 1 hour of treatment and continuing through the 6 hour regimen (Figure 3-7A). Accumulation of ATF6(N) coincided with the induction of ATF4 expression, which was readily detected following 2 hours of the ER stress. During the time course of tunicamycin exposure, there was also a gradual decrease of ATF6-FL/G coincident with increasing ATF6-FL/UG. The ATF6-FL/UG is suggested to represent ATF6 that is newly synthesized during ER stress, as the addition of cycloheximide, a potent inhibitor of protein synthesis, along with tunicamycin resulted in minimal detection of ATF6-FL/UG (Figure 3-7B). Thapsigargin treatment also triggered accumulation of ATF6(N); however in this case there was no detectable ATF6-FL/UG (Figure 3-7A). As a consequence we did not detect measureable reduction of ATF6-FL/G during the time course of thapsigarin treatment, as the synthesis of ATF6 is sufficient to replace that being processed into the activated ATF6(N). Treatment with DTT resulted in rapid processing of ATF6 that exceeded the rate of protein synthesis resulting in no detectable ATF6-FL/G at the early time points (1 and 2 hours). However, this ATF6 synthesis was partially recovered at the later time points (3-6 hours).

Similar ER stress treatments of *PERK*$^{-/-}$ MEF cells revealed a substantial reduction of ATF6(N) after 6 hours of tunicamycin or thapsigargin exposure, although there was some cleaved ATF6(N) product at the earlier time points (Figure 3-7, C and D). *A/A* MEF cells expressing eIF2 containing alanine substituted for the phosphorylation

residue, serine-51, also showed reduced ATF6(N) levels following tunicamycin or thapsigargin treatments (Figure 3-8, A and B). This was most apparent after 6 hours of ER stress, with minimal detectable ATF6(N) in the mutant cells devoid of eIF2~P. It is noted that some ATF6(N) was detected in the *A/A* cells at earlier exposure times to tunicamycin or thapsigargin. As expected, induced eIF2~P levels were significantly reduced in the *PERK*$^{-/-}$ cells in response to these ER stress conditions, and eIF2 α ~P was absent in the *A/*A cells (Figures 3-6C, 3-6D, 3-7A, and 3-7B). These results indicate that PERK mediated eIF2~P is required for full activation of ATF6 in response to different ER stress conditions both *in vivo* and in cultured cells.

To determine if reduced ATF6(N) protein in *PERK*$^{-/-}$ and *A/A* MEF cells also resulted in lowered ATF6 transcriptional activity, we used an ATF6 sensitive luciferase reporter expressed from a promoter containing five optimized UPREs [99]. This reporter system is potently induced by ATF6, although it is noted that that XBP1 has also been shown to contribute to activation of the UPRE based promoters [36]. WT cells transfected with this reporter plasmid showed about a 12-fold increase in ATF6 transcriptional activity after 6 hours of tunicamycin treatment (Figure 3-8C). By comparison, ATF6 activity was lowered by over 50% in the *PERK*$^{-/-}$ and *A/A* mutant cells during ER stress. Collectively, these results indicate that disruption of PERK phosphorylation of eIF2 reduces both ATF6 proteolysis and transcriptional activity.

3.4 ATF4 is required for activation of ATF6

Because PERK facilitates eIF2~P leading to the preferential translation of *ATF4*, we next sought to determine if *ATF4* was required for ATF6 activation in response to ER

stress. In response to thapsigargin, there was a significant reduction of ATF6(N) in the *ATF4*$^{-/-}$ MEF cells, and ATF6-FL/G was substantially reduced by 6 hours of treatment (Figure 3-7D). We also addressed the role of ATF4 in the activation of ATF6 in response to up to 8 hours of tunicamycin treatment (Figure 3-8E). In the absence of stress (0 hours) there was a greater than 40% reduction of ATF6-FL/G in *ATF4*$^{-/-}$ MEF cells when compared to the WT control. Thus in both thapsigargin and tunicamycin treatments, there was minimal accumulation of ATF6(N) in *ATF4*$^{-/-}$ MEF cells. Following the time course, we also found that in WT MEF cells there was a greater rate of reduction of ATF6-FL/G, and as a consequence more accumulation of active ATF6(N), when compared to *ATF4*$^{-/-}$ MEF cells (Figure 3-8E). Furthermore, the accumulation of the newly synthesized ATF6-FL/UG required to replenish ATF6 protein levels was delayed in *ATF4*$^{-/-}$ cells during the exposure to tunicamycin (Figure 3-8E).

The next question addressed was whether preconditioning of the ISR and induction of ATF4 could restore ATF6 activation in *PERK*$^{-/-}$ MEF cells treated with ER stress (Figure 3-8F). For this experiment, induction of ATF4 was achieved by treating *PERK*$^{-/-}$ MEF cells with a derivative of salubrinal (Sal003), which is an inhibitor of the PP1c regulatory subunits, CReP and GADD34, that are required for eIF2~P dephosphorylation [57]. The Sal003 treatment for 1 hour prior to adding the ER stress agent tunicamycin resulted in ATF4 protein levels that were sustained in *PERK*$^{-/-}$ cells during the ER stress time course. Induction of ATF4 expression in *PERK*$^{-/-}$ cells with this treatment regimen also rescued the processing of ATF6, supporting the idea that eIF2~P and ATF4 are required for ATF6 activation (Figure 3-8F). These results indicate that the ATF4 transcription factor is also central to activation of ATF6 in response to

different ER stress conditions. Further supporting this finding, loss of *ATF4* resulted in significantly reduced ATF6 transcriptional activity upon ER stress, as measured by the luciferase reporter plasmid containing the optimized ATF6-binding sites (Figure 3-8C).

We considered three models to explain the underlying mechanisms by which the PERK/eIF2~P/ATF4 pathway facilitates ATF6 activation, and it is noted that these ideas are not mutually exclusive. The first is the Stability model, in which the PERK pathway facilitates stabilization of ATF6(N), thus contributing to enhanced levels of this activated form of ATF6. The second is the Synthesis model, which posits that ATF4 enhances *ATF6* expression, therefore increasing the amount of full-length ATF6 entering into the secretory pathway for processing in the Golgi. Lastly, the Trafficking model, focuses on ER to Golgi transport and suggests that the PERK/eIF2~P/ATF4 pathway is important for key features of ATF6 anterograde transport to the Golgi for cleavage by S1P and S2P. These models of, Stability, Synthesis, and Trafficking, are depicted in Figure 3-6 and will be experimentally addressed below.

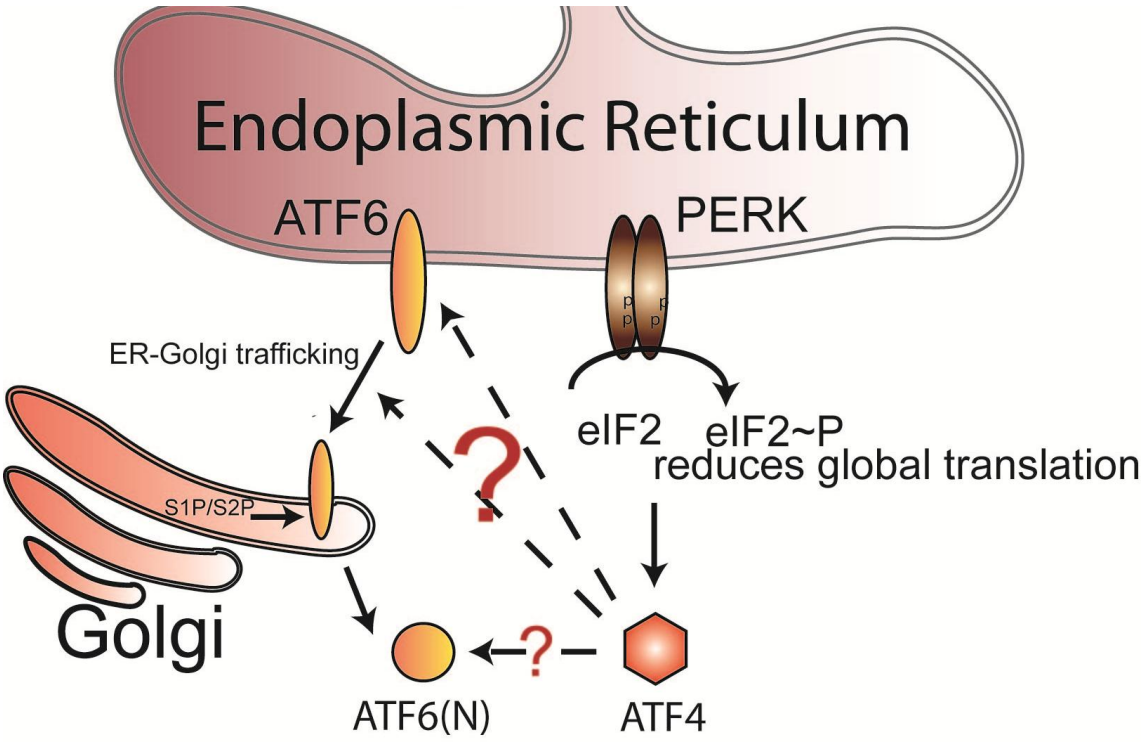

Figure 3-6 Model for the ISR requirement in the activation of ATF6. The PERK/eIF2~P/ATF4 pathway is proposed to be required for the synthesis, ER-Golgi trafficking, and/or stability of ATF6. These three possible models are depicted with red "?" marks and dashed arrows. These models will be tested empirically in this thesis.

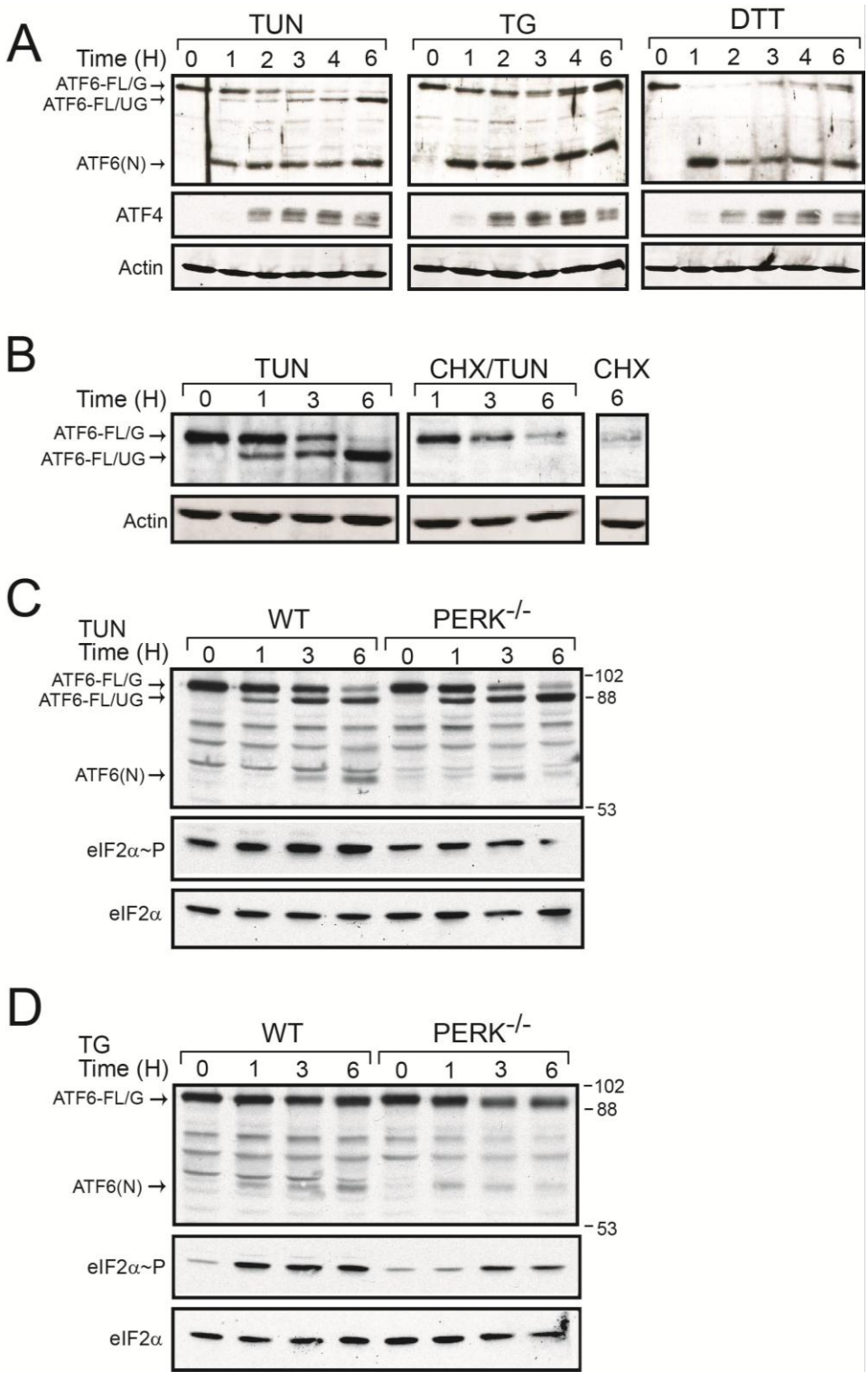

Figure 3-7 PERK is required for full activation of ATF6 in MEF cells in response to different ER stress conditions. (A) WT MEF cells were treated with 2 μM tunicamycin

(TUN), 1 μM thapsigargin (TG) or for between 1 and 6 hours, as indicated, or with no stress treatment (0). Equal amounts of the protein lysates prepared from the cultured cells were separated by SDS-PAGE, and the levels of ATF6, ATF4, and actin were measured by immunoblot analysis. The arrows indicate the glycosylated (ATF6-FL/G) and unglycosylated (ATF6-FL/UG) versions of full-length ATF6, and the cleaved ATF6(N) proteins. (B) WT MEF cells were treated with 2 μM tunicamycin (TUN), tunicamycin and 50 μg/ml cycloheximide (TUN/CHX), or cycloheximide alone (CHX) for up to 6 hours as indicated. The levels of ATF6-FL/G, ATF6-FL/UG, and actin were measured by immunoblot analysis. (C and D) WT and *PERK*$^{-/-}$ MEF cells were treated with tunicamycin (TUN) or thapsigargin (TG) for up to 6 hours, and the levels of ATF6, eIF2~P, and total eIF2 were measured by immunoblot. The position of the molecular weight standards (kDa) are shown to the right of the ATF6 panel.

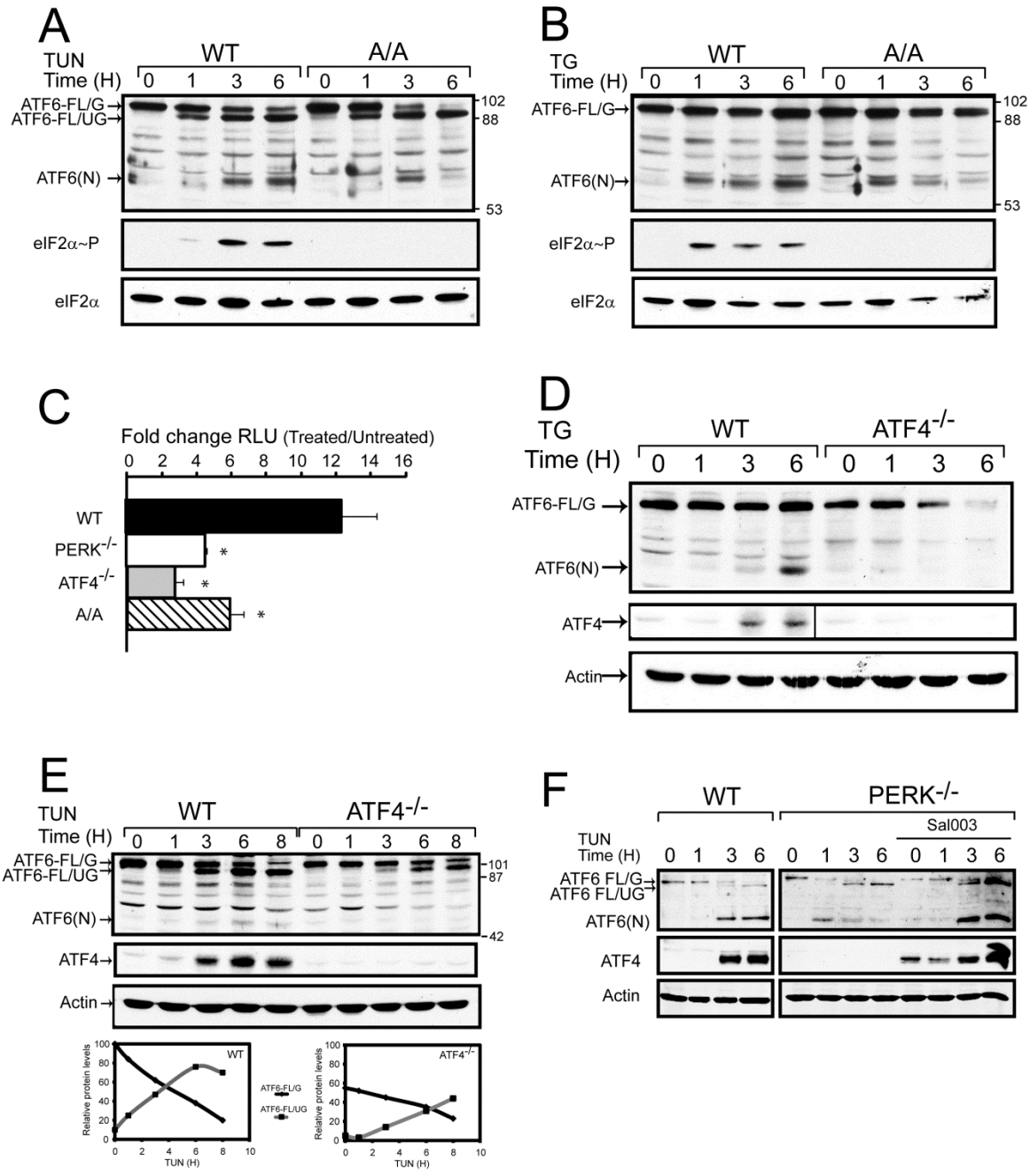
A
TUN
Time (H)
WT
A/A
0 1 3 6 0 1 3 6
ATF6-FL/G
ATF6-FL/UG
ATF6(N)
102
88
53
eIF2α~P
eIF2α
B
TG
Time (H)
WT
A/A
0 1 3 6 0 1 3 6
ATF6-FL/G
ATF6(N)
102
88
53
eIF2α~P
eIF2α
C
Fold change RLU (Treated/Untreated)
0 2 4 6 8 10 12 14 16
WT
PERK-/-
ATF4-/-
A/A
*
*
*
D
TG
Time (H)
WT
ATF4-/-
0 1 3 6 0 1 3 6
ATF6-FL/G
ATF6(N)
ATF4
Actin
E
TUN
Time (H)
WT
ATF4-/-
0 1 3 6 8 0 1 3 6 8
ATF6-FL/G
ATF6-FL/UG
ATF6(N)
101
87
42
ATF4
Actin
Relative protein levels
WT
ATF4-/-
ATF6-FL/G
ATF6-FL/UG
TUN (H)
F
WT
PERK-/-
Sal003
TUN
Time (H)
0 1 3 6 0 1 3 6 0 1 3 6
ATF6 FL/G
ATF6 FL/UG
ATF6(N)
ATF4
Actin

Figure 3-8 Phosphorylation of eIF2 and ATF4 facilitate activation of ATF6 in response to ER stress. (A and B) WT and *A/A* MEF cells were treated with 2 μM tunicamycin (TUN) or 1 μM thapsigargin (TG) for between 1 and 6 hours, as indicated, or with no stress treatment (0). Equal amounts of the protein lysates prepared from the cultured cells were analyzed by immunoblot analysis using antibodies specific to ATF6, eIF2~P, and total eIF2. The arrows indicate full-length ATF6-FL/G and ATF6-FL/UG, and the cleaved ATF6(N) proteins. Molecular weight standards in kDal are shown to the right of the panels. (C) To measure ATF6 transcriptional activity, a firefly luciferase reporter with a promoter containing 5X ATF6-binding elements was co-transfected with a *Renilla* normalization plasmid into *PERK*$^{-/-}$, *ATF4*$^{-/-}$, *A/A*, and WT MEF cells. The transfected cells were treated with thapsigargin for 6 hours or no stress agent and the ATF6 transcriptional activity was measured by using a dual luciferase reporter assay. The values represent the fold-change in relative light units (RLU) after treatment with ER stress for each transfected cell type. The error bar represents the S.D. and the "*" indicates a significant (p<0.05) difference when compared to WT cells. (D) WT and *ATF4*$^{-/-}$ MEF cells from two independently derived cell lines were treated with thapsigargin (TG) and the levels of ATF6, ATF4, and actin were measured by immunoblot. (E) WT and *ATF4*$^{-/-}$ MEF cells were treated with tunicamycin (TUN) for up to 8 hours as indicated levels of ATF6, ATF4 and actin were measured by immunoblot. Panels are representative of three independent experiments. (F) Quantitative analysis of ATF6-FL/G and ATF6-FL/UG in WT and ATF4$^{-/-}$ MEF cells. This Figure shows three experimental replicates of WT and ATF4 treated with tunicamycin for up to 10 hours as indicated, levels of the ATF6-FL/G and ATF6-FL/UG proteins from the immunoblot

analysis were measured by densitometry. The graphs below indicate the fraction of ATF6 protein relative to the ATF6-FL/G in the untreated (0 hours) controls. Measurements from WT cells are shown as a solid black line (diamonds) and measurements for *ATF4*$^{-/-}$ cells are shown as a dotted line (open squares). (G) WT and *PERK*$^{-/-}$ MEF cells were treated with tunicamycin for up 6 hours, or no ER stress (0). Where indicated, Sal003 was added to the *PERK*$^{-/-}$ cells 1 hour prior to addition of tunicamycin. Sal003 was either 'removed' after 1 hour or 'left in' during the ER stress time course. Levels of ATF6, ATF4, and actin were measured by immunoblot.

3.5 Stability of ATF6 is independent of PERK and ATF4

The first model to be addressed concerns the role of the PERK pathway in the stabilization of ATF6. ATF6(N) is suggested to have a short half-life ($t_{1/2}$~ 1 hour) by a mechanism involving degradation through the ubiquitin/proteasome pathway [103]. Basic zipper (bZIP) transcription factors, such as ATF6 and ATF4, are often labile and have been shown to require partner proteins for stability [24, 104, 105]. We sought to determine if induction of the PERK/eIF2~P/ATF4 pathway stabilized ATF6(N). First, WT and *ATF4*$^{-/-}$ MEF cells were treated with tunicamycin in the presence or absence of MG132, a potent proteasome inhibitor [106]. Enhanced ATF6(N) levels were detected in both WT and *ATF4*$^{-/-}$ cells, although the total accumulation of ATF6(N) was significantly greater in WT cells (Figure 3-8A). This finding is consistent with the earlier report suggesting that ATF6 is subject to degradation by the proteasome pathway. It is also noted in these MEF cells that 6 hours of treatment with MG132 alone does not induce ER stress, as judged by accumulation of ATF6(N) and splicing of *XBP1* mRNA [107]. As a control, other ISR inducible transcription factors, ATF4 and CHOP, which are also short-lived [104, 105], showed similar increases when MG132 was combined with the tunicamycin treatment in WT cells. In the *ATF4*$^{-/-}$ cells, there was no detectable ATF4 transcription factor and its target CHOP showed some enhanced accumulation in the combined tunicamycin and MG132 treatments, although significantly less than that measured in WT cells. Consistent with our earlier experiments, there were also minimal detectable ATF6-FL/UG levels in the *ATF4*$^{-/-}$ cells in response to tunicamycin treatment in the presence or absence of MG132 (Figure 3-8A). This finding suggests that ATF4

contributes to the synthesis of ATF6 in response to ER stress, an idea that will be explored more fully below.

We next directly measured the half-life of ATF6(N) in WT and *ATF4*$^{-/-}$ cells. Because the steady-state levels of ATF6(N) are a consequence of both the processing of full-length ATF6 and the turnover of ATF6(N), a HA-tagged version of ATF6(N) containing amino acid residues 1-373 (HA-ATF6-1-373) was expressed in both WT and *ATF4*$^{-/-}$ MEF cells. The synthesis of the HA-ATF6-1-373 would therefore occur independent of intramembrane proteolysis and the HA tag would allow for the expressed ATF6 protein to be distinguishable from endogenous ATF6. MEF cells expressing HA-ATF6-1-373 were either untreated or exposed to tunicamycin for 3 hours. Induction of CHOP was used as a control, as it is robustly induced after 3 hours of ER stress by a mechanism requiring ATF4. These cells were then subjected to treatment with cycloheximide and the rate of turnover of the tagged ATF6(N) protein was monitored. There was no appreciable difference in the rate of decay of the HA-ATF6-1-373 protein in the WT MEF cells in the presence or absence of ER stress (Figure 3-8B). In both cases, the activated version of ATF6 displayed a half-life of about 3 hours. Furthermore, loss of *ATF4* did not alter the rate of turnover of the HA-ATF6-1-373 protein (Figure 3-8C). Based on these findings, we conclude that the PERK/ATF4 pathway is not a significant contributor to the stability of ATF6-FL and the activated ATF6(N).

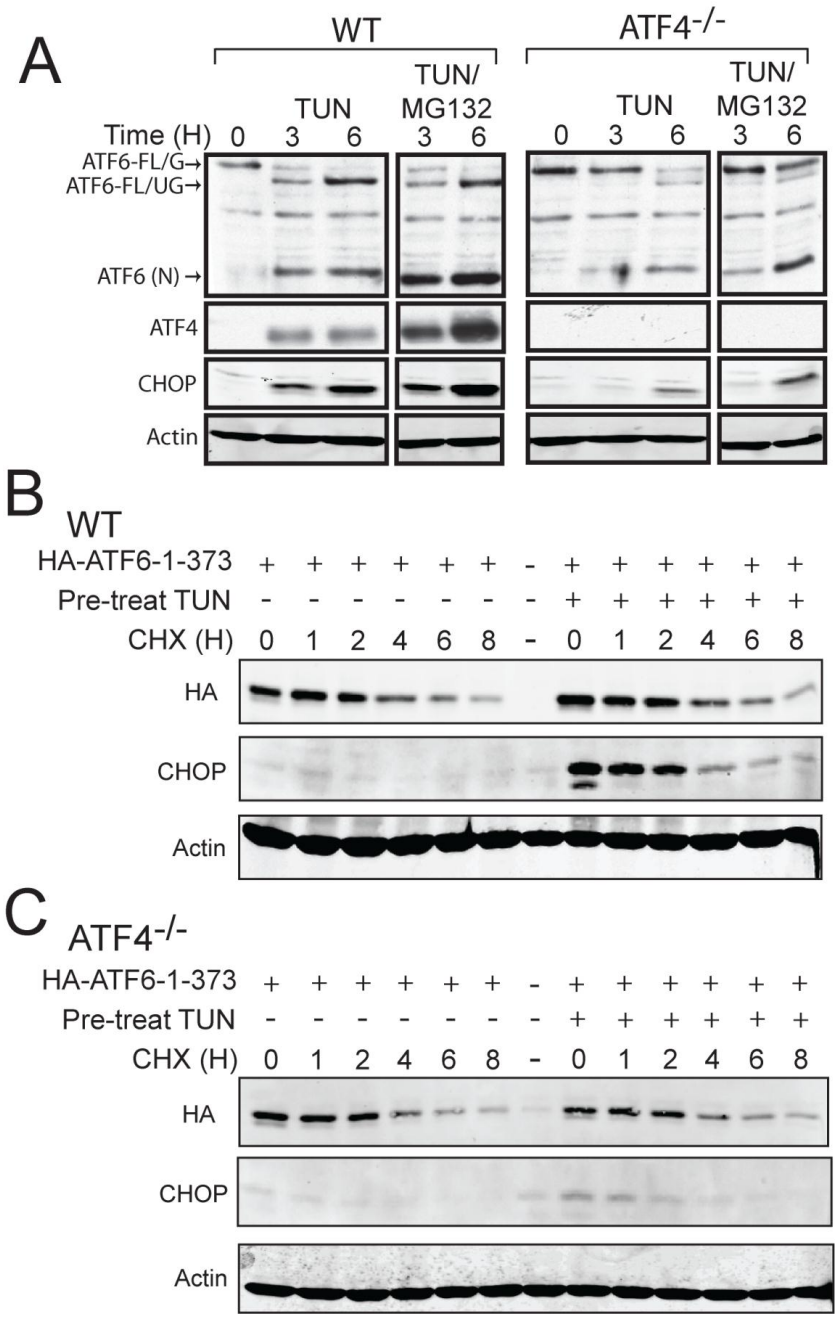

Figure 3-9 ATF6(N) protein has a short-half life that is independent of ATF4. (A) WT and *ATF4*$^{-/-}$ MEF cells were treated with tunicamycin (TUN), or co-treated with tunicamycin and MG132 (TUN/MG132) for up to 6 hours, as indicated. The levels of ATF6-FL/G, ATF6-FL/UG, ATF6(N), ATF4, CHOP, and actin were measured by

immunoblot analysis. Each panel was derived from a single immunoblot and is representative of three independent experiments. (B and C) WT and *ATF4*$^{-/-}$ cells were subject to the same treatment regimen. The half-life of ATF6(N) was measured in these cells by introducing a plasmid expressing an HA-tagged version of ATF6 encoding residues 1-373 (HA-ATF6-1-373). Cells were pre-treated with 2 μM tunicamycin for 3 hours, or exposed to no ER stress, followed by the addition of 50 μg/ml cycloheximide. Cells were then cultured for up to 8 hours as indicated, and the HA-ATF6-1-373 (HA), CHOP, or actin proteins were measured by immunoblot analysis. (D) WT and ATF4-/- cells were treated with 50 μg/ml cycloheximide for the indicated times and the levels of ATF6-FL/G was measured by immunoblot analysis.

3.6 The PERK/eIF2~P/ATF4 pathway facilitates increased ATF6 expression during the UPR

An important contributing factor to the activation of ATF6 during ER stress is induced synthesis of the full-length ATF6 protein. This continual renewal of full length ATF6 is required to replenish the full-length ATF6 that is irreversibly cleaved to generate ATF6(N). The Synthesis model suggests that disruption of the PERK/eIF2~P/ATF4 pathway lowers the levels of ATF6(N) by blocking the induced synthesis of full-length ATF6. Synthesis of the full-length protein is required for continued availability of this substrate for intramembrane proteolysis during ER stress. We initially addressed this by determining the requirement for global transcription in the accumulation of ATF6(N). Increasing amounts of ATF6(N) were detected between 1 and 6 hours of tunicamycin treatment (Figure 3-9A). This was accompanied by a depletion of ATF6-FL/G that was nearly absent by 6 hours of exposure to tunicamycin and by accumulation of ATF6-FL/UG, which represented the ATF6 protein newly synthesized during the ER stress condition. By comparison, a 30 minute pretreatment with actinomycin D, a potent inhibitor of RNA polymerase II, led to a more rapid depletion of ATF6-FL/G, and reduced levels of ATF6-FL/UG and ATF6(N) during the time course of tunicamycin treatment. These results suggest that transcription is an important contributor to accumulation of ATF6(N) during ER stress. This result is consistent with the idea that synthesis of ATF6 replenishes the processing pathway of ATF6, insuring a continued source of full length ATF6 for cleavage into the labile ATF6(N) transcription factor.

Induced ATF6 synthesis is suggested to involve increased transcription of *ATF6*, as there was a 2 to 3-fold increase in *ATF6* mRNA during tunicamycin treatment (Figure

3-9B). As described earlier in the LsPERK-KO mice (Figure 3-4A), loss of *PERK* or *ATF4* in the MEF cells blocked the increase in *ATF6* mRNA in response to ER stress (Figure 3-9B). Also consistent with the earlier LsPERK-KO experiments, there was significantly lowered induction of total and spliced *XBP1* mRNA levels during tunicamycin treatment in $PERK^{-/-}$ or $ATF4^{-/-}$ cells (Figure 3-9). To further support the idea that ATF4 facilitates the transcription of *ATF6*, we measured the activity of the *ATF6* promoter fused to a firefly luciferase reporter that was transfected into WT or $ATF4^{-/-}$ MEFs. While there was about 1.5-fold increase in the *ATF6* promoter activity in WT cells upon treatment with tunicamycin, loss of *ATF4* blocked induction of the *ATF6* promoter (Figure 3-9C). These results indicate that ATF4 enhances the transcription of the *ATF6* gene.

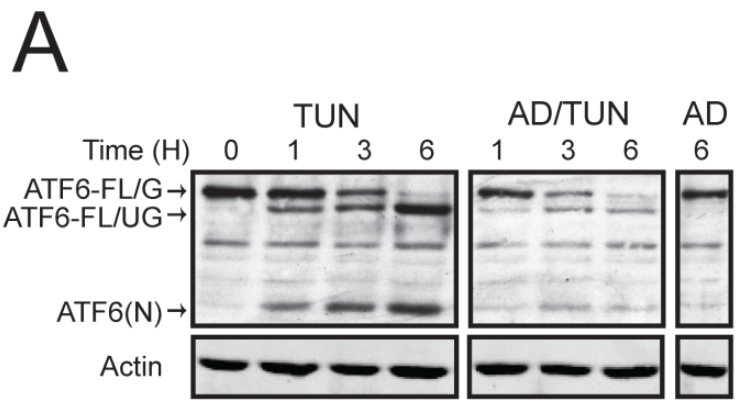
A
TUN
AD/TUN
AD
Time (H) 0 1 3 6 1 3 6 6
ATF6-FL/G→
ATF6-FL/UG→
ATF6(N)→
Actin

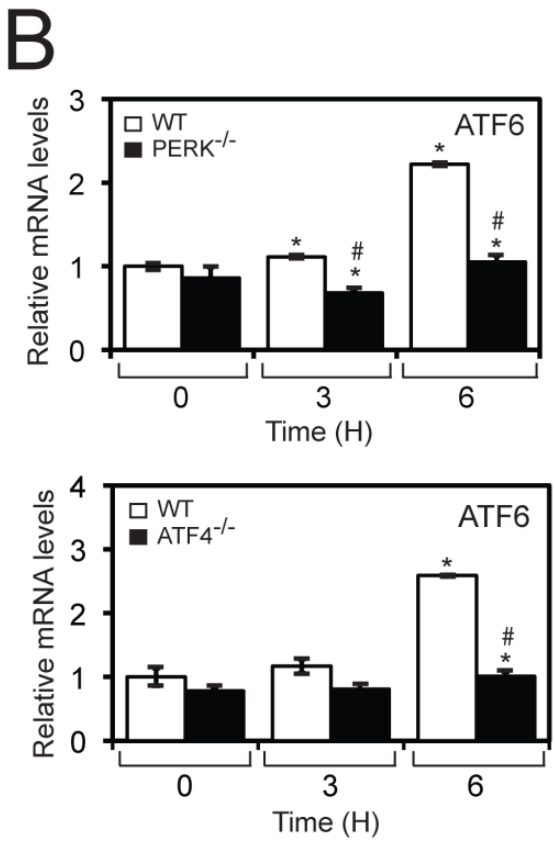
B
Relative mRNA levels
WT
PERK-/-
ATF6
Time (H)
Relative mRNA levels
WT
ATF4-/-
ATF6
Time (H)

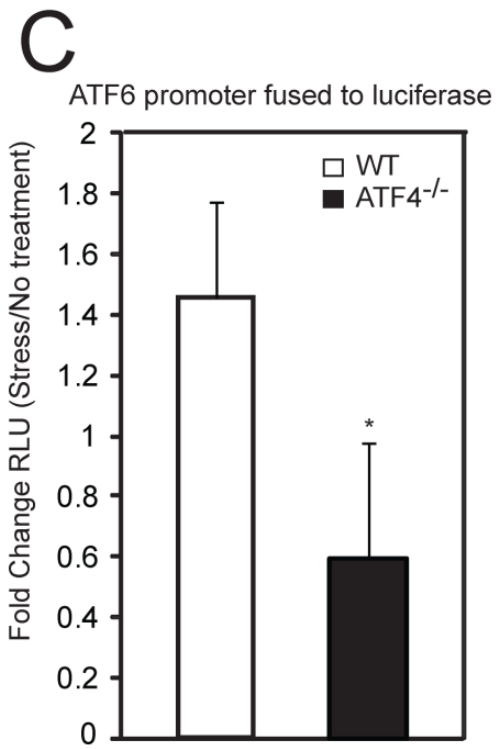
C
ATF6 promoter fused to luciferase
Fold Change RLU (Stress/No treatment)
WT
ATF4-/-

A

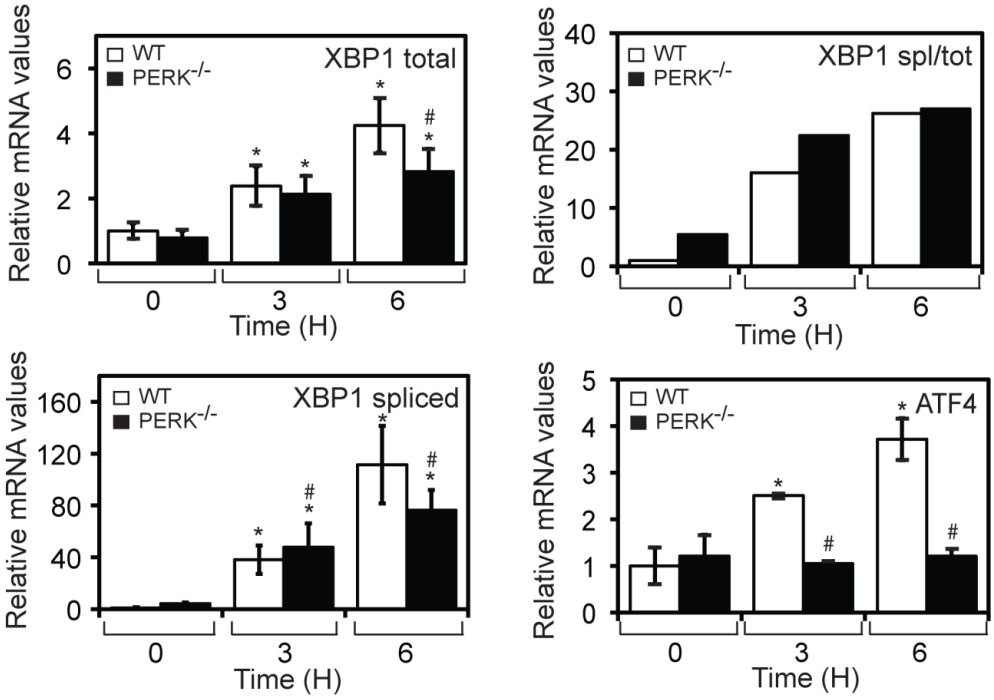
Relative mRNA values
WT
PERK-/-
XBP1 total
XBP1 spl/tot
XBP1 spliced
ATF4
Time (H)
0
3
6

B

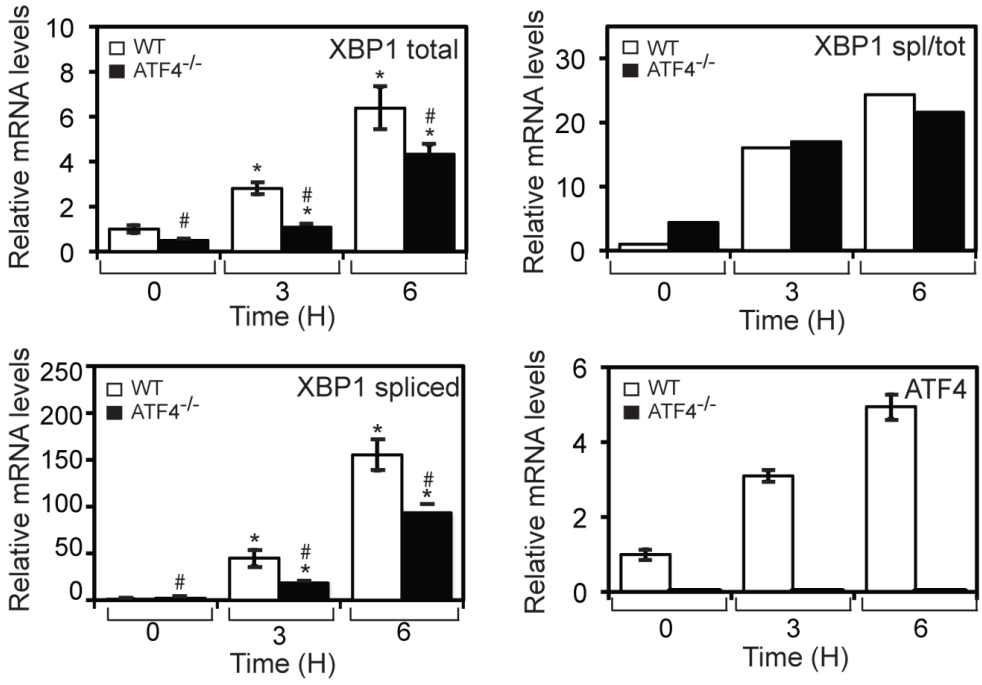
Relative mRNA levels
WT
ATF4-/-
XBP1 total
XBP1 spl/tot
XBP1 spliced
ATF4
Time (H)
0
3
6

Figure 3-10 PERK and ATF4 facilitate increased expression of the *ATF6* gene in response to ER stress. (A) WT MEF cells were treated with tunicamycin (TUN), 10 μM actinomycin D and tunicamycin (AD/TUN), or actinomycin D (AD) alone for up to 6 hours, as indicated. The levels of ATF6-FL/G, ATF6-FL/UG, and actin were measured by immunoblot analysis. (B) *PERK*$^{-/-}$ and *ATF4*$^{-/-}$ MEF cells, and their WT counterparts, were treated with tunicamycin for up to 6 hours, and the levels of *ATF6* mRNA were measured by qPCR. (C) A 1.5-kb segment (-1500 to -1) of the *ATF6* promoter was fused to a firefly luciferase reporter and assayed for expression in MEF cells treated with tunicamycin for 6 hours, or no stress agent. The fold-change in *ATF6* promoter activity in response to ER stress was determined by the dual luciferase assay. In panels B and C, the error bar represents the S.D., and the "*" indicates significance between untreated and treated samples; the "#" indicates significance between cell types, with a $p<0.05$. (E) WT and *PERK*$^{-/-}$ MEF cells were treated with 2 μM tunicamycin (TUN), as indicated, and mRNA levels for spliced *XBP1*, total *XBP1*, and *ATF4* were measured by qPCR. The "*" symbol indicates a significant difference ($p<0.05$) between tunicamycin treated and non-stressed samples, and the "#" symbol represents a significant difference between cell types. (F) WT and *ATF4*$^{-/-}$ MEF cells were treated with 2 μM tunicamycin (TUN), as indicated. The mRNA levels for spliced *XBP1*, total *XBP1*, and *ATF4* were determined by qPCR. The "*" symbol highlights a significant difference ($p<0.05$) between tunicamycin treated and non-stressed samples, and the "#" symbol indicates a significant difference between WT and *ATF4*$^{-/-}$ cells.

3.7 ATF4 facilitates trafficking of ATF6 from the ER to the Golgi

A final model to explain the role of the PERK/eIF2~P/ATF4 pathway in the activation of ATF6 suggests that this pathway facilitates the cellular trafficking of ATF6 during ER stress. In support of this model, our earlier observations showed that the rate of decrease of ATF6-FL/G in response to ER stress was slower in the *ATF4*$^{-/-}$ cells versus WT, which was accompanied by reduced levels of cleaved ATF6(N) (Figure 3-8E). We employed two experimental approaches to address whether ATF4 facilitates ATF6 trafficking. First, we used brefeldin A, a chemical inhibitor of anterograde ER-Golgi vesicle trafficking that causes S1P and S2P relocalization from the Golgi compartments to the ER [33, 34, 108]. We reasoned that brefeldin A would trigger a redistribution of Golgi proteins, including the S1P and S2P proteases, to the ER causing cleavage of ATF6 that was independent of trafficking. Consistent with an earlier study [34], there was an accumulation of ATF6(N) in WT cells within 2 hours of brefeldin A exposure (Figure 3-10A). This was accompanied by accumulation of ATF4 beginning at 3 hours of treatment, suggesting that at later time points brefeldin A can stress the ER organelle. Importantly, this pattern of ATF6 activation by brefeldin A was not changed in the absence of *ATF4*, with similar levels of ATF6(N) accumulated at each of the time points (Figure 3-10A). This finding demonstrates that the S1P and S2P proteases are active in the *ATF4*$^{-/-}$ cells, and supports the idea the ATF4 is required to facilitate passage of ATF6 from the ER to Golgi.

Trafficking and activation of ATF6 is suggested to involve multiple steps, including the reduction of the disulfide bonds which facilitates deoligomerization of ATF6 into ATF6 monomers, the release of inhibitor BiP [35, 72], and the loading of

ATF6 into COPII vesicles for transport from the ER to Golgi [31]. Prywes and colleagues showed that deletion of the BiP binding domain and the cysteine residues from the luminal portion of ATF6 (1-500 Δ431-475) leads to a constitutively active transcription factor that is transported to the Golgi for cleavage independent of ER stress [72]. Consistent with this idea, we found that expression of ATF6-1-500 Δ431-475 in non-stressed WT MEF cells led to a significant increase in ATF6 activity as measured by luciferase reporter expressed from a promoter with optimized ATF6-binding elements (Figure 3-10B). However, the ATF6 activity was blocked when the ATF6-1-500 Δ431-475 was expressed in the *ATF4*$^{-/-}$ cells. In contrast, when WT and *ATF4*$^{-/-}$ MEF cells were transfected with the ATF6(N) (residues 1-373) construct that is not dependent on Golgi processing, transcriptional activity was similarly induced in both WT and *ATF4*$^{-/-}$ cells. These results suggest that even when ATF6 is readily released from the ER, loss of ATF4 function interferes with the passage of ATF6 to the Golgi for processing by S1P to S2P proteases.

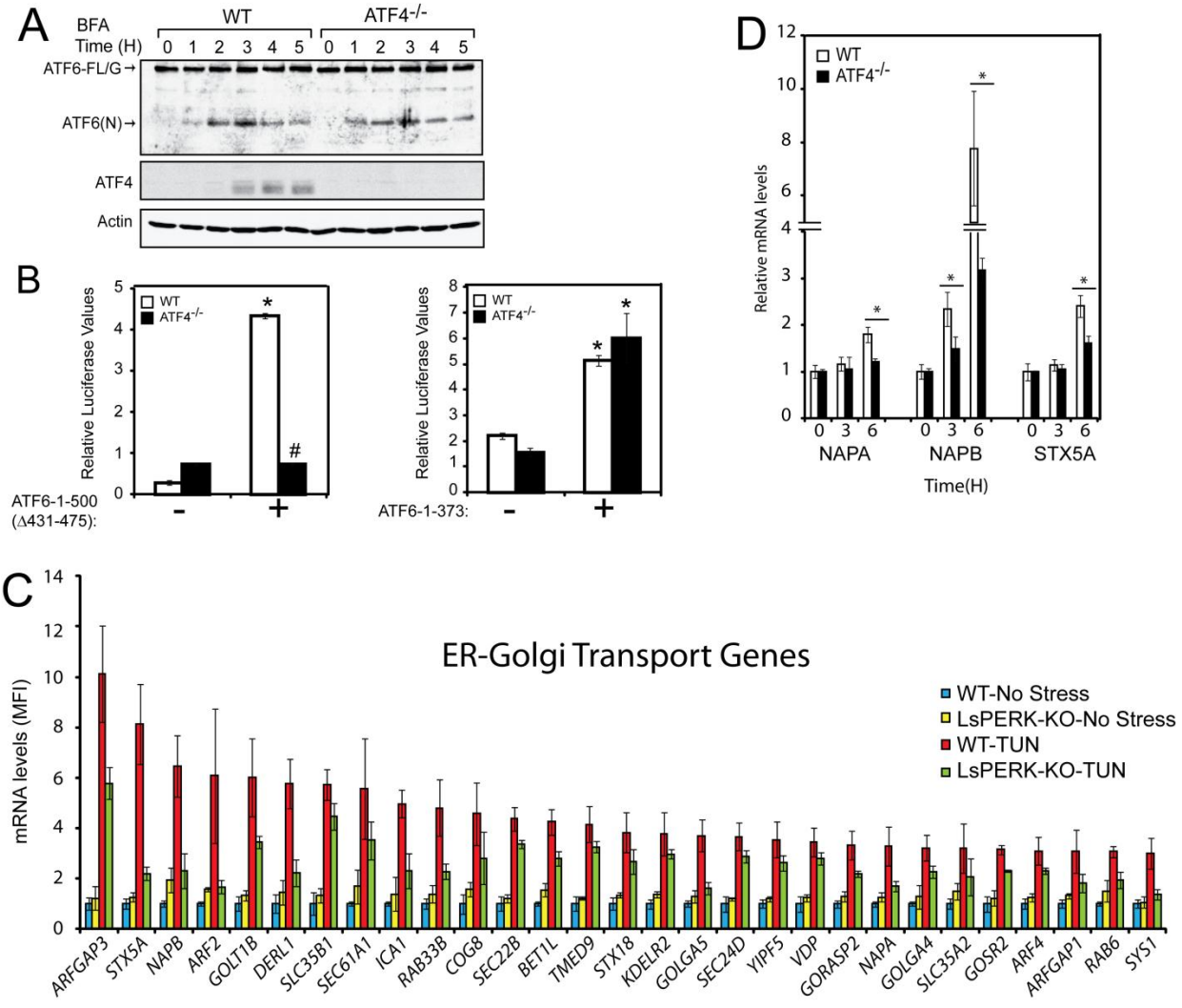

Figure 3-11 ATF4 is dispensable for activation of ATF6 in response to brefeldin A treatment. (A) WT and *ATF4*$^{-/-}$ MEF cells were treated with 5 μg/ml Brefeldin A (BFA) for up to 5 hours, and the levels of ATF6-FL/G, ATF6(N), ATF4, and actin were measured by immunoblot analysis. (B) Plasmids encoding ATF6-1-500Δ431-475 or ATF6-1-373 (indicated by "+"), along with a firefly luciferase reporter containing a

promoter with 5X ATF6-binding elements, were introduced into WT and *ATF4*$^{-/-}$ MEF cells. Luciferase values normalized to a Renilla internal control are shown and a "*" symbol represents significance (p<0.05) with respect to untransfected control and the "#" symbol shows significance between cell types, the error bars represent the S.D. (C) Graphical representation of the expression of genes involved in ER-Golgi trafficking that are Perk dependent. The mean fluorescent intensity (MFI) for each transcript is shown as a histogram, along with the S.D. (D) WT and *ATF4*$^{-/-}$ MEF cells were treated with tunicamycin for up to 6 hours, as indicated. The mRNA levels of *NAPA*, *NAPB*, and *STX5A* were measured by qPCR. The "*" indicates a significant difference was detected between the cell types.

3.8 ATF4 facilitates gene expression important for trafficking to the Golgi

Given that ATF4 facilitates trafficking of ATF6 from the ER to Golgi, we reasoned that ATF4 may induce the expression of genes involved in ER to Golgi transport. In our microarray analysis, a number of the genes that showed a *PERK*-dependent induction in response to tunicamycin are known to participate in this trafficking process (Figure 3-11C). These genes include COPII vesicle coat proteins, GTPase activating proteins (GAPs), and genes associated with vesicle formation and fusion such as *STX5a* [109, 110] and *α/β-SNAP* required for recycling of SNARE complexes at target membranes [111]. Further supporting this idea, measurements of *STX5a* and *α/β-SNAP* mRNAs by qPCR confirmed that ATF4 contributes to increased expression of these ER to Golgi trafficking genes in MEF cells during ER stress (Figure 3-11D). These results suggest that the PERK/eIF2~P/ATF4 pathway directs increased expression of genes involved in protein trafficking, and highlights the importance of the ISR in facilitating ATF6 transport from the ER to the Golgi for cleavage by S1P and S2P.

CHAPTER 4. RESULTS: THE ISR IS REQUIRED FOR ATF5 ACTIVATION

4.1 CHOP is required for expression transcriptional regulators in the ISR

While the ISR activates essential adaptive functions in response to stress, a topic of the preceding chapter, unabated induction of these stress responses can contribute to morbidity. Enhanced *CHOP* expression is one hallmark of this adaptive to maladaptive switch which leads to apoptotic cell fate decisions. Accumulation and sustained levels of CHOP are suggested to trigger maladaptive cell fates in response to disruptions in protein homeostasis. With this in mind, we measured CHOP-dependent changes in the transcriptome by comparative microarray analysis of WT and *CHOP*$^{-/-}$ MEF cells upon treatment with 1 μM MG132 for 8 hours. MG132 is a proteasome inhibitor and potent pharmacological inducer of eIF2~P and CHOP [107]. 8,321 genes as defined by probe sets were significantly changed in response to MG132 treatment (Table 4.1.) Among these genes 3,316 (39.8%) were found to be *CHOP*-dependent, with 46% (1,520 genes) enhanced and 54% (1,796 genes) lowered in response to proteasome inhibition. These findings are also illustrated in Figure 4-1A, which features a scatter-plot analysis between the stress-induced transcriptome changes in WT cells (x-axis) versus *CHOP*$^{-/-}$ cells (y-axis). The *CHOP* requirement for changes in the transcriptome is supported by the large number of probe sets which were increased in the WT cells upon stress, but induced to a lesser extent in *CHOP*$^{-/-}$ cells. Pathway analysis of the *CHOP*-dependent genes was performed using IPA analysis to group genes into functional categories. The top functional groups are depicted in Figure 4-1 C where CHOP-dependent gene networks were found to be associated with a range of molecular and cellular functions in the categories of cell death, cellular growth and proliferation, cell cycle, cellular assembly,

organization, and maintenance. This suggests that although CHOP-dependent genes participate in cell death properties they are also found to play a role in a diverse set of cellular functions. Classification of the CHOP-dependent genes by role within the cell revealed that CHOP was required for increased expression of *HSPA1A* and *DNAJA4* involved in protein folding, *NOXA, APAF1, and GAS5* involved in cell death, and about 200 genes involved in regulation of transcription (Figure 4-1B) including *MLF1*, *ATF7IP2*, and, *ATF5*. The *ATF5* transcript was 3.6-fold higher in the WT cells under basal conditions and 2-fold higher under stressed conditions when compared to *CHOP*$^{-/-}$ cells. This suggests that CHOP is required for *ATF5* mRNA synthesis in both basal and stressed conditions. It was previously reported that *ATF5* was subject to preferential translation in response to eIF2~P/ATF4 [70], however the transcriptional regulation, placement within the ISR pathway, and biological significance was not defined. The characterization of these important aspects of ISR signaling and the CHOP dependent regulation of the *ATF5* gene will be a focus of this chapter.

Table 4-1 CHOP-dependent genes induced by MG132.

		Fold Change (Treated/Untreated)[a]			
Dependence	Total	> 1.0	≥ 2.0	< 1.0	≤ 0.5
Total 8h MG132	8321[b]	3607	695	4714	966
CHOP-dep 8h MG132 (%)	3316(39.8)[c]	1520(42.1)	332(47.7)	1796(38.1)	350(36.2)

[a] Expression profile summary of gene transcripts, as defined by genes that were significantly changed after treatment with MG132 (1 μM). The number of induced genes are shown for both the >1.0 fold and ≥ 2.0 fold thresholds. The repressed genes are also shown for the < 1.0 and < 0.5 fold thresholds.
[b] The total number of transcripts significantly changed ($p \leq 0.05$) by proteasome inhibition.
[c] The number of CHOP-dependent transcripts that were significantly changed by proteasome inhibition.

Table 4-2 Functional classification of CHOP specific genes.

Probe ID[a]	Gene name	Gene Symbol	Fold-NT (WT/KO)[b]	Fold-MG132 (WT/KO)[c]
	TRANSCRIPTION FACTOR			
1417516_at	DNA-damage inducible transcript 3	CHOP	2.8	19.5
1422912_at	bone morphogenetic protein 4	BMP4	6.4	14.2
1416967_at	SRY-box containing gene 2	SOX2	9.6	13.9
1418271_at	basic helix-loop-helix family, member e22	BHLHE22	2.8	6.6
1440275_at	runt related transcription factor 3	RUNX3	7.7	4.4
1421469_a_at	signal transducer and activator of transcription 5A	STAT5A	3.1	3.4
1416981_at	forkhead box O1	FOXO1	3.7	2.9
1427938_at	c-myc binding protein	MYCBP	1.4	2.2
1425927_a_at	activating transcription factor 5	ATF5	3.6	1.8
1418589_a_at	myeloid leukemia factor 1	MLF1	2.1	2.5
1427603_at	activating transcription factor 7 interacting protein 2	ATF7IP2	2.2	6.4
1448135_at	activating transcription factor 4	ATF4	0.7	0.6
	TRANSLATION INITIATION			
1435904_at	eukaryotic translation initiation factor 2C, 3	EIF2C3	1.9	1.9
	APOPTOSIS			
1418203_at	phorbol-12-myristate-13-acetate-induced protein 1	NOXA	2.5	3.3
1436222_at	growth arrest specific 5	GAS5	2.8	2.1
1435448_at	BCL2-like 11 (apoptosis facilitator)	BIM	0.7	1.3
	PHOSPHATASE ACTIVITY			
1429514_at	phosphatidic acid phosphatase type 2B	PPAP2B	33.7	21.6
1415834_at	dual specificity phosphatase 6	DUSP6	0.5	2.3
1448325_at	myeloid differentiation primary response gene 116	GADD34	1.6	1.4

1455728_at	phosphatase and tensin homolog	PTEN	1.9	1.2
	PROTEIN FOLDING			
1419625_at	Heatshock protein 1A	HSPA1A	2.7	3.0
1434196_at	DnaJ (Hsp40 homolog, subfamily A, member 4	DNAJA4	1.1	2.7
1426260_a_at	UDP glycosyltransferase 1 family, polypeptide A6	UGT1A6	4.2	7.2
1455346_at	mannan-binding lectin serine peptidase 1	MASP1	3.3	3.7
	CYTOKINE SIGNALLING			
1451798_at	interleukin 1 receptor antagonist	IL1RN	9.0	12.8
1417625_s_at	chemokine (C-X-C motif) receptor 7	CXCR7	1.9	5.6
1436861_at	interleukin 7	IL7	1.7	2.1
	MISCELLANEOUS			
1421001_a_at	carbonic anhydrase 6	CAR6	2.7	24.9
1436555_at	solute carrier family 7, member 2	SLC7A2	3.3	4.5
1434714_at	ERO1-like beta (S. cerevisiae)	ERO1LB	1.7	2.4
1424048_a_at	cytochrome b5 reductase 1	CYB5R1	1.1	1.8
1418599_at	collagen, type XI, alpha 1	COL11A1	5.9	3.9
1417421_at	S100 calcium binding protein A1	S100A1	4.1	3.6
1443250_at	regulator of G-protein signaling 2	RGS2	1.0	1.9
	FATTY ACID SYNTHESIS			
1439478_at	acyl-CoA thioesterase 2	ACOT2	2.1	11.5
1424097_at	ELOVL family member 7, elongation of long chain fatty acids	ELOVL7	8.7	7.8

[a]Affymetrix Mouse 430 2.0 array, probe set identifier.
[b]Mean Flourescent intensity fold difference between WT and $CHOP^{-/-}$ cells, No treatment (NT).
[c]Mean Flourescent intensity fold difference between WT and $CHOP^{-/-}$ cells, MG132 (8 hours).

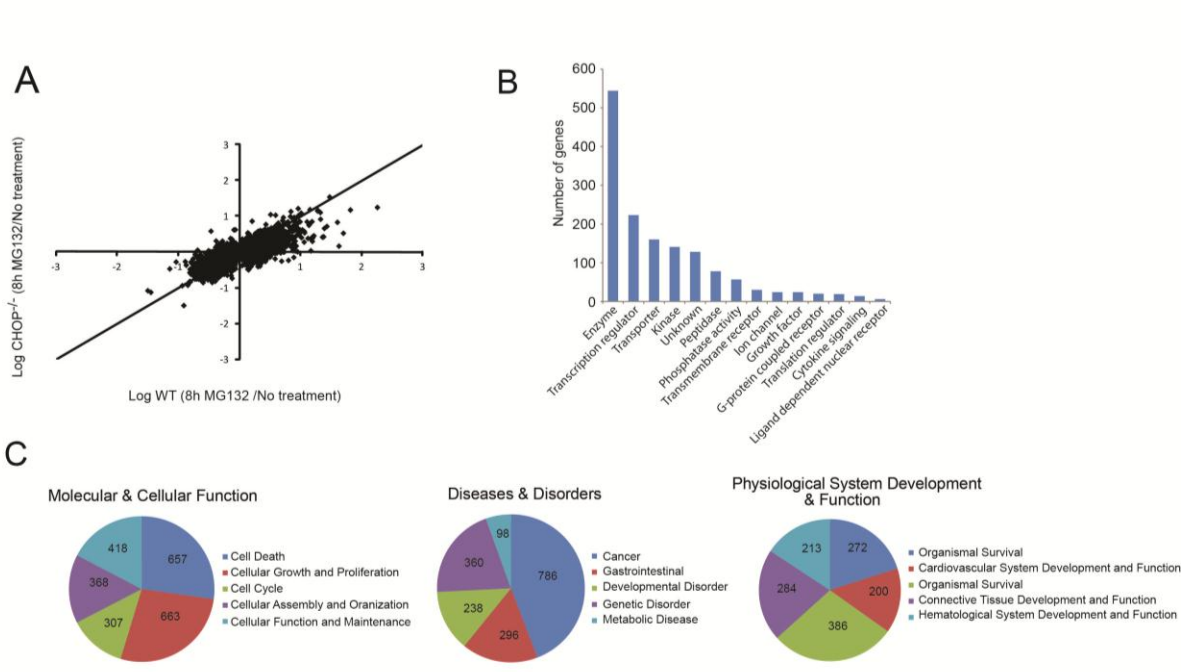

Figure 4-1 Genome-wide analysis of CHOP-dependent genes.

(A) The scatter plot is the log ratio of stressed versus no stress for WT (x-axis) and *CHOP*$^{-/-}$ MEF cells (y-axis). This comparative analysis of gene transcripts as defined by probe sets (p<0.05) in WT or *CHOP*$^{-/-}$ MEF cells following treatment with 1 μM MG132 for 8 hours. (B) IPA comparison of CHOP-dependent genes classified by functional roles. (C) IPA pie charts highlighting functional classes of CHOP-dependent genes.

4.2 CHOP is required for transcriptional expression of *ATF5* via binding to CARE elements in the *ATF5* promoter

The importance of CHOP for induced *ATF5* mRNA in the ISR was further analyzed by using qPCR and RNA prepared from the WT and *CHOP*$^{-/-}$ cells. In response to treatment with MG132, there was a 1.5-fold increase in *ATF5* mRNA levels in WT cells, while in *CHOP*$^{-/-}$ cells the amount of *ATF5* transcript was reduced about 50% upon proteasome inhibition (Figure 4-2A). The requirement of CHOP for increased *ATF5* mRNA was also seen when these MEF cells were treated with thapsigargin, which elicits ER stress and eIF2~P due to calcium disruption in this organelle (Figure 4-2B). In wild-type cells, there was a 4-fold in increase in *ATF5* mRNA, which was significantly lowered in *CHOP*$^{-/-}$ cells. As expected, *CHOP* mRNA levels were dramatically increased in WT cells during either stress arrangement, and there were no detectable *CHOP* transcripts in the *CHOP*$^{-/-}$ cells (Figures 4-2A and B). Consistent with earlier reports, we found that CHOP was required for full induction of *GADD34* mRNA during proteasome inhibition (Figure 4-2A) [56]. Supporting the idea that ATF4 is an upstream activator of *CHOP* transcription in the ISR, the amount of *ATF4* mRNA was enhanced in WT and *CHOP*$^{-/-}$ cells exposed to MG132 or thapsigargin. In fact, the *ATF4* transcripts were further elevated in the stress *CHOP*-deficient cells (Figure 4-2A and B), suggesting there is an extended ISR response with loss of expression of *CHOP* and its downstream target gene *GADD34*, which facilitates feedback control of the ISR. Together these results indicate that CHOP is required for induced *ATF5* mRNAs in response to different stress conditions that activate the ISR.

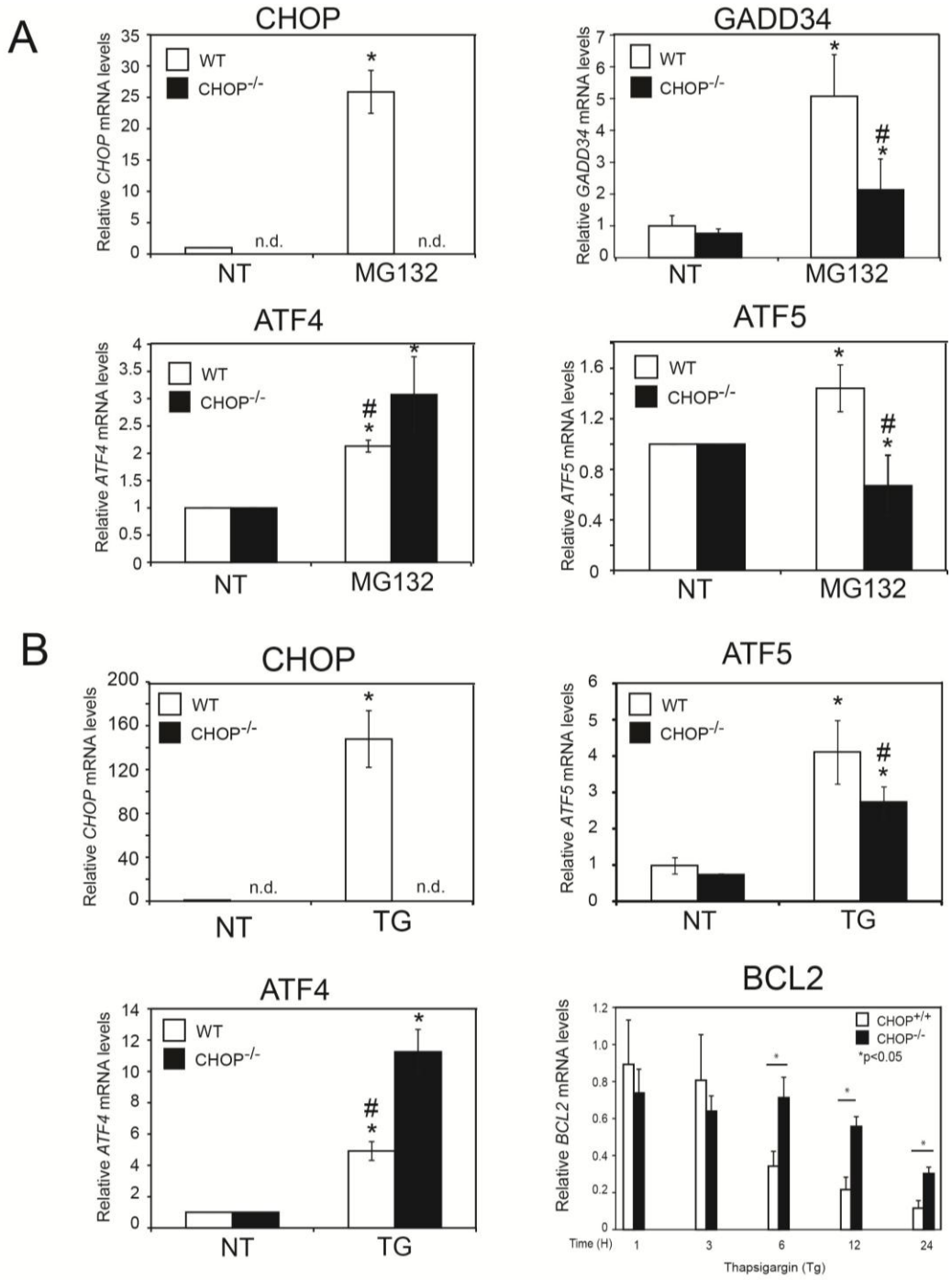

Figure 4-2 CHOP is required for enhanced levels of *ATF5* mRNA transcripts.

WT or *CHOP*$^{-/-}$ MEF cells were treated with 1 µM MG132 (A) or 1µM TG (B) for 8 hours, and relative levels of *ATF4*, *CHOP*, *ATF5*, and *GADD34* mRNAs were determined by qPCR. The "*" represents statistical significance ($p<0.05$) with respect to

the untreated control and the "#" represents a significant difference ($p<0.05$) between cell types.

Several potential CHOP binding elements are situated in the *ATF5* promoter from -2500 to -3000 bp region relative to the *ATF5* transcriptional start site. These binding sites termed CARE elements can be placed in either orientation [62, 112], and in the *ATF5* promoter these were designated CARE-1 (5'-TGATGGAAA-3') and CARE-2 (5'-TGATGCAAC-3') (Figure 4-3A). We therefore carried out ChIP analyses to measure ATF4 and CHOP occupancy on the *ATF5* promoter at these CARE sites. Both CHOP and ATF4 were both found to associate with DNA including the CARE-2 element (designated P2) in the *ATF5* promoter, with significantly enhanced binding in response to MG132 (Figure 4-3B), or thapsigargin treatment (Figure 4-3C). Conversely, there was minimal binding of ATF4 and CHOP to the CARE-1 segment (designated P1), which is predicted to be a suboptimal CHOP binding site due to a G in the 6^{th} position [113, 114]. The third site tested is located in an exon (designated P3) and was used as a negative control. As expected, there was minimal ATF4 or CHOP binding at the P3 site in the presence of absence of the stresses (Figsure 4-3B and C). Finally, no signal was detected using a non-specific IgG in the ChIP assay (Figure 4-3B). These results support the idea that both CHOP and ATF4 bind directly to the *ATF5* promoter to facilitate increased transcription in response to diverse stress conditions that elicit the ISR.

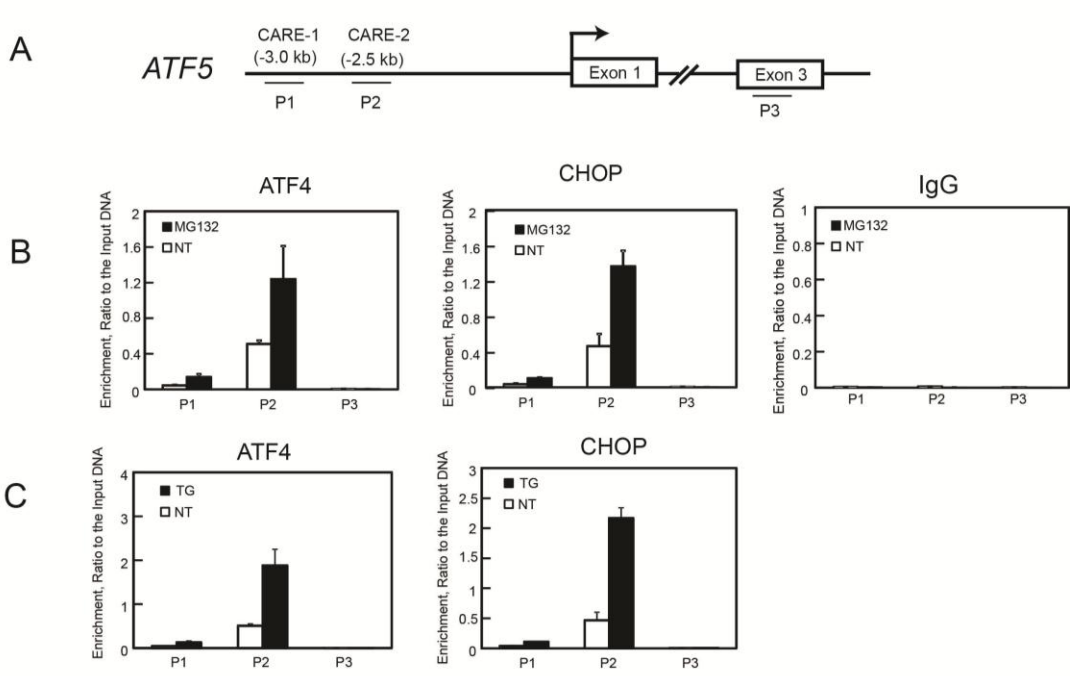

Figure 4-3 CHOP is required for transcriptional activation of ATF5 by binding to CARE elements in the *ATF5* promoter. (A) Diagram of CARE elements found in the *ATF5* promoter region. The -2.5 kb and -3.0 kb positions are relative to the transcriptional start site. Cells were treated with MG132 (B), TG (C), or left untreated (NT) and Chromatin immunoprecipitation was carried out using antibody for ATF4, CHOP or IgG negative control. qPCR was performed and the enrichment relative to input DNA is shown for each of the DNA sites labeled in diagram. Sites P1 and P2 contain CARE sequences in the *ATF5* promoter, and the site P3 located in exon 3 does not contain a CARE site.

4.3 CHOP is required for ATF5 protein expression during diverse stress conditions

Because ATF5 is also regulated at the level of mRNA translation it was important to determine whether CHOP was required for increased ATF5 protein. WT and *CHOP*$^{-/-}$ MEF cells were treated with MG132 for up to 24 hours and the levels of eIF2~P and downstream ISR effectors, ATF4 and CHOP proteins, were enhanced early within 1 to 3 hours of proteasome inhibition (Figure 4-4A). As expected, no CHOP protein was detected in the *CHOP*$^{-/-}$ cells, whereas induction of ATF4 protein and another ISR transcription factor ATF3 was largely unaffected. While ATF5 protein was increased within 3 hours of treatment of WT cells with MG132, there were significantly lowered levels of ATF5 in the *CHOP*$^{-/-}$ cells, with only modest levels of ATF5 protein after 12 hours of proteasome inhibition. Stable expression of WT *CHOP* into the *CHOP*$^{-/-}$ MEF cells significantly enhanced ATF5 proteins upon MG132 treatment (Figure 4-4B). Furthermore, we used a lentiviral system and shRNA to stably knockdown *CHOP* expression in mouse liver Hep1-6 cells subjected to proteasome inhibition. Using clones derived from three different validated shRNAs, we found that reduced CHOP levels in the Hep1-6 cells led to sharply reduced expression of ATF5 protein upon treatment with MG132 (Figure 4-4C).

Given that eIF2~P and the ISR are induced by many different stress conditions, we also addressed whether CHOP facilitates increased ATF5 protein in response to treatment with thapsigargin, arsenite, or histidinol (Figure 4-5). In each stress condition, there was a significant diminishment and delay in the induction of ATF5 protein in the *CHOP*$^{-/-}$ cells as compared to WT. These results support the idea that CHOP is required

for full induction of *ATF5* expression in the ISR during different stress conditions and in multiple cell types.

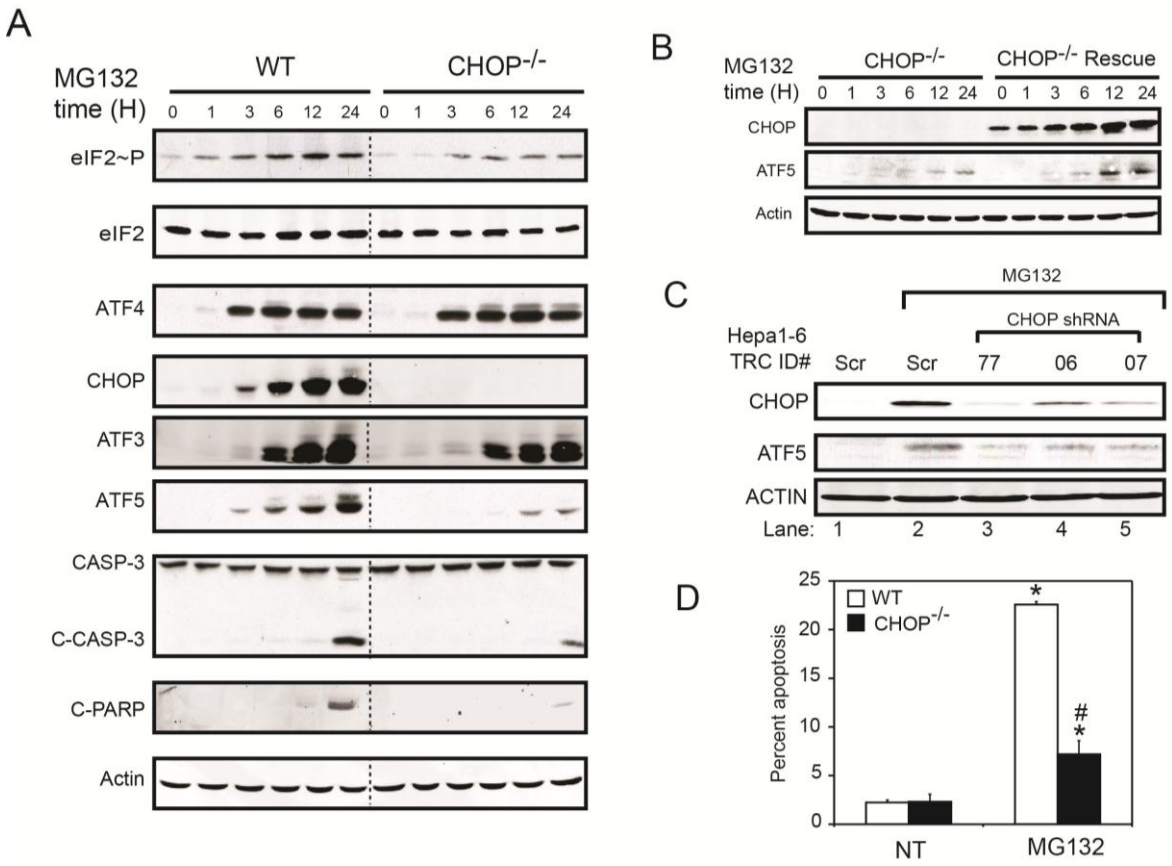

Figure 4-4 CHOP is required for ATF5 protein expression in response to proteasome inhibition. (A) WT and *CHOP*$^{-/-}$ MEF cells were treated with 1 μM MG132 for a time course of up to 24 hours as indicated. Levels of eIF2α ~P, eIF2α, ATF4, CHOP, ATF3, ATF5, caspase-3, parp, and actin were determined by immunoblot analysis using antibody specific to the protein of interest. (B) *CHOP*$^{-/-}$ cells and *CHOP*$^{-/-}$ cells stably expressing a translationally active CHOP from an FRT locus (see materials and methods for details) were subjected to up to 24 hours of treatment with 1 μM MG132. Levels of CHOP, ATF5, and actin proteins were determined by immunoblot analysis. (D) HEPA1-6 cells stably expressing a control scrambled shRNA or different shRNAs that knocked down *CHOP* expression were treated with 1μM MG132 for 8 hours. The RNA Consortium (TRC) ID# indicates the last two digits in the validated

shRNA identification number obtained from Sigma. Levels of CHOP, ATF5 and actin proteins were determined by immunoblot analysis. (D) WT and *CHOP*$^{-/-}$ MEF cells were exposed to μM MG132 for 24 hours, or not treated (NT). Cells were then analyzed by fluorescence-activated cell sorting (FACS) and Annexin V-FITC/PI staining.

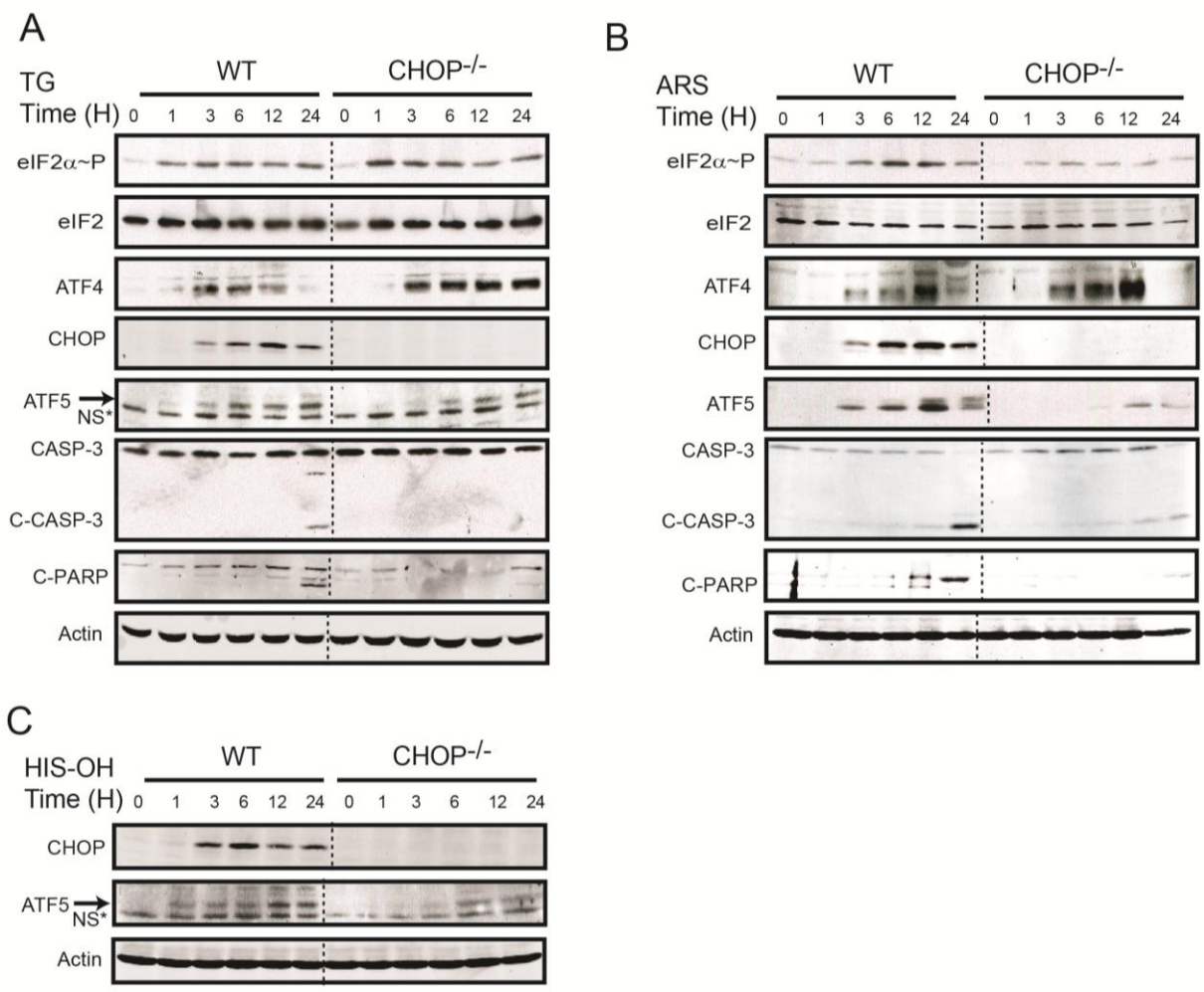

Figure 4-5 CHOP is required for ATF5 protein expression in response to diverse stress conditions. WT and *CHOP*$^{-/-}$ MEF cells were treated with (A) 1 µM thapsigargin (TG) or (B) 20 µM arsenite for up to 24 hours, as indicated. Levels of eIF2α~P, eIF2α, ATF4, CHOP, ATF5, cleaved Caspase-3, cleaved PARP, and actin were determined by immunoblot analysis using specific antibodies. (C) WT and *CHOP*$^{-/-}$ MEF cells were subject to 5 mM histidinol (His-OH) treatment for up to 24 hours. Levels of CHOP, ATF5 and actin proteins were determined by immunoblot analysis. The "*" indicates an un-specified protein recognized by the antibody.

4.4 CHOP and ATF5 facilitate apoptosis during proteasome inhibition

CHOP has a potent pro-apoptotic function in the ISR during extended stress arrangements. This idea is illustrated by the observations that while cleavage of PARP, a marker of apoptosis, was present in WT cells following 24 hours of MG132 exposure, there was minimal detected cleaved PARP in *CHOP*$^{-/-}$ cells (Figure 4-4C). Furthermore, cleavage of Caspase 3 was reduced during this stress regimen upon loss of *CHOP*. Consistent with the idea that CHOP can facilitate cell death in response to cellular stresses, *CHOP*$^{-/-}$ cells showed significantly lower levels of apoptosis during MG132 treatment as compared to WT cells (Figure 4-4D). Lowered cleaved Caspase 3 and PARP were also seen in the *CHOP*$^{-/-}$ cells upon thapsigargin and arsenite treatments (Figure 4.5) supporting the notion that CHOP can signal apoptosis during different chronic stresses.

Having established that *ATF5* expression was dependent on CHOP, the next objective was to investigate the role of ATF5 in cell survival during stress**.** To achieve this goal, lentiviral transduction of shRNA was used to stably knockdown ATF5 in MEF cells. Using a collection of different shRNAs, we were able to achieve 58% to 72% knockdown of the *ATF5* transcripts compared to no significant difference in knockdown in the scramble control (Figure 4-6A). Two cell lines designated *ATF5*-KD1 and *ATF5*-KD2, with the highest percentage knockdown of *ATF5* mRNAs (58% and 72%, respectively) were selected for further characterization. ATF5 protein levels in these knockdown cells were also sharply lowered following up to 24 hours of MG132 treatment (Figure 4-6B). Supporting the idea that ATF4 and CHOP proteins are upstream

activators of ATF5 expression, the levels of ATF4 and CHOP upon exposure to MG132 were unchanged in WT cells compared to the *ATF5* knockdown cells (Figure 4-6B).

The role of ATF5 for cell survival was addressed by treating WT and the *ATF5* knockdown cells with a proteasome inhibitor, followed by the MTT assay to measure cell viability. In this experiment WT, *CHOP*$^{-/-}$, *ATF5*-KD1, and *ATF5*-KD2 cells were exposed to MG132 for between 1 and 18 hours as outlined in Figure 4-6C. Following each stress time point, fresh media was added with no drug and cells were allowed to recover from the stress insult for the remainder of the time course (total 24 hours). Both the *ATF5*-KD1 and *ATF5*-KD2 cell lines showed enhanced survival at each time point of MG132 compared to WT cells (Figure 4-6D). The increased survival of the *ATF5* knockdown cells was similar to that determined for *CHOP*$^{-/-}$ cells. Furthermore, there were significantly lowered levels of cleaved Caspase 3 and PARP in the ATF5-KD1 and *ATF5*-KD2 cells treated with MG132 as compared to WT (Figure 4-6B). These results support the idea that both CHOP and ATF5 facilitate apoptosis during perturbations in protein homeostasis.

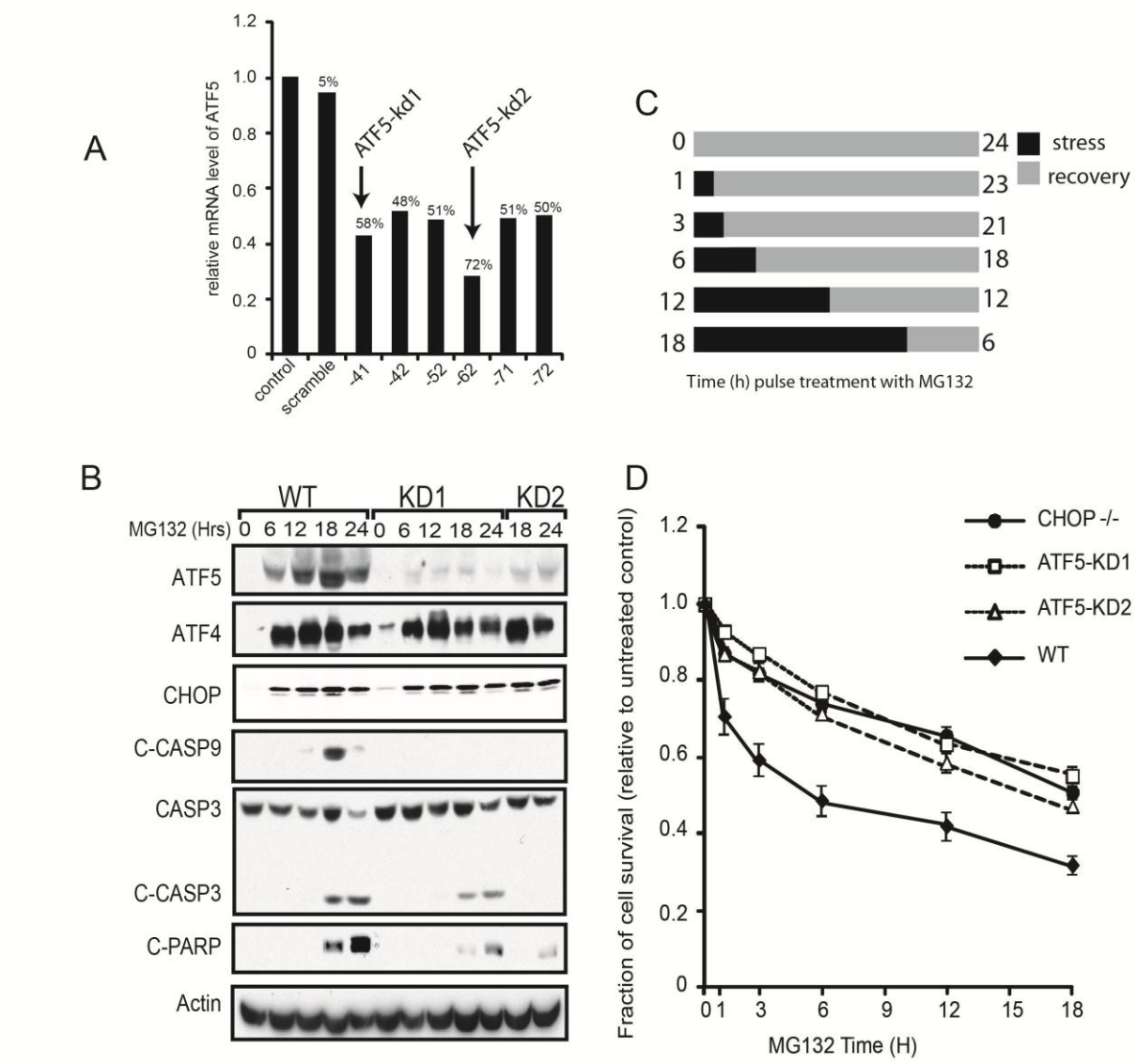

Figure 4-6 ATF5 is required for apoptosis in response to MG132. (A) RNA was isolated from MEF cells stably expressing a scramble shRNA or an *ATF5* targeted shRNA, *ATF5* mRNA levels were determined by qPCR relative to non-shRNA expressing control. Additionally, percentage of ATF5 knockdown was determined relative to a non-shRNA expressing control and is also indicated. (B) WT, *ATF5*-KD1, and *ATF5*-KD2 MEF cells were treated with the proteasome inhibitor MG132 for the

indicated times. Levels of ATF4, CHOP, ATF5, cleaved Caspase-9 and Caspase-3, cleaved PARP, and actin proteins were measured by immunoblot analysis using antibody specific to the protein of interest. (C and D) Treatment regimen and cell survival as determined by MTT assay. Survival was normalized to the untreated controls for each cell type.

4.5 ATF5 is required for activation of proapoptotic target genes in response to proteasome inhibition

To determine the transcriptome changes directed by ATF5 transcription factor, and its possible impact in the regulation of apoptosis, we carried out a microarray analysis of WT of *ATF5-KD2* cells treated with MG132 or no stress. A total of 8,055 genes as defined by probe sets were significantly changed in response to MG132 treatment (Table 4.3). Among these genes, 3,075 (38%) were dependent on ATF5, with 1,714 (44%) increased and 1,361 (32%) reduced. We again utilized IPA software to analyze the functional classes of ATF5-dependent genes which are depicted in Figure 4-7A. Complete data for this second microarray can be found under the GEO accession number GSE4367. The ATF5-dependent gene network is associated with several different functional classes when compared to the networks characterized for CHOP-dependent genes. In the ATF5-dependent gene network, we found classes involved with infectious disease and inflammatory responses, as well as genes involved in protein synthesis, protein degradation, and gene expression (Figure 4-7A). We compared the set of genes requiring ATF5 for full induction with our previous microarray dataset of *CHOP*-dependent genes and found 348 genes (23%) that overlapped in genes dependent on both CHOP and ATF5. Protein folding genes, *HSPA1A* and *DNAJA4* were found to be dependent on both CHOP and ATF5. The transcription factors *ATF7IP2* and *MLF1*, and proapoptotic genes *GAS5* and *NOXA* were also noted to be dependent on both CHOP and ATF5 for induced expression (Figure 4-7C). There was also a subset of genes that were found to be dependent on ATF5 alone, including *APAF1* and *TXNIP* that are involved in apoptosis and the inflammatory response, respectively. Therefore there are

three classes in the ISR-directed transcriptome: genes that are ATF5-dependent, CHOP-dependent, and those requiring both transcription factors for full induction in response to MG132 treatment. As noted further below, we have confirmed by qPCR several of the key findings in this microarray dataset. Furthermore we confirmed by qPCR and by immunoblot that *ATF5* mRNA and protein is depleted in the *ATF5*-KD2 cells and that upstream *CHOP* expression is unaffected (Figures 4-7A and B).

Table 4-3 Number of ATF5 dependent genes induced by MG132.

		Fold Change (Treated/Untreated)[a]			
Dependence	Total	> 1.0	≥ 2.0	< 1.0	≤ 0.5
Total 8h MG132	8055[b]	3833	69	4222	72
ATF5-dep 8h MG132 (%)	3075(38.1)[c]	1714(44.7)	52(75.3)	1361(32.2)	41(56.9)

[a] Expression profile summary of gene transcripts, as defined by genes that were significantly changed after treatment with MG132 (1 μM). The number of induced genes are shown for both the >1.0 fold and ≥ 2.0 fold thresholds. The repressed genes are also shown for the < 1.0 and < 0.5 fold thresholds.
[b] The total number of transcripts significantly changed ($p \leq 0.05$) by proteasome inhibition.
[c] The number of ATF5-dependent transcripts that were significantly changed by proteasome inhibition.

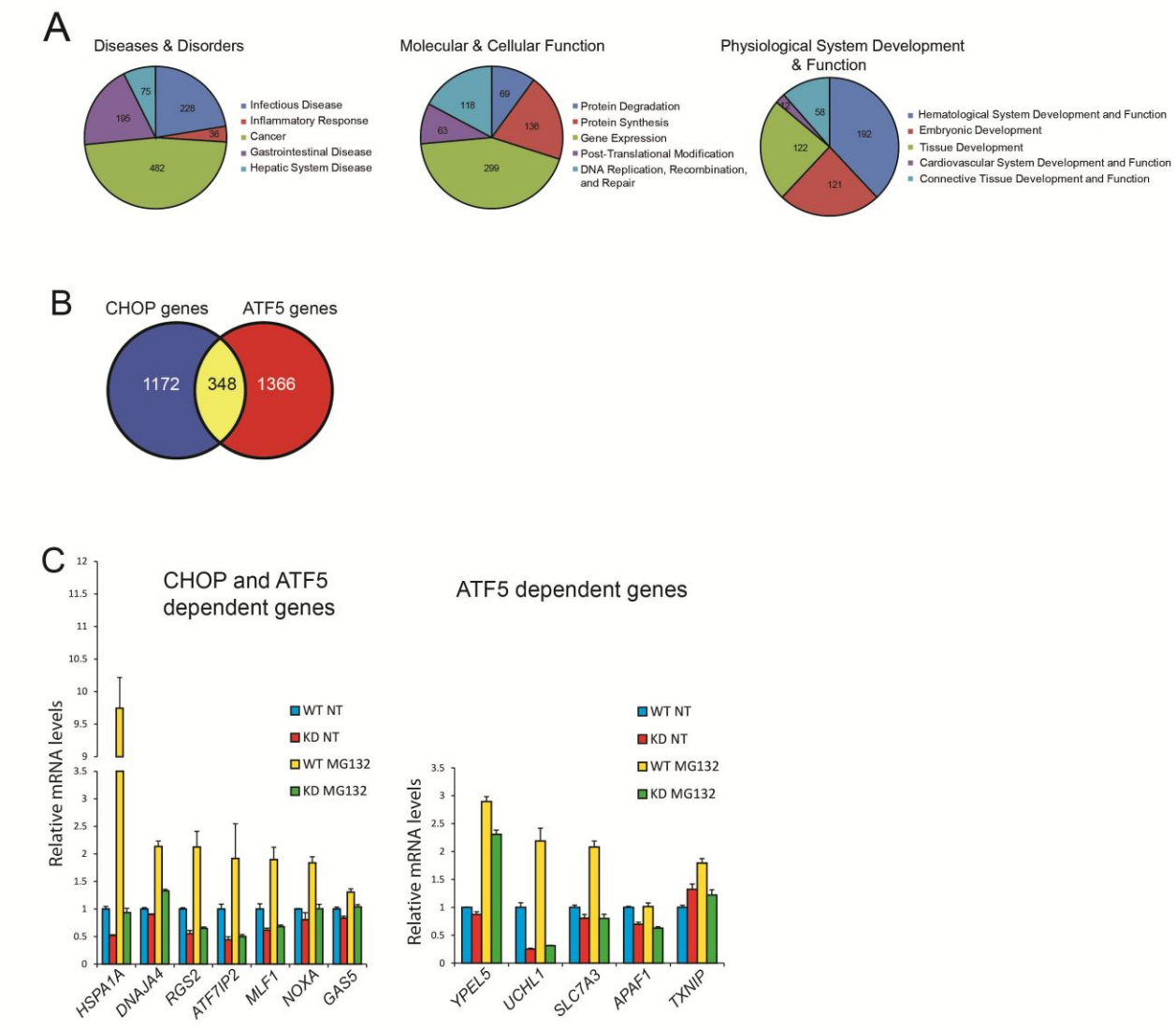

Figure 4-7 Microarray analysis shows ATF5 is required for activation of proapoptotic mRNA transcripts in response to ER stress. (A) IPA analysis of ATF5-dependent gene networks that highlights functional classes as depicted in the pie charts. (B) The numbers of CHOP-only, ATF5-only, and CHOP and ATF5 target genes are illustrated in Venn diagrams. (C) Comparative bar graph showing the top ATF5-target genes, with values representing relative levels of gene transcripts in in mean fluorescent intensities (MFI) in WT and *ATF5*-KD2 cells in the presence or absence of 1 μM MG132 treatment for 8 hours.

ATF5 was required for full mRNA induction of several known proapoptotic genes including *NOXA (PMAIP1)*, *APAF1*, and *TXNIP* (Figure 4-8B). *TXNIP* is an example of an ATF5-specific gene reported to be involved in apoptosis. ATF5 was recently reported to facilitate increased expression of thioredoxin-interacting protein (TXNIP) during ER stress, and knockdown of *TXNIP* was found to alleviate inflammation and subsequent apoptosis in the beta cells [115]. By comparison, induction of *GADD34* mRNA in response to MG132 was not significantly altered upon knockdown of *ATF5*, indicating that this gene is an example of a *CHOP*-specific gene that can facilitate apoptosis during chronic stress. NOXA has been previously shown to be important for activation of apoptosis in response to ER stress [116]. We found that *NOXA* mRNA levels were increased in an *ATF5* and *CHOP*-dependent fashion in our microarray datasets (Figure 4-8C and Table 4-2). Importantly, *NOXA* transcripts were diminished as judged by qPCR in both *ATF5*-KD1 and *ATF5*-KD2 cells lines treated with MG132 as compared to WT cells. These results suggest that ATF5 and CHOP are nodes in an ISR transcription factor network that participates in the cellular decision to invoke apoptosis during extended disruptions in protein homeostasis.

4.6 The ATF5 target gene *NOXA* is required for increased apoptosis in response to proteasome inhibition

To address the role of ATF5 and CHOP-target gene *NOXA* in the regulation of cell survival during proteasome inhibition, we utilized shRNA to knockdown *NOXA* mRNA in both MEF and Hepa1-6 cells. *NOXA* knockdown was confirmed by qPCR, with substantial reductions in *NOXA* mRNA levels in both of the shRNA expressing cell

lines (Figure 4-8A). The MEF cells depleted for *NOXA* expression were treated with MG132 for 24 hours and found to significantly enhance cell viability, as judged by the MTT assay. The increase in cell viability was comparable to that determined for the *CHOP*$^{-/-}$ cells, further supporting the idea that NOXA is an important target for the ISR (Figure 4-8B). These results support the model that ATF5 is a downstream of CHOP, and together these transcription factors can facilitate apoptosis during proteasome inhibition.

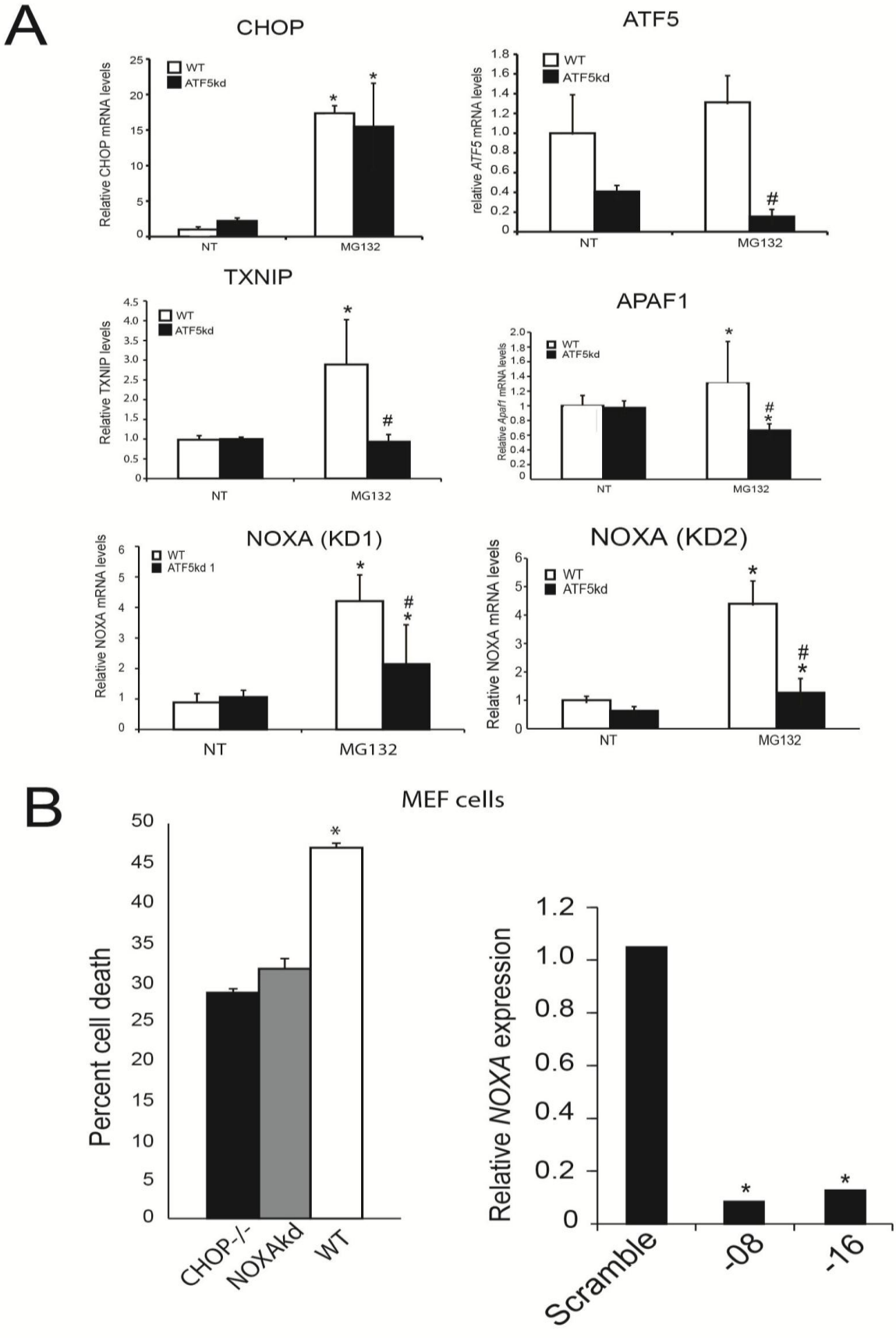
A
CHOP
Relative CHOP mRNA levels
WT
ATF5kd
NT
MG132
ATF5
relative ATF5 mRNA levels
TXNIP
Relative TXNIP levels
APAF1
Relative Apaf1 mRNA levels
NOXA (KD1)
Relative NOXA mRNA levels
ATF5kd 1
NOXA (KD2)
B
MEF cells
Percent cell death
CHOP-/-
NOXAkd
WT
Relative NOXA expression
Scramble
-08
-16

Figure 4-8 Knockdown of *NOXA* by shRNA protects cells from MG132 stress.

(A) WT and *ATF5*-KD2 MEF were treated for 8 hours with 1 μM MG132 or subjected to no stress treatment. Levels of *CHOP*, *ATF5*, *NOXA*, *TXNIP* and *APAF1* mRNA were quantified by qPCR. The "*" indicates statistical significance ($p<0.05$) (B) MEF cells expressing an shRNA targeting *NOXA*, or scramble control, were treated with 1 μM MG132 for 8 hours. *NOXA* mRNA levels were measured by qPCR. The "*" indicates statistical significance ($p<0.05$).

CHAPTER 5. DISCUSSION

5.1 ISR signaling is important for cell survival

Phosphorylation of eIF2 and activation of the ISR are important for signaling events that can determine whether a cell survives a stress insult or induces apoptosis. The role of eIF2~P in both outcomes were studied in this thesis. Results in Chapter 3 focused on ISR pathways directing cell survival. eIF2~P by PERK triggers not only translational control in response to ER stress, but also facilitates the activation of ATF6 and the transcriptional phase of the UPR. Among the UPR genes induced by 2-fold, 74% showed a significant reduction in gene expression in the LsPERK-KO livers (Table 3-1 and Figure 3-3A). Furthermore, activation of ATF6 in response to ER stress was significantly diminished with loss of *PERK* (Figure 3-4). These central findings were observed not only in liver tissues, but also in MEF cells containing mutations that blocked each of the steps in the PERK/eIF2~P/ATF4 pathway (Figures 3-7 and 3-8).

ATF4 facilitates induction of ATF6 during ER stress by at least two mechanisms. First, ATF4 enhances the transcription of the *ATF6* gene, ensuring that there are sufficient amounts of newly synthesized ATF6 available for continued processing into activated ATF6(N) (Figures 3-8 and 3-10). Second, ATF4 contributes to the trafficking of ATF6 from the ER to the Golgi for subsequent proteolysis and activation by S1P and S2P. Supporting this idea is the finding that mutations that adversely affect each step of the PERK/eIF2~P/ATF4 pathway significantly diminish the levels of activated ATF6(N) in response to either tunicamycin or thapsigargin treatments (Figures 3-7 and 3-8). By comparison, ATF4 is dispensable for the processing of ATF6(N) in MEF cells upon exposure with brefeldin A, which triggers redistribution of S1P and S2P to the ER

(Figure 3-11B). This suggests that while S1P and S2P are functional in *ATF4*$^{-/-}$ cells, the passage of ATF6 to the Golgi is impeded with loss of ATF4. ATF4 contributes to the expression of many genes involved in ER to Golgi transport (Figure 3-11, C and D), and diminished levels of key proteins that are important for ATF6 trafficking is suggested to be an important underlying reason for the reduced activation of ATF6(N) in *ATF4*-deficient cells. These findings provide a mechanistic understanding for earlier reports that suggested that PERK may affect the expression of ER chaperones and the efficiency of secretory processes [17, 37, 54]. In this regard, this study suggests that ATF4 plays a role in the expression of genes contributing to the assembly and processing of secretory proteins, in addition to its earlier described role in regulating genes involved in metabolism, resistance to oxidative stress, and regulation of apoptosis [40].

5.2 The PERK/eIF2~P/ATF4 pathway alleviates ER stress by multiple mechanisms

Phosphorylation of eIF2 by PERK directs essential adaptive functions that alleviate cellular injury during ER stress. This is illustrated by our finding that the LsPERK-KO livers showed enhanced activation of Caspase-3 and apoptosis during ER stress (Figure 3-2). One underlying mechanism by which PERK can alleviate stress damage is by reducing translation, which would lower the influx of nascent proteins into the ER organelle that is inundated with misfolded proteins [117]. Our study suggests that the PERK/eIF2~P/ATF4 pathway is also central for activation of ATF6 during ER stress, and as a consequence is critical for full implementation of the transcription of UPR genes, including those involved in protein folding, ERAD, and trafficking in the secretory system. This reconfiguration of the transcriptome would contribute to the

expansion of the processing capacity of the secretory pathway, which would be essential for returning the stressed ER to homeostasis. Consistent with these ideas, the livers of *ATF6*$^{-/-}$ mice also showed increased apoptosis when challenged with tunicamycin [26]. It was suggested that lowered protein chaperone expression in the *ATF6*-deficient mice compromised the ability of the ER to cope with stresses that disrupt protein folding and assembly. Livers from the *ATF6*$^{-/-}$ mice treated with tunicamycin also exhibited significantly more intracellular triglycerides compared with WT, accompanied by evidence of microvesicular steatosis [17]. This suggests that perturbations in the hepatic lipid homeostasis in the ER-stressed LsPERK-KO mice may result at least in part from the failure to appropriately activate ATF6 and its targeted gene expression (Figures 3-3 and 3-4)

PERK is also suggested to contribute to cell death during prolonged and severe ER stress. Although the underlying mechanisms by which eIF2~P can contribute to apoptosis is not well understood, it is thought that chronic ER stress can induce *CHOP* expression to a certain threshold that induces the expression of genes critical for triggering cell death [2, 3]. In this sense, PERK has a dynamic and balanced range of cellular responsiveness that is optimal for cellular adaption to ER stress [118]. The eIF2~P by PERK would lower protein synthesis and facilitate activation of the UPR, which would serve to expand the secretory pathway. Perturbations in the ISR that lead to levels of eIF2~P outside this adaptive zone would trigger extremes in translational control that would be detrimental to cells. For example, hypophosphorylation of eIF2, as can be seen in Wolcott-Rallison Syndrome (WRS), can prevent proper implementation of UPR transcription, along with heightened protein synthesis, which

can exacerbate protein trafficking deficiencies during ER stress. This can lead to cell death by mechanisms independent of CHOP induction [39]. Hyperphosphorylation of eIF2 during chronic ER stress can heighten *CHOP* expression, which is linked to signaling pathways that can culminate in apoptosis.

The range of eIF2~P levels is important to consider when examining the biological effects of eIF2~P and the UPR during different stress conditions. Chemically-induced ER stress, such as that elicited by tunicamycin used in this study, can produce an acute and terminal stress response, whereas physiological stresses that the liver can encounter may be more transient and within the adaptive zone [119, 120]. For example, a high-fat diet can elicit eIF2~P in the liver, and it was reported that attenuated eIF2~P in transgenic animals expressing elevated levels of GADD34 can diminish liver triglycerides and hepatosteatosis [121]. In this case dephosphorylation of eIF2 would be viewed as protective in the liver, while our LsPERK-KO study would suggest an important role for the ISR for cellular survival. The mechanistic rationale for these differences is not well understood. Clearly the expression of important regulators of intermediary metabolism, including those involved in lipogenesis and lipid oxidation, are affected by the PERK pathway. The expression of these genes may be influenced by the diversity, intensity and duration of the critical stress signals triggered by physiological changes in the liver.

Earlier studies have suggested divergent effects of PERK and IRE1 on cell viability [122, 123]. Sustained PERK signaling was proposed to be maladaptive to cells, while similar durations of IRE1 activation were suggested to be restricted to remedying ER stress. These ideas are complicated by the findings that PERK is

required for full activation of ATF6 and implementation of the UPR transcriptome. Furthermore, the PERK/eIF2~P/ATF4 pathway reduced *XBP1* expression, although it did not appear to alter IRE1 activity as measured by splicing of *XBP1* mRNA (Figures 3-4A). Therefore, each branch of the UPR is fully integrated, and perturbations of PERK can reduce the critical signaling functions required for cell survival during ER stress.

IRE1 is also suggested to be a contributor to apoptosis during certain ER stress arrangements. IRE1 can bind the scaffolding protein TRAF2, which serves to activate JNK, a potent inducer of apoptosis [3, 124]. This may be an important underlying explanation for the enhanced apoptosis of LsPERK-KO livers during ER stress (Figure 3-3). IRE1 dependent JNK signaling is suggested to be significantly enhanced with reductions in *XBP1* expression [14], and the levels of *XBP1* mRNA were significantly reduced in LsPERK-KO livers, despite IRE1 endonuclease activity being fully retained (Figure 3-4A).

5.3 Role of ATF4 in implementing the UPR

ATF4 is suggested to be required for full activation of ATF6 in response to ER stress by enhancing *ATF6* transcription and by facilitating the expression of genes that facilitate ATF6 trafficking from the ER to the Golgi. ATF4 may carry out these functions by directly binding to the promoters of UPR genes, through additional transcription factors targeted by ATF4, or by critical cellular changes resulting from ATF4-directed transcription. *ATF4*-deficient cells are suggested to be defective for the expression of genes involved in nutrient import and metabolism that predisposes cells to

oxidative stress [40]. This may interfere with cellular processes such as the release of ATF6 from the ER, which requires the reduction of disulfide linkages within ATF6 to promote deoligomerization required for loading and passage into COPII vesicles for anterograde transport to the Golgi [35].

5.4 ISR signaling is arranged as a binary switch

Cells recognize and respond to environmental stresses that disrupt protein homeostasis. Depending on the extent and duration of these protein disruptions, stress response pathways, such as the ISR, may not be able to restore proteostatic control and instead switch to a terminal outcome that features elevated expression of the transcription factor CHOP. The dual nature of the ISR signaling during endoplasmic reticulum stress has been referred to as a "binary switch" [12, 13] and the focus of the study presented in Chapter 4 was to define the mechanisms by which CHOP directs gene regulatory networks that determine these cell fate decisions. We find that in response to disruption of protein homeostasis by proteasome inhibition, CHOP induces the expression of ~200 transcription regulators, including ATF5 (Figure 4-1, Table 4-2). Transcriptional expression of ATF5 is directly activated by both CHOP and ATF4 (Figure 4-3), coincident with the preferential translation of ATF5 during eIF2~P [70]. Like CHOP, ATF5 functions to enhance apoptosis during perturbations in protein homeostasis. Knockdown of *ATF5* expression resulted in improved cell survival in response to proteasome inhibition, accompanied by lowered levels of biochemical markers of apoptosis (Figure 4-6). Microarray analysis of ATF5-dependent genes revealed novel targets involved in apoptosis (Figure 4-7). One of these genes, *NOXA*, was shown to be important for inducing cell death during proteasome inhibition (Figure 4-8) [116]. This

study indicates that CHOP and the ISR activate a network of transcriptional regulators, including ATF5, which function in the binary switch toward apoptosis upon disturbances in protein homeostasis.

5.5 The ISR features a network of transcription factors arranged in a feed-forward loop

This study describes three transcriptional factors in the ISR, with a network of interactions featuring a feed-forward loop (Figure 5-1) [125]. The transcriptional expression of each transcription factor node-ATF4, CHOP, and ATF5 is increased during proteasome inhibition. ATF4 directly enhances *CHOP* and *ATF5* mRNA levels, whereas CHOP facilitates the induction of *ATF5* transcripts (Figure 5-1). Currently, we do not know the underlying processes by which the transcriptional expression of ATF4 is enhanced in the ISR, but eIF2~P is suggested to be a contributing factor [126]. Accompanying this transcriptional mode of regulation, *ATF4*, *CHOP*, and *ATF5* mRNAs are preferentially translated in response to eIF2~P (Figure 5-1). Therefore, the activities of each transcription factor is tightly linked to eIF2~P levels in the ISR. With chronic disruptions of protein homeostasis there can be high levels of uninterrupted eIF2~P, which will amplify the levels of each transcription factor to a proposed threshold that will switch the ISR to a terminal outcome. Added to this ISR amplification, ancillary stress response pathways can contribute to the binary switch. Heterodimerization with other bZIP transcription factors, post-translational modifications, and subcellular localization, can also contribute to the biological functions of ATF4, CHOP, and ATF5 [84, 104, 127, 128]

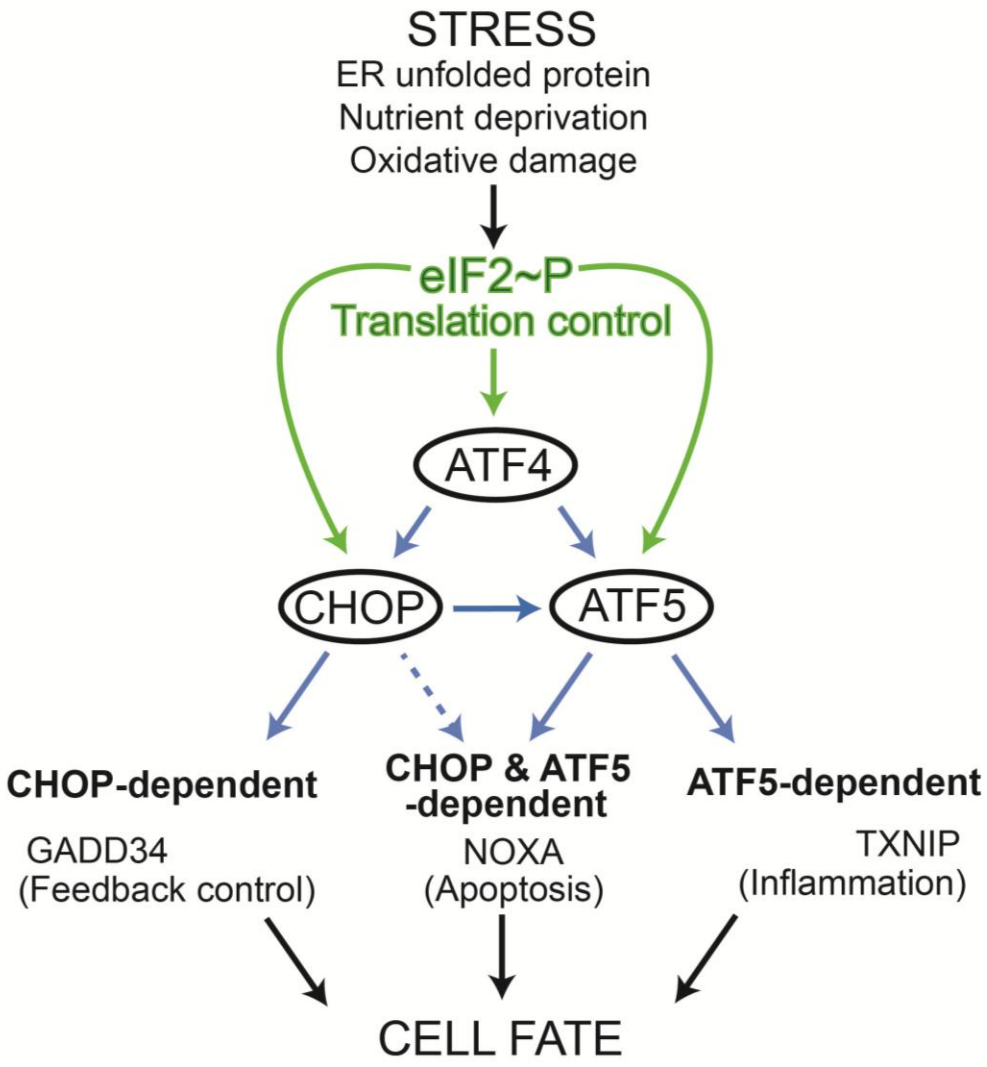

Figure 5-1 The ISR network. Proposed model of ISR signal integration and the ATF4, CHOP, and ATF5 network arranged as a feed-forward loop. Green arrows represent eIF2~P dependent translation control. Blue arrows represent transcriptional control. Three groups of genes are presented downstream of the network: ATF5-dependent, CHOP-dependent, and those target genes requiring both ATF5 and CHOP for full induction.

The network of transcription factors can induce the expression of three classes of target genes (Figure 5-1). The first group is dependent on only the ATF5 transcription factor. Included among the ATF5-specific genes is *TXNIP*. Elevated levels of TXNIP can dampen the function of thioredoxins, increasing reactive oxygen species (ROS), and enhancing caspase-1 cleavage and interleukin-1b production through TXNIP binding to the NLRP3 inflammasome, which together can trigger caspase-3 cleavage and cell death [115, 129]. It is noted that ATF5 levels are sharply reduced in the absence of *CHOP*, suggesting that the promoters of genes targeted solely by ATF5 would have a higher affinity for this transcription factor. The second group includes CHOP-specific genes, exemplified by *GADD34*, encoding a targeting subunit for Type 1 protein phosphatase that can dephosphorylate eIF2~P in a feedback control of the ISR (Figure 5-1) [130, 131]. CHOP induction of *GADD34* expression is suggested to lower cell survival during chronic stress, as premature resumption of protein synthesis can lead to further protein misfolding and aggregation [56]. The third group contains genes requiring both CHOP and ATF5 for full expression (Figure 5-1). This co-dependence may be the consequence of CHOP facilitating elevated expression of ATF5 protein in response to proteasome inhibition, aiding the binding of this transcription factor to the promoters of targeted genes. Additionally, CHOP and ATF5 could activate this group of genes by jointly associating with their respective promoters. Included among this third group is *NOXA*, which can induce apoptosis during stresses, such as proteasome inhibition [116, 132-134]. NOXA is suggested to specifically bind and inhibit BCL2 pro-survival family member MCL1, which can facilitate permeabilization of the mitochondrial membrane that leads to release of cytochrome C and subsequent activation of the apoptosome

complex and cleavage of caspases 3/9. Additionally, ATF5 facilitates expression of APAF1 (Figure 4-8), a key regulator of the apoptosome and apoptosis [135]. Coincident with this ATF5-dependent regulation, CHOP can independently repress the transcriptional expression of pro-survival *BCL2* and enhance that of pro-apoptotic *BIM* (Figure 4-2) [64, 65]. Therefore, CHOP and ATF5 regulate expression of multiple regulators of the intrinsic pathway of apoptosis in response to disruptions in protein homeostasis, with the overarching theme of induction of pro-apoptotic factors and repression of those facilitating survival.

5.6 Biological roles of ATF5

Published research on ATF5 has largely focused on its functions in neural development and tumorigenesis. *ATF5* mRNA was first detected in sensory neurons during embryonic development of the olfactory epithelium and vomeronasal organs, suggesting a role for ATF5 in olfactory neuron differentiation [68]. Indeed a recent study of mice deleted for *ATF5* showed neonatal death due to impaired differentiation and survival of olfactory sensory neurons, leading to a competitive suckling defect [136]. ATF5 was suggested to be directly involved in the transcription of genes important for olfactory function, including *KIRREL2* and *RTP2*, by processes that may involve retinoic acid. Neither of these genes was significantly changed in MEF cells in response to MG132 treatment, suggesting there are differences between the cell types studied and/or stress signals. ATF5 is also suggested to have a role in the differentiation of other types of neuroprogenitor cells, including astrocytes and oligodendrocytes [137-139].

Elevated *ATF5* mRNA has also been observed in gliobastomas and other selected tumors, and it was suggested that *ATF5* expression, which is diminished following neural development, can be restored upon cancer differentiation [140]. Genetic disruption of *ATF5* contributes to survival of glioblastomas and other tumor-derived cell lines, but not in corresponding nonneoplastic cell types [141]. These studies suggested that ATF5 is a significant contributor to proliferation of certain cancers. However, in other cell types, ATF5 was reported to reduce cell viability. For example, ectopic expression of *ATF5* in HeLa cells increased apoptosis upon treatment with cisplatin [128, 142], and *ATF4* and *ATF5* expression in B-cell lymphoma cells treated with the proteasome inhibitor bortezomib were associated with increased apoptosis [143]. In this way ATF5 may contribute to either cell survival or death depending on the cell type, developmental stage, or environmental stress arrangement.

We still have much to learn about the networks controlling the expression and transcriptional activities of *ATF5*. This study indicates that ATF4 and CHOP are upstream effectors of *ATF5* expression in the ISR, and CHOP and ATF5 can selectively target genes that adversely affect cells during proteasome inhibition. It is noted that basal levels of *ATF5* mRNA can vary between tissues, with elevated amounts in liver and selected neural regions [68]. This would suggest that there are variances in the networks that control *ATF5* transcript levels among cell types. Furthermore, there are two *ATF5* mRNAs isoforms that contain identical *ATF5* coding sequences, but differ in their 5'-leader sequences and their mode of translation. The predominant *ATF5α* mRNA isoform contains a 5'-leader with two uORFs that renders its translation dependent on induced eIF2~P [70, 144] whereas the *ATF5*β transcript contains a 5'-leader derived from another

exon and its translation is not suggested to be regulated by stress or eIF2~P [68, 144]. An important question for future studies is to determine whether eIF2~P and the ISR also contributes to *ATF5* expression and its functions in cell fate in neural development and in proliferation and treatment of cancers.

5.7 Binary switches in biological systems

There is room for the binary switch model in the description of complex cellular circuitry provided this system is clearly defined before it is applied to a biological process. For example a binary switch model could be used to describe two alternate cell fate outcomes (alive/dead) but when used in the process of cell survival or the process of cell death further definition is needed. Figure 5-2 illustrates an example of the cellular response to stress. The y-axis represents the relative level of a given adaptive or maladaptive stress responsive effector. The x-axis is a measurement of stress that could be representative of stress duration or dosage. An inflection point, where the levels of adaptive and maladaptive effectors switch is represented by a dotted line dividing the x-axis. Contrary to a classic binary switch, it is noted that the adaptive and maladaptive effectors are present on both sides of the dotted line and change gradually over time. However expressing these effectors as a ratio (maladaptive/adaptive) allows for binary quantification where at the inflection point the ratio switches. Therefore the essence of the stress responsive "binary switch" can be defined as the switching from the *absence* of a maladaptive dominant ratio to the *presence* of maladaptive dominant ratio.

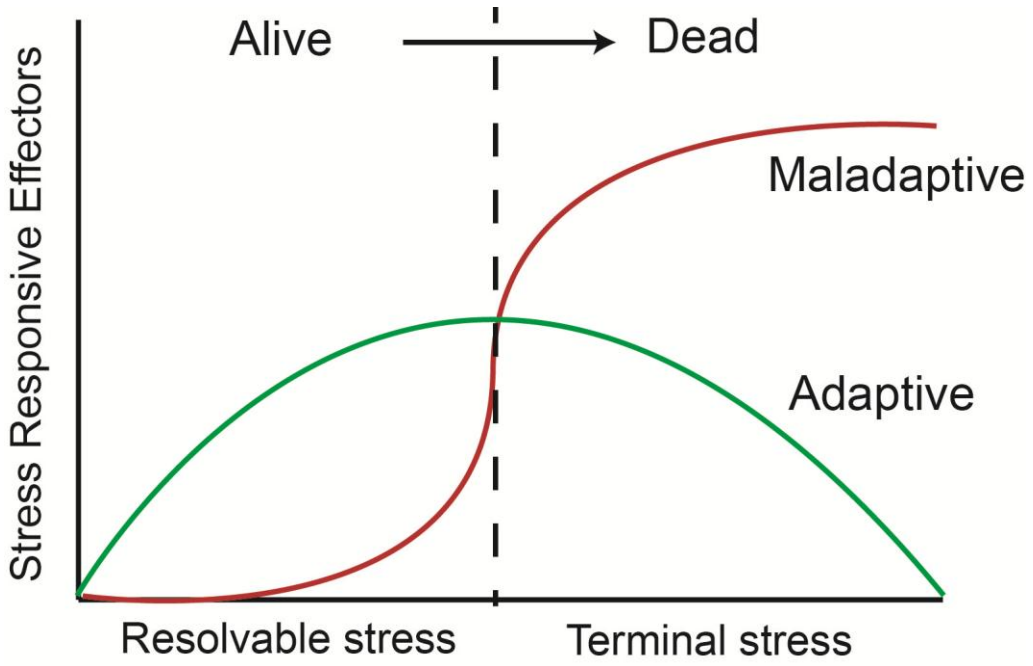

Figure 5-2 Stress responses: a binary switch model. The y-axis shows relative levels of stress responsive effectors. Levels of adaptive stress responsive effectors are shown by the green line and levels of maladaptive stress responsive effectors are shown by the red line. The x-axis indicates relative stress measurements that could be represent duration or dosage. The dotted line represents the inflection point where the stress response ratio switches from adaptive dominant to maladaptive dominant.

REFERENCES

1. Hotamisligil, G.S., *Endoplasmic reticulum stress and the inflammatory basis of metabolic disease.* Cell, 2010. 140(6):900-917.
2. Marciniak, S.J. and D. Ron, *Endoplasmic reticulum stress signaling in disease.* Physiol Rev, 2006. 86(4):1133-1149.
3. Ron, D. and P. Walter, *Signal integration in the endoplasmic reticulum unfolded protein response.* Nat Rev Mol Cell Biol, 2007. 8(7):519-529.
4. Schroder, M. and R.J. Kaufman, *The mammalian unfolded protein response.* Annu Rev Biochem, 2005. 74:739-789.
5. Wek, R.C. and D.R. Cavener, *Translational control and the unfolded protein response.* Antioxid Redox Signal, 2007. 9(12):2357-2371.
6. Hollien, J. and J.S. Weissman, *Decay of endoplasmic reticulum-localized mRNAs during the unfolded protein response.* Science, 2006. 313(5783):104-107.
7. Hollien, J., et al., *Regulated Ire1-dependent decay of messenger RNAs in mammalian cells.* J Cell Biol, 2009. 186(3):323-331.
8. Belmont, P.J., et al., *Regulation of microRNA expression in the heart by the ATF6 branch of the ER stress response.* J Mol Cell Cardiol, 2012. 52(5):1176-1182.
9. Papa, F.R., *Endoplasmic Reticulum Stress, Pancreatic beta-Cell Degeneration, and Diabetes.* Cold Spring Harb Perspect Med, 2012. 2(9)1-10.
10. Vattem, K.M. and R.C. Wek, *Reinitiation involving upstream open reading frames regulates ATF4 mRNA translation in mammalian cells.* Proc Natl Acad Sci U.S.A., 2004. 101:11269-11274.

11. Baird, T.D. and R.C. Wek, *Eukaryotic initiation factor 2 phosphorylation and translational control in metabolism.* Adv Nutr, 2012. 3(3):307-321.

12. Oslowski, C.M. and F. Urano, *The binary switch that controls the life and death decisions of ER stressed beta cells.* Curr Opin Cell Biol, 2011. 23(2):207-215.

13. Oslowski, C.M. and F. Urano, *A switch from life to death in endoplasmic reticulum stressed beta-cells.* Diabetes Obes Metab, 2010. 12(Suppl 2):58-65.

14. Glimcher, L.H., *XBP1: the last two decades.* Ann Rheum Dis, 2010. 69 (Suppl 1):i67-71.

15. Back, S.H., et al., *Cytoplasmic IRE1alpha-mediated XBP1 mRNA splicing in the absence of nuclear processing and endoplasmic reticulum stress.* J Biol Chem, 2006. 281(27):18691-18706.

16. Iwawaki, T., et al., *Function of IRE1 alpha in the placenta is essential for placental development and embryonic viability.* Proc Natl Acad Sci U S A, 2009. 106(39):16657-16662.

17. Rutkowski, D.T., et al., *UPR pathways combine to prevent hepatic steatosis caused by ER stress-mediated suppression of transcriptional master regulators.* Dev Cell, 2008. 15(6):829-840.

18. Teske, B.F., et al., *The eIF2 kinase PERK and the integrated stress response facilitate activation of ATF6 during endoplasmic reticulum stress.* Mol Biol Cell, 2011. 22(22):4390-4405.

19. Bertolotti, A., et al., *Increased sensitivity to dextran sodium sulfate colitis in IRE1beta-deficient mice.* J Clin Invest, 2001. 107(5):585-593.

20. Lee, A.H., et al., *Regulation of hepatic lipogenesis by the transcription factor XBP1.* Science, 2008. 320(5882):1492-1496.

21. Reimold, A.M., et al., *An essential role in liver development for transcription factor XBP-1.* Genes Dev, 2000. 14(2):152-157.

22. Upton, J.P., et al., *IRE1alpha cleaves select microRNAs during ER stress to derepress translation of proapoptotic Caspase-2.* Science, 2012. 338(6108):818-822.

23. Thuerauf, D.J., L. Morrison, and C.C. Glembotski, *Opposing roles for ATF6alpha and ATF6beta in endoplasmic reticulum stress response gene induction.* J Biol Chem, 2004. 279(20):21078-21084.

24. Thuerauf, D.J., et al., *Effects of the isoform-specific characteristics of ATF6 alpha and ATF6 beta on endoplasmic reticulum stress response gene expression and cell viability.* J Biol Chem, 2007. 282(31):22865-22878.

25. Haze, K., et al., *Identification of the G13 (cAMP-response-element-binding protein-related protein) gene product related to activating transcription factor 6 as a transcriptional activator of the mammalian unfolded protein response.* Biochem J, 2001. 355(1):19-28.

26. Wu, J., et al., *ATF6alpha optimizes long-term endoplasmic reticulum function to protect cells from chronic stress.* Dev Cell, 2007. 13(3):351-364.

27. Yamamoto, K., et al., *Transcriptional induction of mammalian ER quality control proteins is mediated by single or combined action of ATF6alpha and XBP1.* Dev Cell, 2007. 13(3):365-376.

28. Yamamoto, K., et al., *Induction of liver steatosis and lipid droplet formation in ATF6alpha-knockout mice burdened with pharmacological endoplasmic reticulum stress.* Mol Biol Cell, 2010. 21(17):2975-2986.

29. Yoshida, H., et al., *XPB1 mRNA is induced by ATF6 and spliced by IRE1 in response to ER stress to produce a highly active transcription factor*. Cell, 2001. 107:881-891.

30. Calfon, M., et al., *IRE1 couples endoplasmic reticulum load to secretory capacity by processing the XBP-1 mRNA.* Nature, 2002. 415(6867):92-96.

31. Schindler, A.J. and R. Schekman, *In vitro reconstitution of ER-stress induced ATF6 transport in COPII vesicles.* Proc Natl Acad Sci U S A, 2009. 106(42):17775-17780.

32. Nadanaka, S., et al., *Activation of mammalian unfolded protein response is compatible with the quality control system operating in the endoplasmic reticulum.* Mol Biol Cell, 2004. 15(6):2537-2548.

33. DeBose-Boyd, R.A., et al., *Transport-dependent proteolysis of SREBP: relocation of site-1 protease from Golgi to ER obviates the need for SREBP transport to Golgi.* Cell, 1999. 99(7):703-712.

34. Shen, J. and R. Prywes, *Dependence of site-2 protease cleavage of ATF6 on prior site-1 protease digestion is determined by the size of the luminal domain of ATF6.* J Biol Chem, 2004. 279(41):43046-43051.

35. Nadanaka, S., et al., *Role of disulfide bridges formed in the luminal domain of ATF6 in sensing endoplasmic reticulum stress.* Mol Cell Biol, 2007. 27(3):1027-1043.

36. Yamamoto, K., et al., *Differential contributions of ATF6 and XBP1 to the activation of endoplasmic reticulum stress-responsive cis-acting elements ERSE, UPRE and ERSE-II.* J Biochem, 2004. 136(3):343-350.

37. Adachi, Y., et al., *ATF6 is a transcription factor specializing in the regulation of quality control proteins in the endoplasmic reticulum.* Cell Struct Funct, 2008. 33(1):75-89.

38. Sonenberg, N. and A.G. Hinnebusch, *Regulation of translation initiation in eukaryotes: mechanisms and biological targets.* Cell, 2009. 136(4):731-745.

39. Harding, H.P., et al., *Regulated translation initiation controls stress-induced gene expression in mammalian cells.* Mol Cell, 2000. 6:1099-1108.

40. Harding, H.P., et al., *An integrated stress response regulates amino acid metabolism and resistance to oxidative stress.* Mol Cell, 2003. 11:619-633.

41. Lu, P.D., H.P. Harding, and D. Ron, *Translation reinitiation at alternative open reading frames regulates gene expression in an integrated stress response.* J Cell Biol, 2004. 167(1):27-33.

42. Wek, R.C., H.Y. Jiang, and T.G. Anthony, *Coping with stress: eIF2 kinases and translational control.* Biochem Soc Trans, 2006. 34(Pt 1):7-11.

43. Anthony, T.G., et al., *Preservation of liver protein synthesis during dietary leucine deprivation occurs at the expense of skeletal muscle mass in mice deleted for eIF2 kinase GCN2.* J Biol Chem, 2004. 279(35):36553-36561.

44. Hinnebusch, A.G., *Translational regulation of GCN4 and the general amino acid control of yeast.* Annu Rev Microbiol, 2005. 59:407-450.

45. Chen, J.J., *Regulation of protein synthesis by the heme-regulated eIF2alpha kinase: relevance to anemias.* Blood, 2007. 109(7):2693-2699.

46. Senee, V., et al., *Wolcott-Rallison Syndrome: clinical, genetic, and functional study of EIF2AK3 mutations and suggestion of genetic heterogeneity.* Diabetes, 2004. 53(7):1876-1883.

47. Julier, C. and M. Nicolino, *Wolcott-Rallison syndrome.* Orphanet J Rare Dis, 2010. 5:29.

48. Delepine, M., et al., *EIF2AK3, encoding translation initiation factor 2-a kinase 3, is mutated in patients with Wolcott-Rallison syndrome.* Nat Genet, 2000. 25:406-409.

49. Zhang, P., et al., *The PERK eukaryotic initiation factor 2 alpha kinase is required for the development of the skeletal system, postnatal growth, and the function and viability of the pancreas.* Molecular and Cellular Biology, 2002. 22:3864-3874.

50. Harding, H., et al., *Diabetes mellitus and exocrine pancreatic dysfunction in Perk -/- mice reveals a role for translational control in secretory cell survival.* Mol Cell, 2001. 7:1153-1163.

51. Li, Y., et al., *PERK eIF2alpha kinase regulates neonatal growth by controlling the expression of circulating insulin-like growth factor-I derived from the liver.* Endocrinology, 2003. 144(8):3505-3513.

52. Zhang, W., et al., *PERK EIF2AK3 control of pancreatic beta cell differentiation and proliferation is required for postnatal glucose homeostasis.* Cell Metab, 2006. 4(6):491-497.

53. Iida, K., et al., *PERK eIF2 alpha kinase is required to regulate the viability of the exocrine pancreas in mice.* BMC Cell Biol, 2007. 8:38.

54. Gupta, S., B. McGrath, and D.R. Cavener, *PERK (EIF2AK3) regulates proinsulin trafficking and quality control in the secretory pathway.* Diabetes, 2010. 59(8):1937-1947.

55. Mumby, M.C. and G. Walter, *Protein serine/threonine phosphatases: structure, regulation, and functions in cell growth.* Physiol Rev, 1993. 73(4):673-99.

56. Marciniak, S.J., et al., *CHOP induces death by promoting protein synthesis and oxidation in the stressed endoplasmic reticulum.* Genes Dev, 2004. 18(24):3066-3077.

57. Costa-Mattioli, M., et al., *eIF2alpha phosphorylation bidirectionally regulates the switch from short- to long-term synaptic plasticity and memory.* Cell, 2007. 129(1):195-206.

58. Tsaytler, P., et al., *Selective inhibition of a regulatory subunit of protein phosphatase 1 restores proteostasis.* Science, 2011. 332(6025):91-94.

59. Scheuner, D., et al., *Translational control is required for the unfolded protein response and in vivo glucose homeostasis.* Mol Cell, 2001. 7(6):1165-1176.

60. Harding, H.P., et al., *Ppp1r15 gene knockout reveals an essential role for translation initiation factor 2 alpha (eIF2alpha) dephosphorylation in mammalian development.* Proc Natl Acad Sci U S A, 2009. 106(6):1832-1837.

61. Masuoka, H.C. and T.M. Townes, *Targeted disruption of the activating transcription factor 4 gene results in severe fetal anemia in mice.* Blood, 2002. 99(3):736-745.

62. Kilberg, M.S., J. Shan, and N. Su, *ATF4-dependent transcription mediates signaling of amino acid limitation.* Trends Endocrinol Metab, 2009. 20(9):436-443.

63. Kilberg, M.S., et al., *The transcription factor network associated with the amino acid response in mammalian cells.* Adv Nutr, 2012. 3(3):295-306.

64. McCullough, K.D., et al., *Gadd153 sensitizes cells to endoplasmic reticulum stress by downregulating BcL2 and perturbing the cellular redox state.* Mol Cell Biol, 2001. 21:1249-1259.

65. Puthalakath, H., et al., *ER stress triggers apoptosis by activating BH3-only protein Bim.* Cell, 2007. 129(7):1337-1349.

66. Rutkowski, D.T., et al., *Adaptation to ER stress is mediated by differential stabilities of pro-survival and pro-apoptotic mRNAs and proteins.* PLoS Biol, 2006. 4(11):e374.

67. Kilberg, M.S., et al., *Nutritional control of gene expression: how mammalian cells respond to amino acid limitation.* Annu Rev Nutr, 2005. 25:59-85.

68. Hansen, M.B., et al., *Mouse Atf5: molecular cloning of two novel mRNAs, genomic organization, and odorant sensory neuron localization.* Genomics, 2002. 80(3):344-350.

69. Wei, Y., et al., *Identification and characterization of the promoter of human ATF5 gene.* J Biochem, 2010. 148(2):171-178.

70. Zhou, D., et al., *Phosphorylation of eIF2 directs ATF5 translational control in response to diverse stress conditions.* J Biol Chem, 2008. 283(11):7064-7073.

71. Liu, D.X., et al., *p300-Dependent ATF5 acetylation is essential for Egr-1 gene activation and cell proliferation and survival.* Mol Cell Biol, 2011. 31(18):3906-3916.

72. Shen, J., et al., *ER stress regulation of ATF6 by dissociation of BiP/GRP78 binding and unmasking of Golgi localization signals.* Developmental Cell, 2002. 3:99-111.

73. Ma, K., K.M. Vattem, and R.C. Wek, *Dimerization and release of molecular chaperone inhibition facilitate activation of eukaryotic initiation factor-2 kinase in response to endoplasmic reticulum stress.* J Biol Chem, 2002. 277(21):18728-18735.

74. Bertolotti, A., et al., *Dynamic interaction of BiP and ER stress transducers in the unfolded-protein response.* Nat Cell Biol, 2000. 2(6):326-332.

75. Pincus, D., et al., *BiP binding to the ER-stress sensor Ire1 tunes the homeostatic behavior of the unfolded protein response.* PLoS Biol, 2010. 8(7):e1000415.

76. Cui, W., et al., *The structure of the PERK kinase domain suggests the mechanism for its activation.* Acta Crystallogr D Biol Crystallogr, 2011. 67(5):423-428.

77. Credle, J.J., et al., *On the mechanism of sensing unfolded protein in the endoplasmic reticulum.* Proc Natl Acad Sci U S A, 2005. 102(52):18773-18784.

78. Kimata, Y., et al., *Two regulatory steps of ER-stress sensor Ire1 involving its cluster formation and interaction with unfolded proteins.* J Cell Biol, 2007. 179(1):75-86.

79. Gardner, B.M. and P. Walter, *Unfolded proteins are Ire1-activating ligands that directly induce the unfolded protein response.* Science, 2011. 333(6051):1891-1894.

80. Jiang, H.Y., et al., *Activating transcription factor 3 is integral to the eukaryotic initiation factor 2 kinase stress response.* Mol Cell Biol, 2004. 24(3):1365-1377.

81. Ubeda, M. and J.F. Habener, *CHOP transcription factor phosphorylation by casein kinase 2 inhibits transcriptional activation.* J Biol Chem, 2003. 278(42):40514-40520.

82. Frank, C.L., et al., *Control of ATF4 persistence by multisite phosphorylation impacts cell cycle progression and neurogenesis.* J Biol Chem, 2010.

83. Elefteriou, F., et al., *ATF4 mediation of NF1 functions in osteoblast reveals a nutritional basis for congenital skeletal dysplasiae.* Cell Metab, 2006. 4(6):441-451.

84. Yang, X., et al., *ATF4 is a substrate of RSK2 and an essential regulator of osteoblast biology; implication for Coffin-Lowry Syndrome.* Cell, 2004. 117(3):387-398.

85. Bunpo, P., et al., *GCN2 protein kinase is required to activate amino acid deprivation responses in mice treated with the anti-cancer agent L-asparaginase.* J Biol Chem, 2009. 284(47):32742-32749.

86. Yoshida, H., *Unconventional splicing of XBP-1 mRNA in the unfolded protein response.* Antioxid Redox Signal, 2007. 9(12):2323-2333.

87. Zhang, K. and R.J. Kaufman, *Identification and characterization of endoplasmic reticulum stress-induced apoptosis in vivo.* Methods Enzymol, 2008. 442:395-419.

88. Winnay, J.N., et al., *A regulatory subunit of phosphoinositide 3-kinase increases the nuclear accumulation of X-box-binding protein-1 to modulate the unfolded protein response.* Nat Med, 2010. 16(4):438-445.

89. Lee, A.H., et al., *Proteasome inhibitors disrupt the unfolded protein response in myeloma cells.* Proc Natl Acad Sci U S A, 2003. 100(17):9946-9951.

90. Park, S.W., et al., *Regulatory subunits of PI3K, p85a and p85b, interact with XBP1 and increase its nuclear translocation.* Nat Med, 2010. in press.

91. Jiang, H.Y. and R.C. Wek, *GCN2 phosphorylation of eIF2alpha activates NF-kappaB in response to UV irradiation.* Biochem J, 2005. 385(Pt 2):371-380.

92. Lu, W., et al., *The role of nitric-oxide synthase in the regulation of UVB light-induced phosphorylation of the alpha subunit of eukaryotic initiation factor 2.* J Biol Chem, 2009. 284(36):24281-24288.

93. Xue, X., et al., *Tumor necrosis factor alpha (TNFalpha) induces the unfolded protein response (UPR) in a reactive oxygen species (ROS)-dependent fashion, and the UPR counteracts ROS accumulation by TNFalpha.* J Biol Chem, 2005. 280(40):33917-33925.

94. Harding, H.P., Y. Zhang, and D. Ron, *Protein translation and folding are coupled by an endoplasmic-reticulum-resident kinase.* Nature, 1999. 397(6716):271-274.

95. Sood, R., et al., *Pancreatic eukaryotic initiation factor-2alpha kinase (PEK) homologues in humans, Drosophila melanogaster and Caenorhabditis elegans that mediate translational control in response to endoplasmic reticulum stress.* Biochem J, 2000. 346(2):281-293.

96. Bobrovnikova-Marjon, E., et al., *PERK-dependent regulation of lipogenesis during mouse mammary gland development and adipocyte differentiation.* Proc Natl Acad Sci U S A, 2008. 105(42):16314-16319.

97. Nair, S., et al., *Toxicogenomics of endoplasmic reticulum stress inducer tunicamycin in the small intestine and liver of Nrf2 knockout and C57BL/6J mice.* Toxicol Lett, 2007. 168(1):21-39.

98. Hochberg, Y. and Y. Benjamini, *More powerful procedures for multiple significance testing.* Stat Med, 1990. 9(7):811-818.

99. Wang, Y., et al., *Activation of ATF6 and an ATF6 DNA binding site by the endoplasmic reticulum stress response.* Journal of Biological Chemistry, 2000. 275:27013-27020.

100. Zhang, K., et al., *Endoplasmic reticulum stress activates cleavage of CREBH to induce a systemic inflammatory response.* Cell, 2006. 124(3):587-599.

101. Lee, K., et al., *IRE1-mediated unconventional mRNA splicing and S2P-mediated ATF6 cleavage merge to regulate XBP1 in signaling the unfolded protein response.* Genes Dev, 2002. 16(4):452-466.

102. Hong, M., et al., *Underglycosylation of ATF6 as a novel sensing mechanism for activation of the unfolded protein response.* J Biol Chem, 2004. 279(12):11354-11363.

103. Thuerauf, D.J., et al., *Coordination of ATF6-mediated transcription and ATF6 degradation by a domain that is shared with the viral transcription factor, VP16.* J Biol Chem, 2002. 277(23):20734-20739.

104. Chiribau, C.B., et al., *Molecular Symbiosis of CHOP and C/EBP{beta} Isoform LIP Contributes to Endoplasmic Reticulum Stress-Induced Apoptosis.* Mol Cell Biol, 2010. 30(14):3722-3731.

105. Lassot, I., et al., *ATF4 degradation relies on a phosphorylation-dependent interaction with the SCF(betaTrCP) ubiquitin ligase.* Mol Cell Biol, 2001. 21(6):2192-2202.

106. Lee, D.H. and A.L. Goldberg, *Proteasome inhibitors: valuable new tools for cell biologists.* Trends Cell Biol, 1998. 8(10):397-403.

107. Jiang, H.Y. and R.C. Wek, *Phosphorylation of the alpha-subunit of the eukaryotic initiation factor-2 (eIF2alpha) reduces protein synthesis and enhances apoptosis in response to proteasome inhibition.* J Biol Chem, 2005. 280(14):14189-14202.

108. Shen, J. and R. Prywes, *ER stress signaling by regulated proteolysis of ATF6.* Methods, 2005. 35(4):382-389.

109. Rowe, T., et al., *Role of vesicle-associated syntaxin 5 in the assembly of pre-Golgi intermediates.* Science, 1998. 279(5351):696-700.

110. Geng, L., et al., *Syntaxin 5 regulates the endoplasmic reticulum channel-release properties of polycystin-2.* Proc Natl Acad Sci U S A, 2008. 105(41):15920-15925.

111. Ungar, D. and F.M. Hughson, *SNARE protein structure and function.* Annu Rev Cell Dev Biol, 2003. 19:493-517.

112. Pan, Y.X., et al., *Activation of the ATF3 gene through a co-ordinated amino acid-sensing response programme that controls transcriptional regulation of responsive genes following amino acid limitation.* Biochemical Journal, 2007. 401(1):299-307.

113. Zhong, C., C. Chen, and M.S. Kilberg, *Characterization of the nutrient-sensing response unit in the human asparagine synthetase promoter.* Biochem J, 2003. 372(2):603-609.

114. Bruhat, A., et al., *Differences in the molecular mechanisms involved in the transcriptional activation of the CHOP and asparagine synthetase genes in response to amino acid deprivation or activation of the unfolded protein response.* J Biol Chem, 2002. 277(50):48107-48114.

115. Oslowski, C.M., et al., *Thioredoxin-interacting protein mediates ER stress-induced beta cell death through initiation of the inflammasome.* Cell Metab, 2012. 16(2):265-273.

116. Wang, Q., et al., *ERAD inhibitors integrate ER stress with an epigenetic mechanism to activate BH3-only protein NOXA in cancer cells.* Proc Natl Acad Sci U S A, 2009. 106(7):2200-2205.

117. Harding, H.P., et al., *Perk is essential for translational regulation and cell survival during the unfolded protein response.* Mol Cell, 2000. 5(5):897-904.

118. Wek, R.C. and T.G. Anthony, *Beta testing the antioxidant function of eIF2alpha phosphorylation in diabetes prevention.* Cell Metab, 2009. 10(1):1-2.

119. Rutkowski, D.T. and R.S. Hegde, *Regulation of basal cellular physiology by the homeostatic unfolded protein response.* J Cell Biol, 2010. 189(5):783-794.

120. Rutkowski, D.T. and R.J. Kaufman, *That which does not kill me makes me stronger: adapting to chronic ER stress.* Trends Biochem Sci, 2007. 32(10):469-476.

121. Oyadomari, S., et al., *Dephosphorylation of translation initiation factor 2alpha enhances glucose tolerance and attenuates hepatosteatosis in mice.* Cell Metab, 2008. 7(6):520-532.

122. Lin, J.H., et al., *IRE1 signaling affects cell fate during the unfolded protein response.* Science, 2007. 318(5852):944-949.

123. Lin, J.H., et al., *Divergent effects of PERK and IRE1 signaling on cell viability.* PLoS One, 2009. 4(1):e4170.

124. Urano, F., et al., *Coupling of stress in the ER to activation of JNK protein kinases by transmembrane protein kinase IRE1.* Science, 2000. 287(5453): p. 664-666.

125. Milo, R., et al., *Network motifs: simple building blocks of complex networks.* Science, 2002. 298(5594):824-827.

126. Harding, H.P., et al., *An integrated stress response regulates amino acid metabolism and resistance to oxidative stress.* Mol Cell, 2003. 11(3):619-633.

127. Liu, X., et al., *Nucleophosmin (NPM1/B23) interacts with activating transcription factor 5 (ATF5) protein and promotes proteasome- and caspase-dependent ATF5 degradation in hepatocellular carcinoma cells.* J Biol Chem, 2012. 287(23):19599-19609.

128. Wei, Y., et al., *Cdc34-mediated degradation of ATF5 is blocked by cisplatin.* J Biol Chem, 2008. 283(27):18773-18781.

129. Lerner, A.G., et al., *IRE1alpha induces thioredoxin-interacting protein to activate the NLRP3 inflammasome and promote programmed cell death under irremediable ER stress.* Cell Metab, 2012. 16(2):250-264.

130. Novoa, I., et al., *Feedback inhibition of the unfolded protein response by GADD34-mediated dephosphorylation of eIF2alpha.* J Cell Biol, 2001. 153:1011-1022.

131. Novoa, I., et al., *Stress-induced gene expression requires programmed recovery from translational repression.* EMBO J, 2003. 22:1180-1187.

132. Rosebeck, S., et al., *Involvement of Noxa in mediating cellular ER stress responses to lytic virus infection.* Virology, 2011. 417(2):293-303.

133. Reuland, S.N., et al., *ABT-737 synergizes with Bortezomib to kill melanoma cells.* Biol Open, 2012. 1(2):92-100.

134. Selimovic, D., et al., *Bortezomib/proteasome inhibitor triggers both apoptosis and autophagy-dependent pathways in melanoma cells.* Cell Signal, 2013. 25(1):308-318.

135. Youle, R.J. and A. Strasser, *The BCL-2 protein family: opposing activities that mediate cell death.* Nat Rev Mol Cell Biol, 2008. 9(1):47-59.

136. Wang, S.Z., et al., *Transcription factor ATF5 is required for terminal differentiation and survival of olfactory sensory neurons.* Proc Natl Acad Sci U S A, 2012. 109(45):18589-18594.

137. Mason, J.L., et al., *ATF5 regulates the proliferation and differentiation of oligodendrocytes.* Mol Cell Neurosci, 2005. 29(3):372-380.

138. Angelastro, J.M., et al., *Downregulation of activating transcription factor 5 is required for differentiation of neural progenitor cells into astrocytes.* J Neurosci, 2005. 25(15):3889-3899.

139. Greene, L.A., H.Y. Lee, and J.M. Angelastro, *The transcription factor ATF5: role in neurodevelopment and neural tumors.* J Neurochem, 2009. 108(1):11-22.

140. Angelastro, J.M., et al., *Selective destruction of glioblastoma cells by interference with the activity or expression of ATF5.* Oncogene, 2005. 25(6):907-916.

141. Monaco, S.E., et al., *The transcription factor ATF5 is widely expressed in carcinomas, and interference with its function selectively kills neoplastic, but not nontransformed, breast cell lines.* Int J Cancer, 2007. 120(9):1883-1890.

142. Wei, Y., et al., *ATF5 increases cisplatin-induced apoptosis through up-regulation of cyclin D3 transcription in HeLa cells.* Biochem Biophys Res Commun, 2006. 339(2):591-596.

143. Shringarpure, R., et al., *Gene expression analysis of B-lymphoma cells resistant and sensitive to bortezomib.* Br J Haematol, 2006. 134(2):145-156.

144. Watatani, Y., et al., *Stress-induced translation of ATF5 mRNA is regulated by the 5' untranslated region.* J Biol Chem, 2007.

CURRICULUM VITAE
Brian Frederick Teske

EDUCATION

Ph. D. Biochemistry and Molecular Biology 2007-2013
Minor: Diabetes and Obesity
Indiana University, Indianapolis, Indiana
Mentor: Dr. Ronald Wek

M. S. Biology 2005-2007
Indiana University-Purdue University, Indianapolis, Indiana
Mentor: Dr. Martin Bard

B. S. Biological Sciences 2001-2005
Ohio University, Athens, Ohio
Mentor: Dr. Soichi Tanda

EMPLOYMENT HISTORY

Research Assistant 2007-2013
Indiana University School of Medicine, Indianapolis

- Worked closely with a core group of researchers to design and carry out experiments. Collaborated with other departments regularly to provide project support of joint project goals. Contributed both experimentally and intellectually to grant writing and technical documents.

Research Assistant/Teaching Assistant 2005-2007
Indiana University-Purdue University, Indianapolis

- As a research assistant, conducted original research in a small lab group to characterize enzyme interactions in yeast lipid biosynthesis.
- As a teaching assistant, responsible for coordination of lab based instruction. Worked with students and instructors to update course material, administered quizzes and exams, submitted final grades.

Research Technician 2004-2005
Ohio University, Athens

- Provided technical support to meet needs of senior researchers in the lab. Helped with sample preparation, data collection, and data management.

RESEARCH GRANTS AND AWARDS

Predoctoral Fellowship 2011-2012

American Heart Association

- Recipient of the American Heart Association Midwest Affiliate Predoctoral Fellowship to investigate the mechanisms that direct cell survival and apoptosis in response to endoplasmic reticulum stress. Grant ID: 11PRE7240012.

Predoctoral Fellowship 2010-2011

Center for Diabetes Research

- Recipient of National Institute of Health Research Training in Diabetes and Obesity, predoctoral fellowship to investigate the relationship of Perk dependent eIF2 phosphorylation and ER stress activation of ATF6 with the goal of identifying mechanisms that contribute to diabetes. Grant ID: T32DK064466.

Travel Awards 2006-2007

- Graduate Student Organization Educational Enhancement Grant
- Graduate Office Travel Fellowship
- School of Science Graduate Student Council Travel Award

Siegfried Maier Undergraduate Research Award 2004-2005

Ohio University, Athens

- Recipient of the Siegfried Maier Undergraduate Research Award to investigate the regulation of Toll-receptors and Methuselah-like proteins in fruit flies.

PROFESSIONAL SERVICE

Student Ambassador 2007-2011

Indiana Biomedical Gateway (IBMG) Program

- Involved in campus visits, poster session, and recruitment of potential graduate students. Served on student panels to answer questions for incoming students. Also served as a mentor to facilitate training and coaching of graduate students in the lab.

Student Member 2009-2012

Indiana University School of Medicine Graduate Student Organization

- Served as the Biochemistry and Molecular Biology student representative, reviewed travel grants, attended student lunches, and answered questions on behalf of the Biochemistry and Molecular Biology department

Tutor, Molecular Biology and Genetics 2008-2009
Indiana University School of Medicine

- Provided one-on-one tutoring for G716 a core graduate course for all students in the Integrated Biomedical Gateway program at the IU School of Medicine.

PRESENTATIONS AND POSTERS

IUPUI Research Day 2012
Indianapolis, Indiana
Title: *The eIF2 kinase PERK and the integrated stress response facilitate activation of ATF6 during endoplasmic reticulum stress.*

Center for Diabetes Research Seminar Series 2010
Indianapolis, Indiana
Title: *Translation Control and ER Stress Induced Hepatic Steatosis.*

Department of Medical Molecular Genetics Seminar Series 2010
Indianapolis, Indiana
Title: *Integrated Signaling Pathways Direct the Unfolded Protein Response.*

8th Annual Yeast Lipids Conference 2007
Torino, Italy
Poster Title: *Mutational Analysis of the Yeast 3-ketoreductase (Erg27p) and the Effects on Ergosterol Biosynthesis.*

PUBLICATIONS

Teske, B.F., Fusakio, M.F., Zhou, D., Shan, J., McClintick J.N., Kilberg, M.S., Wek, R.C. Chop induces activating transcription factor 5 (ATF5) to trigger apoptosis in response to perturbations in protein homeostasis. 2013 (MBoC submitted).

Dey, S., Savant, S., **Teske, B.F.,** Hatzoglou, M., Calkhoven, C.F., and Wek, R.C. Transcriptional repression of *ATF4* by C/EBPβ differentially regulates the Integrated Stress Response. *Journal of Biological Chemistry*. 2012;287(26):21936-21949.

Teske, B.F., Wek, S.A., Bunpo, P., Cundiff, J.K., McClintick, J.N., Anthony, T.G., Wek R.C. (2011) The eIF2 kinase PERK and the integrated stress response facilitate activation of ATF6 during endoplasmic reticulum stress. *Molecular Biolology of the Cell*. 2011;22(22):4390-4405 (featured article, nominated for paper of year candidate 2012).

Teske, B.F., Baird, T.D., Wek, R.C. Methods for analyzing eIF2 kinases and translation control in the unfolded protein response. *Methods In Enzymology*. 2011;490:333-356.

Taramino, S., **Teske, B.,** Oliaro-Bosso, S., Bard,M., Balliano, G. Divergent interactions involving the oxidosqualene cyclase and the steroid-3-ketoreductase in the sterol biosynthetic pathway of mammals and yeasts. *Biochimica Biophysica Acta*. 2010;1801(11):1232-1237.

Taramino, S., Valachovic, M., Oliaro-Bosso, S., Viola, F., **Teske, B.,** Bard, M., Balliano, G. Interactions of oxidosqualene cyclase (Erg7p) with 3-ketoreductase (Erg27p) and other enzymes of sterol biosynthesis in yeast. *Biochimica Biophysica Acta*. 2010;1801(2):156-162.

Teske, B., Taramino, S., Bhuiyan, M. S. A., Kumaraswami, N. S., Randall, S., Barbuch, R, Eckstein, J., Balliano, G., Bard, M. Genetic analyses involving interactions between the ergosterol biosynthetic enzymes, lanosterol synthase (Erg7p) and 3-ketoreductase (Erg27p), in the yeast *Saccharomyces cerevisiae*. *Biochimica Biophysica Acta*. 2008;1781(8):359-366.